



HAL
open science

Formation Control of Multiple Nonholonomic Wheeled Mobile Robots

Xhaoxia Peng

► **To cite this version:**

Xhaoxia Peng. Formation Control of Multiple Nonholonomic Wheeled Mobile Robots. Other. Ecole Centrale de Lille, 2013. English. NNT : 2013ECLI0006 . tel-00864197

HAL Id: tel-00864197

<https://theses.hal.science/tel-00864197>

Submitted on 20 Sep 2013

HAL is a multi-disciplinary open access archive for the deposit and dissemination of scientific research documents, whether they are published or not. The documents may come from teaching and research institutions in France or abroad, or from public or private research centers.

L'archive ouverte pluridisciplinaire **HAL**, est destinée au dépôt et à la diffusion de documents scientifiques de niveau recherche, publiés ou non, émanant des établissements d'enseignement et de recherche français ou étrangers, des laboratoires publics ou privés.

N° d'ordre:

2	1	8
---	---	---

ÉCOLE CENTRALE DE LILLE

THÈSE

présentée en vue d'obtenir le grade de

DOCTEUR

en

Automatique, Génie Informatique, Traitement du Signal et Image

par

Zhaoxia PENG

DOCTORAT DELIVRE PAR L'ÉCOLE CENTRALE DE LILLE

Titre de la thèse :

**Contribution à la Commande d'un Groupe de Robots Mobiles
Non-holonomes à Roues**

**Formation Control of Multiple Nonholonomic Wheeled Mobile
Robots**

Soutenue le 9 July 2013 devant le jury d'examen :

Président	M. Pierre BORNE	Professeur, École Centrale de Lille, Lille
Rapporteur	M. Rachid ALAMI	Directeur de Recherche CNRS, LAAS, Toulouse
Rapporteur	M. François CHARPILLET	Directeur de Recherche INRIA, LORIA, Nancy
Rapporteur	M. Qiang ZHAN	Professeur, Beihang University, Chine
Examineur	M. Yongguang YU	Professeur, Beijing Jiaotong University, Chine
Examineur	M. Nacer K.M'SIRDI	Professeur, Polytech Marseille, Marseille
Directeur de thèse	M. Ahmed RAHMANI	Maître de Conférences HDR, École Centrale de Lille

Thèse préparée dans le Laboratoire d'Automatique, Génie Informatique et Signal

L.A.G.I.S., CNRS UMR 8219 - École Centrale de Lille

École Doctorale SPI 072

PRES Université Lille Nord-de France

*À mes parents,
à toute ma famille,
à mes professeurs,
et à mes chère(s) ami(e)s.*

Acknowledgements

This research work has been accomplished in École Centrale de Lille, in the “Laboratoire d’Automatique, Génie Informatique et Signal (LAGIS)”, with the research team “Méthodes & Outils pour la Conception Intégrée de Systèmes (MOCIS)”.

First and foremost I offer my most sincere gratitude to my supervisors, Mr. Ahmed Rahmani who has provided his supervision, advices, and guidance as well as given me extraordinary experiences throughout the work. With their enormous helps, I have obtained a lot of research experiences in Intelligent Robots Control. Mr. Rahmani has provided an oasis of ideas for this report by a lot of discussions with me and my colleagues. I am indebted to them more than they know.

Mr. Francois Charpillet, Mr. Rachid Alami and Mr. Qiang Zhan used their precious times to review this PhD report before publication and gave various critical comments for shaping the final version of this report. They helped me refine the most delicate issues and present them from a more comprehensive perspective. I also would like to thank the member of the jury: Mr. Pierre Borne, Mr. Nacer K.M’Sirdi and Mr. Yongguang Yu for their time, interest, and helpful comments.

I would like to thank Mr. Belkacem Ould Bouamama, the team leader of MOCIS, who organized many scientific workshops helping us to exchange ideas. I also would like to thank Mrs. Genevieve Dauphin-Tanguy. During the three years of my thesis, she was always close to us and encouraged us with enthusiasm for our research. I am grateful to her noble characters. I would like to thank Mr. Hieu N.PHAN, he gives me a lot of useful suggestions during my thesis. I would like to thank his kindness and helps. In addition, I would like to thank Director of Ecole Centrale de Lille Etienne Craye.

For the "Accueil à la française", I would like to thank Christine Yvoz, Daniel Rivière, Patrick Gallais, Régine Duplouich, Tram Nguyen, Vanessa Fleury and

ACKNOWLEDGEMENTS

Virginie Leclercq who helped us with the administrative matters. I am also grateful to all my PhD student colleagues: Eugene Tarassov, Baisi Liu, Hui Wang, Huarong Wang, Hui Liu, Jian Liu, Jin Bai, Jiangfeng Liu, Jinlin Gong, Lamine Chalal, Li Zhi, Minzhi Luo, Yingcong Ma, Mayank Shekhar Jha, Naima Hadji, Noe Barrera-G, Wenhua Tang, Xiaojian Fu, Yang Qian, Yahong Zheng, Yang Tian, Yongliang Huang, Yue Yu, Cuicui Li, Youwei Dong, Ran Zhao, Wenhao Fang, etc.

All my gratitude goes to Ms. H el ene Catsiapis who showed us the French language and culture. She made possible all those interesting and unforgettable voyages in France. My knowledge and interest in the French culture is inspired by her work and enthusiasm, she managed to open our appetite for art, history and cuisine/wine.

My PhD study was supported and funded by the ERASMUS MUNDUS TANDEM. therefore I would like to thank Ms. Monique Bukowski, Prof. Zoubeir Lafhaj and all the people who have built this relationship and contributed to select candidates for interesting research projects. I am extremely grateful to ERASMUS MUNDUS TANDEM.

At last, but not the least, I convey special acknowledgement to my husband, Guoguang WEN, my parents Lianglong PENG and Houming ZHOU as well as the rest of my family for their love and support. Their encouragement and understanding during the course of my research work have greatly help me in the pursuit of my advanced academic degree.

Villeneuve d'Ascq, France
Mars, 2013

Zhaoxia PENG

Résumé en français

La commande coopérative des systèmes multi-robots mobiles connaît un essor considérable ces dernières années, en raison des vastes applications, comme le sauvetage, le déplacement des objets volumineux, la surveillance, les réseaux de capteurs, le transport coopératif, etc. L'idée est que des véhicules autonomes qui collaborent peuvent obtenir de meilleurs résultats. Dans cette thèse, nous nous intéressons à la commande d'un groupe de robots mobiles non-holonomes. L'objectif est de concevoir des commandes adaptées à chaque robot pour que le groupe de robots mobiles puisse exécuter une tâche prédéfinie ou suivre une trajectoire désirée, tout en maintenant une configuration géométrique souhaitée.

Cette thèse comporte 5 chapitres résumés ci-dessous:

Le chapitre est consacré à l'état de l'art et rappels des notions utilisés, en particulier, ceux liés à la théorie des graphes.

Dans le chapitre 2, le problème du leader-suiveur pour robots mobiles non-holonomes a été étudié en se basant sur l'approche backstepping. Le contrôle de suivi de trajectoire pour un seul robot mobile non-holonyme a été étendu à la commande d'un groupe de robots mobiles non-holonomes. Le suiveur peut suivre son leader en temps réel à l'aide du contrôleur proposé cinématique. En raison de la contrainte non-holonyme de chaque robot et de l'objectif leader-suiveur, un contrôleur auxiliaire de commande de la vitesse angulaire a été développé pour garantir la stabilité asymptotique globale des suiveurs et de continuer à garantir la stabilité asymptotique locale de la formation entière. Ainsi, un contrôleur asymptotiquement stable a été développé, garantissant à tous les robots mobiles d'atteindre, et de maintenir, la formation souhaitée, mais aussi à tous les robots suiveurs de suivre, en temps réel, la trajectoire du robot leader.

RÉSUMÉ EN FRANÇAIS

Comme l'utilisation de la technologie backstepping peut conduire à un saut de vitesse, en cas d'erreur de suivi, une approche neurodynamique bioinspirée a été développée pour résoudre le problème de saut de vitesse. Il est démontré que chaque robot possède une vitesse lisse, continue avec une valeur initiale nulle en utilisant l'approche neurodynamique bioinspirée. L'analyse de stabilité a été effectuée en utilisant la théorie de Lyapunov. L'efficacité de l'algorithme de commande proposé a été démontrée par simulation.

Dans le chapitre 3, le problème de la commande distribuée d'un système multi-robots mobiles non-holonomes utilisant l'approche basée sur le consensus a été étudiée. Tout d'abord, une transformation a été effectuée afin de convertir le problème de la commande distribuée d'un système multi-robots mobiles non-holonomes en un problème de consensus.

Puis les lois de commande, permettant au groupe de robots mobiles non-holonomie de converger vers une configuration géométrique souhaitée tout en se déplaçant le long de la trajectoire de référence spécifiée, ont été proposées. Dans ce chapitre, la trajectoire de référence spécifiée a été représentée par l'état d'un leader virtuel dont l'information en sortie est sa position qui est disponible pour seulement un sous-ensemble d'un groupe de suiveurs. Comme les lois de commande proposées dans ce chapitre soient distribuées, il n'est pas nécessaire de connaître l'information globale de l'ensemble des robots et de l'environnement. En effet, chaque robot peut obtenir des informations provenant uniquement de ses voisins.

Dans ce chapitre, il a été montré, que la topologie de communication considérée ne possède pas nécessairement une structure en arbre d'informations, et que nos lois de commande proposées garantissent aux robots mobiles non-holonomes de converger exponentiellement vers le modèle géométrique souhaitée, ainsi que le centre de gravité géométrique de la formation qui converge exponentiellement vers la trajectoire de leader virtuel.

Dans le chapitre 3, les lois de commande proposées sont fondées sur des modèles cinématiques, ce qui suppose que la vitesse de suivi est " parfaite ". Mais, dans de nombreuses situations pratiques, la dynamique du robot ne doit pas être ignorée et des lois de commande basées sur les modèles cinématique et dynamique doivent être mise en œuvre. C'est pour cela, que dans le chapitre 4, nous abordons le problème de la commande adaptative distribuée d'un système

multi robots mobiles non-holonomes à roues en tenant compte des modèles cinématiques et dynamiques avec des paramètres inconnus. L'objectif est de mettre au point des lois de commande distribuées, de telle sorte qu'un groupe de robots mobiles non-holonomes sur roues converge asymptotiquement vers une configuration géométrique souhaitée le long de la trajectoire de référence désirée. Pour cela, le problème de la commande d'un système multi robots est transformé en un problème de consensus. Nous supposons que la trajectoire de référence désirée peut être considérée comme la trajectoire d'un leader virtuel et que l'information provenant du leader est disponible pour seulement un sous-ensemble de ses suiveurs voisins. Les suiveurs sont supposés n'avoir qu'une seule interaction locale. Ensuite, parce que les paramètres dynamiques inconnus auront une incidence sur la poursuite de trajectoire, des lois de commande adaptatives ont été proposées. Des conditions suffisantes sont obtenues afin de garantir la stabilité asymptotique des systèmes multi robots non holonome à roues. Elles sont basées sur la théorie des graphes, sur la théorie des matrices, et sur l'approche de Lyapunov. Ces lois de commandes ont été validées par simulation.

Il est bien connu qu'en pratique, les frottements et les perturbations bornées ne doivent pas être ignorés. Dans le chapitre 5, le modèle dynamique du robot mobile non holonome à roues considéré, fait apparaître un coefficient de frottement et une perturbation bornée. Sous l'hypothèse de la connaissance partielle de la dynamique du robot mobile, un régulateur de couple asymptotiquement stable a été proposé en utilisant des techniques robustes de contrôle adaptatif pour tenir compte de la dynamique des perturbations bornées. Ensuite, toute la dynamique du robot mobile a été supposée inconnue, et la propriété d'approximation universelle des réseaux de neurones a été utilisée pour relaxer l'hypothèse de la connaissance de la dynamique du système, et une commande asymptotiquement robuste adaptative augmentée a été proposée afin de garantir un suivi asymptotique.

RÉSUMÉ EN FRANÇAIS

Contents

Table of Contents	8
List of Figures	11
1 Introduction	17
1.1 Background and Motivation	17
1.2 Overview of Related Works	20
1.2.1 Control Structures	20
1.2.2 Control Approaches	22
1.3 Preliminaries	26
1.3.1 Graph Theory	26
1.3.2 Nonsmooth analysis	30
1.3.3 Nonholonomic Systems	31
1.3.4 Lyapunov Theory	33
1.4 Contributions and Outline of Dissertation	35
2 Leader-Follower Formation Control of Multiple Nonholonomic Mobile Robots Using a Bioinspired Neurodynamic based Approach	39
2.1 Introduction	40
2.2 Mathematical Model of a Nonholonomic Mobile Robot	41
2.3 Leader-Follower Formation Control	43
2.3.1 A Leader-Follower Formation Model	43
2.3.2 Formation Control Objective	45
2.3.3 The Error Dynamics of Leader-Follower Formation	46
2.4 Backstepping Control Algorithm	48

CONTENTS

2.5	The Bioinspired Neurodynamics Applying to Backstepping Control Algorithm	49
2.5.1	The Bioinspired Neurodynamics Model	50
2.5.2	Backstepping-based Algorithm with a Bioinspired Neurodynamics Model	51
2.6	Simulations Results	53
2.6.1	Validation and Comparison of the Proposed Backstepping Controllers (2.16) and (2.25)	53
2.6.2	Validation for Leader-Follower Formation Control Based on Bioinspired Neurodynamics	58
2.7	Conclusion	64
3	Distributed Consensus-Based Formation Control for Multiple Nonholonomic Mobile Robots with A Specified Reference Trajectory	65
3.1	Introduction	65
3.2	Mathematical Model of a Nonholonomic Mobile Robot	67
3.3	Problem Statement	68
3.4	Distributed Control Algorithm	70
3.5	Simulation Results	76
3.6	Conclusion	83
4	Distributed Adaptive Formation Control for Multiple Nonholonomic Wheeled Mobile Robots	85
4.1	Introduction	85
4.2	Problem Formulation and Preliminaries	87
4.2.1	Dynamics of Nonholonomic Wheeled Mobile Robot	87
4.2.2	Problem Description	89
4.3	Distributed Control Algorithm	90
4.4	Adaptive Dynamic Controller Design	95
4.4.1	Robot Model and Its Properties	95
4.4.2	Controller Design	96
4.5	Simulation	101
4.6	Conclusion	106

5 Distributed Consensus-Based Formation Control for Nonholonomic Wheeled Mobile Robots Using Adaptive Neural Network	107
5.1 Introduction	108
5.2 Preliminary	108
5.2.1 Dynamics of Nonholonomic Wheeled Mobile robot	110
5.2.2 Neural Network	111
5.2.3 Problem Description	113
5.3 Distributed Control Algorithm	114
5.4 Adaptive Dynamic Controller Design	116
5.4.1 Robot Model and its Properties	116
5.4.2 Controller Design	117
5.5 Neural Network Control Design	122
5.6 Simulation	129
5.6.1 Verification of Formation Control Based on Robust Adaptive Techniques	130
5.6.2 Verification of Formation Control Based on Neural Network Techniques	134
5.7 Conclusion	140
Conclusions and Perspective	141
References	145

CONTENTS

List of Figures

1.1	Examples of biological systems exhibiting formation behaviors in nature: (a) flocks of birds, (b) schools of fishes, (c) team of ants, (d) swarms of bees.	18
1.2	Examples of formation in practice applications.(a)Unmanned Air Vehicles (UAVs);(b) Autonomous Underwater Vehicles (AUVs); (c)Mobile Robots Systems (MRSs);(d)Manipulation.	19
1.3	Example of the Formation Control Objective	20
1.4	$l - \varphi$ controller (Desai <i>et al.</i> (1998))	23
1.5	$l - l$ controller (Desai <i>et al.</i> (1998))	25
1.6	Information flow from j to i	27
1.7	A graph $G = (\mathcal{V}, \mathcal{E})$ with $\mathcal{V} = \{1, 2, 3, 4, 5, 6\}$	29
1.8	A unicycle mobile robot.	32
2.1	A nonholonomic mobile robot.	42
2.2	A leader-follower formation scheme.	43
2.3	The real-time trajectories of robots: (a) by using the controller(2.16); (b) by using the controller (2.25).	54
2.4	The tracking errors of the follower: (a) by using the controller(2.16); (b) by using the controller (2.25).	55
2.5	The linear velocities and angular velocities of follower: (a) by using the controller(2.16); (b) by using the controller (2.25).	56
2.6	The reference angular velocities of follower and the angular velocities of the leader: (a) by using the controller(2.16); (b) by using the controller (2.25).	57
2.7	Leader-follower formation with five mobile robots.	58
2.8	The trajectory of Leader-Follower formation.	60

LIST OF FIGURES

2.9	The errors between the angular velocity of leader L and the reference angular velocity w_j^d of each follower Fj	60
2.10	The angular velocities and linear velocities of robots.	61
2.11	The tracking errors of the follower in Leader-follower Formation .	63
3.1	Differential wheel mobile robot.	67
3.2	Communication graph of a group of six followers and one virtual leader.	77
3.3	Desired geometric pattern of formation.	78
3.4	Formation pattern of the six follower robots at some time, the trajectory of virtual leader(black line), and the trajectory of the six follower robots' centroid (blue line).	79
3.5	(a)The trajectories of x_0 (blue line) and the centroid of x_i ($1 \leq i \leq 6$)(red line); (b)The position error between x_0 and the centroid of x_i	80
3.6	(a)The trajectories of y_0 (blue line) and the centroid of y_i ($1 \leq i \leq 6$)(red line); (b)The position error between y_0 and the centroid of y_i	81
3.7	The tracking errors: (a)between w_i ($1 \leq i \leq 6$) and w_0 ; (b)between θ_i ($1 \leq i \leq 6$) and θ_0	82
4.1	The trajectory of virtual leader (black line), the trajectory of centroid of the six followers (blue line), and the formation positions and pattern of the six followers at some moments.	101
4.2	The trajectories of x_0 (blue line) and the centroid of x_i ($1 \leq i \leq 6$)(red line).	102
4.3	The trajectories of y_0 (blue line) and the centroid of y_i ($1 \leq i \leq 6$)(red line).	103
4.4	The tracking error \tilde{u}_{wi} for ($1 \leq i \leq 6$).	103
4.5	The tracking error \tilde{u}_{vi} for ($1 \leq i \leq 6$).	104
4.6	The tracking errors $w_i - w_0$ ($1 \leq i \leq 6$).	104
4.7	The tracking errors $\theta_i - \theta_0$ ($1 \leq i \leq 6$).	105
5.1	Two-layer feedforward Neural Network structure	112

LIST OF FIGURES

5.2	Path of the six robots' centroid(blue line), the desired trajectory of the centroid of the robots(black line), and the formation of the six robots at several moments under the distributed kinematic controller (5.31),(5.32) and the torque controller (5.44).	130
5.3	(a)The trajectories of x_0 (blue line) and the centroid of x_i ($1 \leq i \leq 6$)(red line); (b)The position error between x_0 and the centroid of x_i	131
5.4	(a)The trajectories of y_0 (blue line) and the centroid of y_i ($1 \leq i \leq 6$)(red line); (b)The position error between y_0 and the centroid of y_i .	132
5.5	The tracking error \tilde{u}_{wi} for ($1 \leq i \leq 6$) using the torque controller (5.44).	133
5.6	The tracking error \tilde{u}_{vi} for ($1 \leq i \leq 6$) using the torque controller (5.44).	133
5.7	Response of the centroid of $w_i - w_0$ for $1 \leq i \leq 6$	134
5.8	Response of the centroid of $\theta_i - \theta_0$ for $1 \leq i \leq 6$	134
5.9	Path of the six robots' centroid(blue line), the desired trajectory of the centroid of the robots(black line), and the formation of the six robots at several moments	135
5.10	(a)The trajectories of x_0 (blue line) and the centroid of x_i ($1 \leq i \leq 6$)(red line); (b)The position error between x_0 and the centroid of x_i	136
5.11	(a)The trajectories of y_0 (blue line) and the centroid of y_i ($1 \leq i \leq 6$)(red line); (b)The position error between y_0 and the centroid of y_i .	137
5.12	The tracking error \tilde{u}_{wi} for ($1 \leq i \leq 6$) under the Neural Network controller (5.60).	138
5.13	The tracking error \tilde{u}_{vi} for ($1 \leq i \leq 6$) under the Neural Network controller (5.60).	138
5.14	Response of the centroid of $w_i - w_0$ for $1 \leq i \leq 6$	139
5.15	Response of the centroid of $\theta_i - \theta_0$ for $1 \leq i \leq 6$	139

LIST OF FIGURES

Chapter 1

Introduction

Contents

1.1	Background and Motivation	17
1.2	Overview of Related Works	20
1.2.1	Control Structures	20
1.2.2	Control Approaches	22
1.3	Preliminaries	26
1.3.1	Graph Theory	26
1.3.2	Nonsmooth analysis	30
1.3.3	Nonholonomic Systems	31
1.3.4	Lyapunov Theory	33
1.4	Contributions and Outline of Dissertation	35

1.1 Background and Motivation

In the recent years, the cooperation of multiple robots has been extensively researched, which arises from the broad potential applications including many military applications such as general marine mine sweeping , exploration, surveillance and tracking, and many civilian applications such as filming motion picture stunts, mining support, geophysical survey, pipeline and power line patrol, search and rescue, farm aerial spraying, timber survey, forest fire suppression, off-shore oil support, etc. Indeed, there are many potential advantages of such systems

1. INTRODUCTION

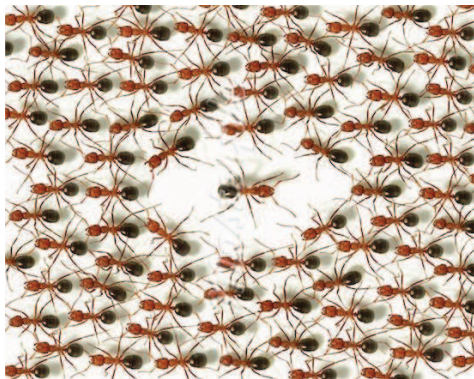
over a single robot, including improving the mission efficiency in terms of time and quality, achieving tasks not executable by a single robot or proving flexibility to the tasks execution, also highly adaptive, low cost and easy maintenance, etc (Gustavi & Hu 2008; Peng *et al.* 2013; Tanner & Piovesan 2010; Wen *et al.* 2012). As a very typical issue in cooperative control, the formation control of multiple robots systems received significant interest in recent years, which aim at forcing robots to converge towards, and maintain, a specific geometric pattern.



(a)



(b)



(c)



(d)

Figure 1.1: Examples of biological systems exhibiting formation behaviors in nature: (a) flocks of birds, (b) schools of fishes, (c) team of ants, (d) swarms of bees.

Many systems in nature exhibit stable formation behaviors, such as, e.g., flocks of birds, schools of fishes, swarms of insects (see Fig. 1.1). In these highly robust systems, individuals follow distant leaders without colliding with neighbors. Similarly, as shown in Fig. 1.2, in many multiple robots applications, such

1.1 Background and Motivation

as Unmanned Air Vehicles (UAVs), Autonomous Underwater Vehicles (AUVs), Mobile Robots Systems (MRSs), manipulation (see, [Chen 2009](#)), using formation of multiple robots to accomplish an objective offers obvious advantages. These include increasing feasibility, accuracy, robustness, flexibility, cost and energy efficiency, and so on.



(a)



(b)



(c)



(d)

Figure 1.2: Examples of formation in practice applications.(a)Unmanned Air Vehicles (UAVs);(b) Autonomous Underwater Vehicles (AUVs); (c)Mobile Robots Systems (MRSs);(d)Manipulation.

Motivated by the above discussions, this dissertation focus on formation control problems of multiple mobile robots. The general objective is to design some new control laws for each robot according to different control tasks and different constraint conditions, such that a group of mobile robots can form and maintain a desired geometric pattern and follow a desired trajectory (See Fig. [1.3](#)).

1. INTRODUCTION

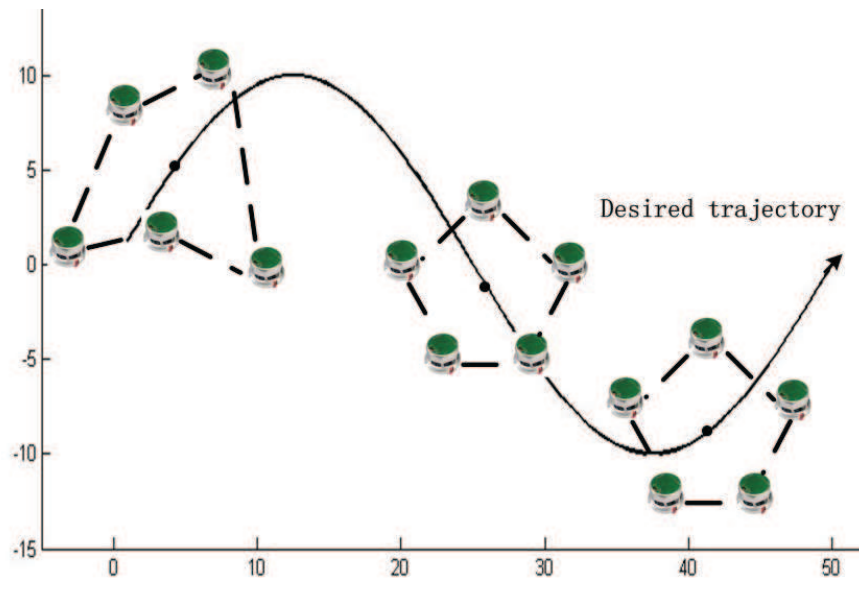


Figure 1.3: Example of the Formation Control Objective

1.2 Overview of Related Works

In the past decade, numerous results for formation control of mobile robots have been obtained. Based on the reference of [Dudek *et al.* \(1996\)](#), there are two fundamental analysis perspectives: control structures and control approaches. In the following, we shall present an overview of the related works belonging to these two perspectives.

1.2.1 Control Structures

It is well known that the robustness of multiple mobile robot systems is strictly related to the control structure used to organize the robots and to obtain the desired formation behaviors. In the field of mobile robots formation control, the control structures can be identified as centralized control structure and distributed control structure.

In the centralized control structure, a single computational unit processes all the information needed to achieve the desired control objectives. Therefore they can ideally yield superior performances and optimal decisions for both the individual members and the formation as a whole ([kanjanawanishkul 2005](#)). In

1.2 Overview of Related Works

recent years, many of the related studies on formation control for multiple mobile robots with centralized control structure have been discussed. In reference of [Egerstedt & Hu \(2001\)](#), a coordination strategy for moving a group of robots in a desired formation over a given trajectory was proposed. In reference of [Koo & Shahruz \(2001\)](#), a centralized path planning method for a group of unmanned aerial vehicles (UAVs) in a desired formation was proposed. In reference of [Belta & Kumar \(2002\)](#), a centralized trajectory computation scheme that uses kinetic energy shaping was developed. The advantages of a centralized structure typically include faster convergence and enhanced stability. These benefits come with a greater financial cost due to the required processing and communications resources needed by the single computational unit. Although these guarantee a complete solution, centralized control schemes require higher computation power and are less robust due to the heavy dependence on a single controller. Additionally, architectures involving a single computational unit typically do not work well for large systems due to limited communication range and limited processing power of the single computational unit (see, [Abel 2010](#)).

For the same formation control purpose, the multiple mobile robots formation control can use a distributed control structure. The distributed control structure is the most used structure to control multi-robot systems, and can be considered as the opposite of the centralized approach. In a mobile robots system with distributed control structure, each robot acts based only on knowledge of local teammates' state and of environment, which can satisfy some practical requirements, for example, limited communication among robots, lack of robot sensing ability to obtain global information and the need to scale robot formation (arbitrarily increase the number of robots in the formation). There are a lot of related results about formation control using distributed control structure (see, [Chen *et al.* 2010](#); [Chen & Wang 2005](#); [Das *et al.* 2002](#); [Desai *et al.* 1998, 2001](#); [Dierks & Jagannathan 2009a,b](#); [Dong 2012](#); [Dong & Farrell 2008, 2009](#); [Mariotini *et al.* 2007](#); [Park *et al.* 2011](#)). This approach typically has a smaller financial cost and works better for larger systems than a centralized structure. However, this approach can result in reduced stability and slower convergence.

1. INTRODUCTION

1.2.2 Control Approaches

There are various strategies and approaches, which can be roughly categorized as behavior-based approach, leader-follower approach, virtual-structure, artificial potential, and graph theory, have been emerged for the formation control of multiple mobile robots (Chen & Wang 2005; Fax & Murray 2004, 2002; Olfati-Saber 2006; Shi *et al.* 2009; Tanner *et al.* 2003a,b; Wang *et al.* 2013).

In the behavior-based approach (Balch & Arkin 1998; Brooks 1985; Brunete *et al.* 2012; Dougherty *et al.* 2004; Lawton *et al.* 2003; Long *et al.* 2005; Zhao 2010), several desired behaviors (e.g. obstacle avoidance, collision avoidance, target attraction, to name a few) are assigned to each robot, and the final control is derived from a weighting of the relative importance of each behavior. In the behavior-based controller, each individual behavior is actually a sub-controller for achieving a certain goal (usually in an elemental level), for example, "form to a specified geometric pattern" can be a behavior, and "avoid obstacles" can be another behavior. If a robot runs on these two behaviors, eventually it will achieve a combination of goals i.e.: "forming to a specified geometric pattern while avoiding obstacles". This method is suitable for a large group of mobile robots. The behavior-based approach is first introduced by Brooks (1985), and is generally used in behavioral robotics applications. Antonelli *et al.* (2008) proposed a control method based on the NSB (Null-Space based behavior) to solve the flocking problem for mobile robots. Monteiro & Bicho (2010) used a nonlinear attractor dynamics to design dynamic control structure, where desired behaviors are generated as an asymptotically stable time series, which further made the entire system asymptotically stable. The advantages of this kind of approach are its parallel, distributed and real-time characteristics, and less information needs to be communicated among robots. Therefore, it is very useful to guide a multiple mobile robots system in an unknown or dynamical changing environment. However, it might be difficult to describe the dynamics of the group and to guarantee the stability of the whole system, and it is difficult to analyze its behavioral performance mathematically.

In the virtual structure approach (Chen & Wang 2005; Egerstedt & Hu 2001; Lewis & Tan 1997; Tan & Lewis 1996), the entire formation is treated as a single entity. The control laws for robots are derived in three steps. First, the dynamics of the virtual structure is defined. Then the motion of the virtual structure is

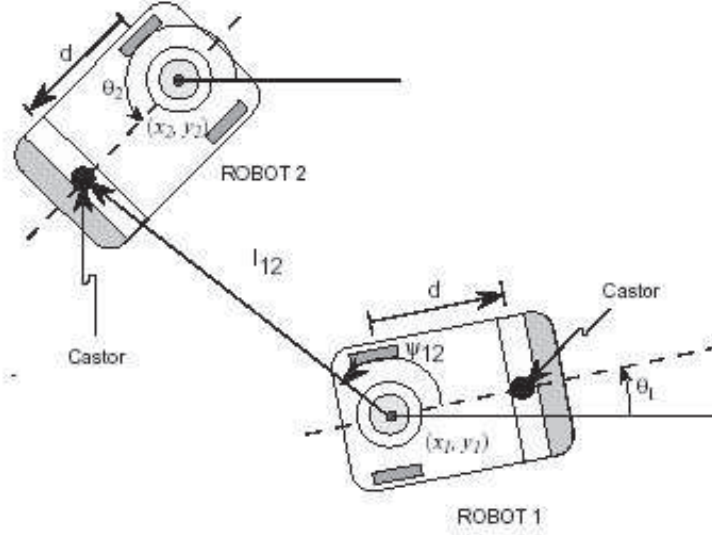


Figure 1.4: $l - \varphi$ controller (Desai *et al.* (1998))

translated into the desired motion for each robot. Finally, the individual tracking controllers for robots are derived. Since Tan & Lewis (1996) proposed the concept of virtual structure, there are already many literatures on formation control using this approach. Ren & Beard (2004) used this approach to implement UAV control. Lalish *et al.* (2006) studied a formation control problem, primarily for a group of aircrafts, and in the first instance introduced a completely decoupled control scheme for robots in formation. Dong & Farrell (2008) studied two formation control problems for nonholonomic mobile robots, in which only constant formation shapes were considered. Kostic *et al.* (2010) studied the time-varying formation shapes control problem using virtual structure approach and proposed a saturated control law where all mobile robots in the formation communicate with all other robots to perform the formation task. Ghommam *et al.* (2010) used a combination of the virtual structure and path following approaches to derive a control strategy for multiple mobile robots coordination. The advantage of this approach is that it is easier to describe the coordinated behavior for the group of formation. However, the controller is not in distributed architecture and may encounter difficulties for solving some formation applications.

In the leader-follower approach (Chen & Wang 2005; Das *et al.* 2002; Desai

1. INTRODUCTION

et al. 1998, 2001; Mariottini *et al.* 2007), one robot acts as leader that generates the reference trajectory for the group of robots, and the rest of robots in the group act as followers that must keep the desired separation and relative bearing with respect to the leader. In fact, once the motion of the leader is given, the desired separation and the desired relative bearing of the follower with the leader can be achieved by choosing a local control law on each follower based on its relative position dynamics. Then the stability of the formation is also guaranteed, i.e. the entire group can achieve and maintain the desired formation. Based on the above observation, formation control problem can be essentially viewed as a natural extension of the traditional trajectory tracking problem. To the best of my knowledge, just few researchers have considered the trajectory tracking problem when dealing with the multi-robot formation problem. Desai *et al.* (1998, 2001) presented a feedback linear control method for the formation of nonholonomic mobile robots using the leader-follower approach, and proposed two control algorithms: $l - \varphi$ control and $l - l$ control. The $l - \varphi$ control aimed to control and maintain the desired separation l_{12}^d and relative bearing φ_{12}^d between the leader and the follower robot as shown in Fig. 1.4 for two nonholonomic wheeled mobile robots. The $l - l$ control considered the relative position of three mobile robots, a follower and two leaders, by keeping the desired separation to its two leaders. The aim is to control and maintain the desired separations l_{13}^d and l_{23}^d between the follower and its two leaders, as shown in Fig. 1.5.

In the artificial potential approach, the obstacle in the environment produces a repulsive force that pushes the robot away from obstacles, the target point produces an attractive force that pulls the robot toward the target point. The repulsive force and attractive force are described as a repulsive potential function and an attractive potential function. Generally, these two kinds of potential functions are used together in practical applications to satisfy the convergence, collision-free and obstacle-free. In fact, the robot will move along the direction that minimizes the potential energy. To the best of my knowledge, the concept of artificial potential is first proposed by Khatib (1986). Since then, a lot of results are obtained. Olfati-Saber (2006) studied the flocking problem using a set of potential functions. Hsieh & Kumar (2006) investigated the pattern generation problem for multiple mobile robots in a potential field framework. Kumar *et al.*

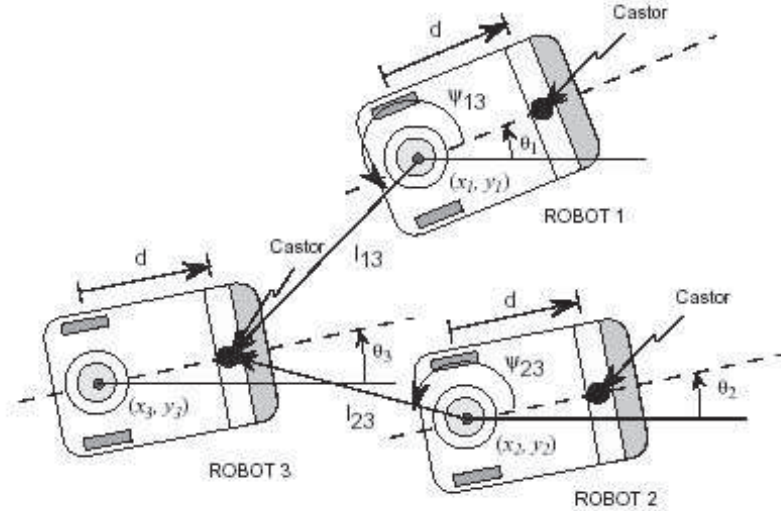


Figure 1.5: $l-l$ controller (Desai *et al.* (1998))

(2008) implemented the group segregation in a potential field framework. Sabatini *et al.* (2009) proposed appropriate control strategies based on the interaction of some artificial potential fields to realize formation of mobile robots with an arbitrary shape. Bennet & McInnes (2010) considered the pattern formation and reconfigurability in a multiple mobile robots system using bifurcation potential field to achieve various patterns through a simple free parameter change. The advantages of this approach are that it requires less calculation, and can be used for real-time control applications. The drawbacks is that it is difficult to design potential field functions satisfying local minimums.

In the graph theory approach, each robot is considered as a node, and each communication or sensing information link between robots is considered as an edge. The research approach uses graph theory, control theory, and dynamics systems theory together to study the formation controller and its stability. Godsil & Royle (2001) made a connection between control theory and graph theory to analyze the formation stabilization. Gazi & Passino (2003) showed the rank of graph Laplacian which is related to connectivity. Olfati-Saber & Murray (2003) considered a spatial adjacency matrix for obtaining the formation among a group of agents which are equipped with limited range sensor. Recently, the graph

1. INTRODUCTION

rigidity and persistence are used in the formation control problem. Since [Eren *et al.* \(2004\)](#) proposed the use of graph rigidity theory for modeling information structure of the formation, numerous results about rigid formation and persistent formation were obtained (See, [Anderson *et al.* 2008](#); [Hendrickx *et al.* 2008](#); [Summers *et al.* 2011](#); [Yu *et al.* 2007](#)). The advantage of this approach is that it is easy to represent any formation by using graph, which has well-developed theory results. The disadvantage is that it is difficult to consider the limitation of the real robot configuration.

Besides the above listed approaches, some other approaches are also used to formation control, i.e., Model predictive control (MPC) approach ([Kanjanawanishkul 2009](#); [Phan & Barlow 2008](#)), Reinforcement learning ([Zuo *et al.* 2010](#)), and hybrid system ([McClintock & Fierro 2008](#)), and so on.

1.3 Preliminaries

In this section, some preliminaries about graph theory and the nonholonomic mobile robots are given, which serve as a basis for the following several chapters.

Notations: Let I_m denote the $m \times m$ identity matrix, $0_{m \times m}$ denote the $m \times m$ zero matrix, and $\mathbf{1}_m = [1, 1, \dots, 1]^T \in \mathbb{R}^m$ ($\mathbf{1}$ for short, when there is no confusion). $\lambda_{\min}(\cdot)$ and $\lambda_{\max}(\cdot)$ are the smallest and the largest eigenvalues of the matrix respectively. For any $y = (y_1, y_2, \dots, y_m)^T \in \mathbb{R}^m$, we denote that $sign(y) = [sign(y_1), sign(y_2), \dots, sign(y_m)]^T$.

1.3.1 Graph Theory

Graph theory has proved to be an important tool in the stability analysis of the formations. A graph is a natural presentation of the interconnection of coordinated robots for information exchange. The characterization of the topology of a graph can be used in the analysis of robot formations stability and controllability . It can also be used to choose an appropriate controller for a specific formation pattern or even decide if such a controller exists, see for example, [Diestel \(1997\)](#) and [Godsil & Royle \(2001\)](#).

A weighted graph is used to represent the communication or sensing links among robots because it can represent both the existence and information communication of each links. Let the weighted graph $\mathcal{G} = (\mathcal{V}, \mathcal{E}, \mathcal{A})$ be a weighted

graph consisting of the finite nonempty set of nodes $\mathcal{V} = \{\nu_1, \dots, \nu_m\}$, the set of edges $\mathcal{E} \subseteq \mathcal{V} \times \mathcal{V}$, and a weighted adjacency matrix $\mathcal{A} = (a_{ij})_{m \times m}$. The quantities $|\mathcal{V}|$ and $|\mathcal{E}|$ are, respectively, called order and size of the graph. Suppose that $|\mathcal{V}| = m$. The edge $(\nu_i, \nu_j) \in \mathcal{E}$ means that the node i get the information from the node j through an information link.



Figure 1.6: Information flow from j to i

Definition 1.1 *The weighted graph $\mathcal{G} = (\mathcal{V}, \mathcal{E}, \mathcal{A})$ is undirected, if for all $\nu_i, \nu_j \in \mathcal{V}$,*

$$(\nu_i, \nu_j) \in \mathcal{E} \iff (\nu_j, \nu_i) \in \mathcal{E},$$

otherwise it is directed.

Definition 1.2 *The weighted adjacency matrix \mathcal{A} of a weighted graph \mathcal{G} is represented as*

$$\mathcal{A} = \begin{bmatrix} a_{11} & a_{12} & \dots & a_{1m} \\ a_{21} & a_{22} & \dots & a_{2m} \\ \vdots & \vdots & \ddots & \vdots \\ a_{m1} & a_{m2} & \dots & a_{mm} \end{bmatrix} \in \mathcal{R}^{m \times m},$$

where a_{ji} is the weight of the link (ν_j, ν_i) , and

$$\begin{cases} a_{jj} = 0 & \text{for any } \nu_j \in \mathcal{V}, \\ a_{ji} = 1 & \text{for } (\nu_j, \nu_i) \in \mathcal{E} \text{ and } i \neq j. \end{cases}$$

Note that here $a_{ji} = a_{ij}, \forall j \neq i$, since $(\nu_j, \nu_i) \in \mathcal{E}$ implies $(\nu_i, \nu_j) \in \mathcal{E}$. We can say ν_j is a neighbor vertex of ν_i , if $(\nu_j, \nu_i) \in \mathcal{E}$. The neighbor set of node j is defined as

$$\mathcal{N}_j = \{i \in \mathcal{V} : a_{ji} \neq 0\} = \{i \in \mathcal{V} : (j, i) \in \mathcal{E}\}.$$

1. INTRODUCTION

Definition 1.3 The degree matrix of the weighted graph \mathcal{G} is a diagonal matrix $\mathcal{D} = \text{diag}\{d_1, \dots, d_m\} \in \mathcal{R}^{m \times m}$, where $d_j = \sum_{i \in N_j}^m a_{ji}$.

Definition 1.4 The Laplacian matrix $L = (l_{ji})_{m \times m} \in \mathcal{R}^{m \times m}$ of the weighted graph \mathcal{G} is defined as

$$l_{ji} = \begin{cases} \sum_{k \in N_j}^m a_{jk} & \text{for } i = j, \\ -a_{ji} & \text{for } (\nu_j, \nu_i) \in \mathcal{E} \text{ and } i \neq j \\ 0 & \text{otherwise.} \end{cases}$$

The Laplacian matrix $L \in \mathcal{R}^{m \times m}$ can be expressed as

$$L = \mathcal{D} - \mathcal{A}. \quad (1.1)$$

It also can express as the following form

$$L = \begin{bmatrix} \sum_{k \in N_1}^m a_{1k} & -a_{12} & \dots & -a_{1m} \\ -a_{21} & \sum_{k \in N_2}^m a_{2k} & \dots & -a_{2m} \\ \vdots & \vdots & \ddots & \vdots \\ -a_{m1} & -a_{m2} & \dots & \sum_{k \in N_m}^m a_{mk} \end{bmatrix}.$$

Hence, we can easily obtain the following equation,

$$L\mathbf{1}_m = 0. \quad (1.2)$$

Example 1.5 From Fig.1.7, the edge set \mathcal{E} of the graph G is $\mathcal{E} = \{(1, 2), (1, 4), (1, 6), (2, 3), (2, 5), (3, 4), (3, 5), (4, 5), (5, 6)\}$. The adjacency matrix, the degree matrix

and the Laplacian matrix of the graph shown in Fig.1.7 can be written as:

$$\mathcal{A} = \begin{bmatrix} 0 & 1 & 0 & 1 & 0 & 1 \\ 1 & 0 & 1 & 0 & 1 & 0 \\ 0 & 1 & 0 & 1 & 1 & 0 \\ 1 & 0 & 1 & 0 & 1 & 0 \\ 0 & 1 & 1 & 1 & 0 & 1 \\ 1 & 0 & 0 & 0 & 1 & 0 \end{bmatrix}, \quad \mathcal{D} = \begin{bmatrix} 3 & & & & & \\ & 3 & & & & \\ & & 3 & & & \\ & & & 3 & & \\ & & & & 4 & \\ & & & & & 2 \end{bmatrix},$$

$$L = \mathcal{D} - \mathcal{A} = \begin{bmatrix} 3 & -1 & 0 & -1 & 0 & -1 \\ -1 & 3 & -1 & 0 & -1 & 0 \\ 0 & 1 & 3 & -1 & -1 & 0 \\ -1 & 0 & -1 & 3 & -1 & 0 \\ 0 & -1 & -1 & -1 & 4 & -1 \\ -1 & 0 & 0 & 0 & -1 & 2 \end{bmatrix}.$$

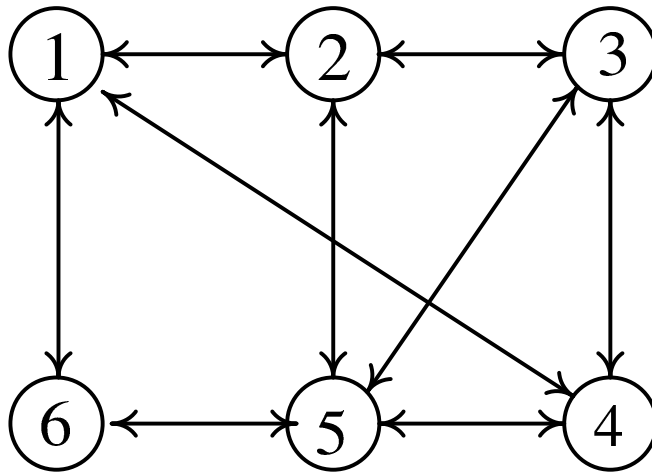


Figure 1.7: A graph $G = (\mathcal{V}, \mathcal{E})$ with $\mathcal{V} = \{1, 2, 3, 4, 5, 6\}$.

Lemma 1.6 (*Chung 1997*): Assume \mathcal{G} is a weighted undirected graph with Laplacian matrix L , then the following two statements are equivalent:

- (1) The matrix L has an eigenvalue zero with multiplicity 1 and corresponding eigenvector $\mathbf{1}$, and all other eigenvalues are positive;

1. INTRODUCTION

(2) \mathcal{G} is connected.

1.3.2 Nonsmooth analysis

In what follows, we introduce some elements from nonsmooth analysis that we use in the next sections. For a differential equation with a discontinuous right-hand side, we have the following definition.

Consider the vector differential equation given by

$$\dot{x} = f(t, x), \tag{1.3}$$

where $f(t, x)$ is measurable and essentially locally bounded. the vector function $x(\cdot)$ is called a Filippov solution of (1.3) Cortes (2008), if $x(\cdot)$ is absolutely continuous and satisfies

$$\dot{x} \in \mathcal{K}[f](t, x)$$

almost everywhere where

$$\mathcal{K}[f](t, x) \equiv \overline{\text{co}}\{\lim_{x_i \rightarrow x} f(x_i) | x_i \notin \Omega_v\},$$

where the Ω_v denotes is the set of measure zero that contains the set of points where f is not differentiable. and $\overline{\text{co}}$ denotes the convex closure.

Lemma 1.7 (Cortes (2008)) *The Filippov set-value map has the following useful properties:*

(1) *Consistency: If $f : \mathbb{R}^d \rightarrow \mathbb{R}^m$ is continuous at $x \in \mathbb{R}^d$, then*

$$\mathcal{K}[f](x) = \{f(x)\}.$$

(2) *Sum Rule : If founction $f_1, f_2 : \mathbb{R}^d \rightarrow \mathbb{R}^m$ are locally bounded at $x \in \mathbb{R}^d$, then*

$$\mathcal{K}[f_1 + f_2](x) \subseteq \mathcal{K}[f_1](x) + \mathcal{K}[f_2](x).$$

Moreover, if either f_1 or f_2 is continuous at x , then equality holds.

Lyapunov theorems have been extended to nonsmooth systems. The following chain rule provides a calculus for the time derivative of the energy function in the nonsmooth case.

Definition 1.8 *Paden & Sastry (1987)* Let $V(x)$ be a locally Lipschitz continuous function. The generalized gradient of $V(x)$ is given by

$$\partial V(x) \triangleq \text{co}\{\lim \nabla V(x) | x_i \rightarrow x, x_i \in \Omega_v \cap \bar{N}\},$$

where co denotes the convex hull, Ω_v is the set of Lebesgue measure zero, where ∇V does not exist, and \bar{N} is an arbitrary set of zero measure.

From the definition, the candidate Lyapunov function V we use is smooth and hence regular, while its generalized gradient is a singleton which is equal to its usual gradient everywhere in the state space: $\partial V(x) = \{\nabla V(x)\}$.

Definition 1.9 (*Cortes (2008)*) Consider the vector differential equation (1.3), a set-valued map $\mathcal{K} : \mathbb{R}^d \rightarrow \mathcal{B}(\mathbb{R})$, the set-valued Lie derivative of V with respect to (1.3) is defined as

$$\dot{\check{V}} \triangleq \bigcap_{\xi \in \partial V} \xi^T \mathcal{K}[f](t, x).$$

A Lyapunov stability theorem in terms of the set-valued map $\dot{\check{V}}$ is stated as follows.

Lemma 1.10 *Shevitz & Paden (1994)* For , let $f(t, x)$ be locally essentially bounded and $0 \in \mathcal{K}[f](t, 0)$ in a region $Q \supset \{t | t_0 \leq t \leq \infty\} \times \{x \in \mathbb{R}^d | \|x\| < r\}$, where $r > 0$. Also, let $V : \mathbb{R}^d \rightarrow \mathbb{R}$ be a regular function satisfying

$$V(t, 0) = 0, \quad \text{and} \quad 0 < V_1(\|x\|) \leq V(t, x) \leq V_2(\|x\|), \quad \text{for } x \neq 0,$$

in Q for some V_1 and V_2 belonging to class \mathcal{K} . If there exists a class \mathcal{K} function $w(\cdot)$ in Q such that the set-valued Lie derivative of $V(x)$ satisfies

$$\max \dot{\check{V}}(t, x) \leq -w(x) < 0, \quad \text{for } x \neq 0,$$

then the solution $x \equiv 0$ is asymptotically stable.

1.3.3 Nonholonomic Systems

The control design for a nonholonomic system has been discussed over the last decade. The nonholonomic system can be described by the nonholonomic con-

1. INTRODUCTION

straints, These so-called nonholonomic constraints most commonly arise in mechanical systems where some constraints are imposed on the motion. These kinds of nonholonomic systems are broadly used in real life, in all kinds of intelligent mechanical systems like manipulators, mobile robots, surface vessels, underwater vehicles, helicopters, spacecrafts, etc (Xiang *et al.* 2009).

In this section, the definitions of nonholonomic system and some related concepts will be introduced (Goldstein 1980; Xiang *et al.* 2009).

1) Holonomic Systems: Consider a system of generalized coordinates q , with the dynamics $\ddot{q} = f(q, \dot{q}, u)$, where u is a vector of external generalized inputs. If the conditions of constraints limiting the motion of the system, can be expressed as the time-derivative of some functions of the generalized coordinates with the form $\Phi(q, t) = 0$, then the constraints are said to be holonomic. This type of constraint is socalled integrated, since the holonomic constraint can be solved by integration.

2) Nonholonomic Systems : In classic mechanics, systems with nonholonomic constraints, which are defined as linear constraints w.r.t. generalized coordinates q , having the form $\Phi(q, t)\dot{q}(t) = 0$. This means the equations of motion constraints are irreducible, and cannot be expressed as time derivative of state function. Therefore, the constraints non-integrable are called nonholonomic constraints. Within nonholonomic systems, the generalized coordinates are not independent from each other.

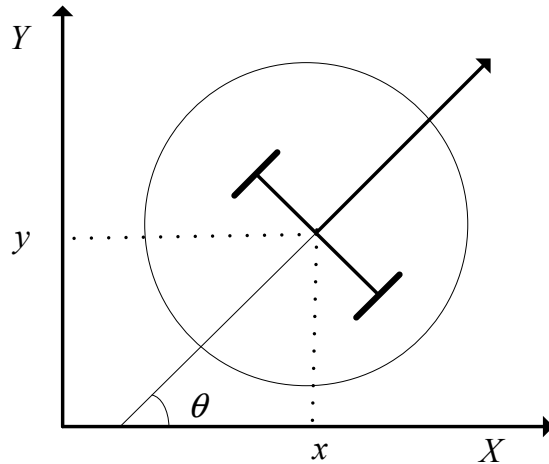


Figure 1.8: A unicycle mobile robot.

The unicycle mobile robot (shown in Fig. 1.8) is a typical nonholonomic system, which can be describe by the nonholonomic constraints. In general, there are two type of constraints: the rolling constraint and the sliding constraint. From the Fig.1.8, the state vector $q = (x, y, \theta)$ denotes posture of the robot. (x, y) of the centre of mass of the robot; And θ is the orientation with respect to the horizontal axis; v and w are the forward velocity and the angular velocity, respectively.

The rolling constraint for the wheel means that all motion along the direction of the wheel plane, which can be expressed as

$$\dot{x} \cos \theta + \dot{y} \sin \theta - r \dot{\varphi} = 0.$$

where $\dot{\varphi}$ is the angular velocity of the wheel, r is the radius of the wheel.

In contrast, the sliding constraint means the wheel's motion orthogonal to the wheel plane must be zero

$$\dot{x} \sin \theta - \dot{y} \cos \theta = 0, \tag{1.4}$$

And the kinematic model of a mobile robot, which can be obtained from the nonholonomic constraints, can be described as

$$\dot{x} = v \cos \theta, \tag{1.5}$$

$$\dot{y} = v \sin \theta, \tag{1.6}$$

$$\dot{\theta} = w. \tag{1.7}$$

It can be shown that the kinematic constraints given by (1.3.3) and (1.4) cannot be integrated, i.e. there does not exist a function $f(x, y, \theta, w)$ such that the constraints are equivalent to $df(x, y, \theta, w)/dt = 0$. This kind of constraints is called nonholonomic. Conversely, if constraints can be integrated, they are named holonomic constraints.

1.3.4 Lyapunov Theory

Before presenting the feedback control laws for the global tracking problem stabilization discussed above, we list two useful lemmas that will be used in the following proof of the main theory.

Assume that f is function of time t only. It should be noted that:

1. INTRODUCTION

1. Having $\dot{f}(t) \rightarrow 0$ does not imply that $f(t)$ has a limit at $t \rightarrow \infty$.
2. Having $f(t)$ approaching a limit as $t \rightarrow \infty$ does not imply that $\dot{f}(t) \rightarrow 0$.
3. Having $f(t)$ lower bounded and decreasing $\dot{f}(t) \leq 0$ implies it converges to a limit. But it does not say whether or not $\dot{f}(t) \rightarrow 0$ as $t \rightarrow \infty$.

Theorem 1.11 (*Barbalat's lemma*) (*Slotine & Li 1991*) *If $f(t)$ has a finite limit as $t \rightarrow \infty$ and if $\dot{f}(t)$ is uniformly continuous (or $\ddot{f}(t)$ is bounded), then $\dot{f}(t) \rightarrow 0$ as $t \rightarrow \infty$.*

Usually, it is difficult to analyze the asymptotic stability of time-varying systems because it is very difficult to find Lyapunov functions with a negative definite derivative.

Lemma 1.12 (*Lyapunov-Like Lemma*) (*Slotine & Li 1991*) *If a scalar function $V(x, t)$ satisfies the following conditions:*

1. $V(x, t)$ is lower bounded.
2. $\dot{V}(x, t)$ is negative semi-definite.
3. $\dot{V}(x, t)$ is uniformly continuous in time (satisfied if \ddot{V} is finite).

then $\dot{V}(x, t) \rightarrow 0$ as $t \rightarrow \infty$.

Example 1.13 (*Slotine & Li 1991*) *Consider a non-autonomous system*

$$\begin{aligned}\dot{e} &= -e + g \cdot w(t) \\ \dot{g} &= -e \cdot w(t).\end{aligned}$$

where $w(t)$ is the input of the system. Assume that the input $w(t)$ is bounded.

Choose the Lyapunov function of the system as

$$V(t) = e^2 + g^2.$$

Taking the derivation of the $V(t)$ obtains $\dot{V}(t) = -2e^2 \leq 0$. It means that $V(t)$ is bounded and $V(t) \leq V(0)$. Hence, e and g are bounded. But it does not say anything about the convergence e of to zero. Moreover, the invariant set theorem cannot be applied, because the dynamics is non-autonomous.

Using Barbalat's lemma:

$$\ddot{V} = -4e(-e + g \cdot w).$$

This is bounded because e and g and w are bounded. This implies $\dot{V} \rightarrow 0$ as $t \rightarrow \infty$ and hence $e \rightarrow 0$. This proves that the error converges.

1.4 Contributions and Outline of Dissertation

This dissertation considers the formation control of multiple nonholonomic mobile robots. The distributed control structure is been used to research the multiple mobile robots formation control problem. The main contributions of this dissertation are summarized as follows:

Chapter 2 investigates the leader-follower formation control problem for non-holonomic mobile robots using a bioinspired neurodynamics based approach. The contribution of this chapter is threefold. First, note from the previous literatures that, in tracking problem for a single robot, the robot tracks the desired trajectory which has been predefined. However, in the leader-follower formation system, the trajectories of the followers are usually not predefined, which are decided by its real-time leader. This chapter extends the trajectory tracking control for a single nonholonomic mobile robot to the formation control for multiple nonholonomic mobile robots based on backstepping technique, in which follower can track its real-time leader using the proposed kinematic controller. And the kinematic controller is proposed according to its leader's information, and desired relative separation and bearing with its leader. Second, due to the nonholonomic constraint of each robot and the leader-follower formation control objective, an auxiliary angular velocity control law is developed to guarantee the global asymptotic stability of the followers and to further guarantee the local asymptotic stability of the entire formation. Finally, it is well known that mobile robot will start with a very large velocity value by using the backstepping technique, and can suffer from impractical velocity jumps when tracking errors suddenly occur. Therefore, a bioinspired neurodynamics based approach according to the backstepping technique is developed to control the leader-follower formation to solve the impractical velocity jumps problem. In comparison to the previous backstepping control technique, the proposed neurodynamics based tracking controller in this

1. INTRODUCTION

chapter is simple and efficient. It is not necessary to use the torque controllers for resolving the velocity jumps.

Chapter 3 investigates the distributed formation control problem for multiple nonholonomic mobile robots using consensus-based approach. The contributions of this chapter are fourfold. Firstly, a transformation is given to convert the formation control problem for multiple nonholonomic mobile robots into a state consensus problem. Secondly, the control laws are established by using the result from graph theory and Lyapunov techniques for accomplishing our formation control objectives: a group of nonholonomic mobile robots converge to a desired geometric pattern with its centroid moving along the specified reference trajectory. In this chapter, the specified reference trajectory is represented by the state of a virtual leader whose outputs is only its position information that is available to only a subset of a group of followers. Thirdly, the distributed kinematic controller is design by the its neighbors' information. It is not necessary for each robot to know the global information. In fact, each robot can obtain information only from its neighbors. Moreover, different with the traditional leader-follower approach, the communication topology does not necessary need to be tree information sensing structures. Finally, our control laws guaranty that the nonholonomic mobile robots can at least exponentially converge to the desired geometric pattern, as well as the geometric centroid of the formation at least exponentially converges to the trajectory of virtual leader.

In the previous Chapter 3, the formation control of nonholonomic wheeled mobile robots is based on kinematic models, which requires "perfect velocity tracking". However, in many practical situations, the dynamics of robot should not be ignored and practical control strategies accounting for both the kinematic and dynamic effect should be implemented. Hence, Chapter 4 investigates the distributed adaptive formation control problem for multiple nonholonomic wheeled mobile robots. The objective is to develop distributed controllers based on the combination of both kinematic model and dynamics systems with unknown parameters, such that a group of nonholonomic wheeled mobile robots asymptotically converge to a desired geometric pattern with its centroid moving along the specified reference trajectory. To achieve this goal, a variable transformation is first given to convert the formation control problem into a state consensus problem.

1.4 Contributions and Outline of Dissertation

Distributed kinematic controllers are then developed. We assume that the specified reference trajectory can be considered as the trajectory of a virtual leader whose information is available to only a subset of the followers. Also the followers are assumed to have only local interaction. Next, it is well known in practice that the dynamics model of the wheel mobile robot has unknown dynamical parameters, which will affect the robust trajectory tracking of the system. Therefore, adaptive computed-torque controllers for mobile robots are developed. Sufficient conditions are derived for accomplishing the asymptotically stability of the systems based on algebraic graph theory, matrix theory, and Lyapunov control approach. Finally, simulation examples illustrate the effectiveness of the proposed controllers.

In the previous Chapter 4, we consider the dynamics model of the wheeled mobile robot without the friction term and bounded disturbance term. In some practical applications, the friction term and bounded disturbance term should not be ignored and practical control strategies accounting for the friction term and bounded disturbance term should be implemented. Therefore, in Chapter 5, we shall consider the formation control problem for the wheeled mobile robots, in which the dynamics model of the wheeled mobile robot has the friction term and bounded disturbance term. First, we consider that the partial knowledge of the mobile robot dynamics is available. An asymptotically stable torque controller is proposed by using robust adaptive control techniques to account for unmolded dynamics and bounded disturbances. Next, we consider that the dynamics of the mobile robot are all unknown. Note from the previous cited literatures the neural network controller can relax the knowledge of the dynamics. Thus the universal approximation property of neural network is used to relax the knowledge of the dynamics system, and an asymptotically robust adaptive controller augmented with the neural network is derived to achieve asymptotic tracking.

1. INTRODUCTION

Chapter 2

Leader-Follower Formation Control of Multiple Nonholonomic Mobile Robots Using a Bioinspired Neurodynamic based Approach

Contents

2.1	Introduction	40
2.2	Mathematical Model of a Nonholonomic Mobile Robot	41
2.3	Leader-Follower Formation Control	43
2.3.1	A Leader-Follower Formation Model	43
2.3.2	Formation Control Objective	45
2.3.3	The Error Dynamics of Leader-Follower Formation . .	46
2.4	Backstepping Control Algorithm	48
2.5	The Bioinspired Neurodynamics Applying to Backstepping Control Algorithm	49
2.5.1	The Bioinspired Neurodynamics Model	50
2.5.2	Backstepping-based Algorithm with a Bioinspired Neurodynamics Model	51
2.6	Simulations Results	53
2.6.1	Validation and Comparison of the Proposed Backstepping Controllers (2.16) and (2.25)	53

2. LEADER-FOLLOWER FORMATION CONTROL OF MULTIPLE NONHOLONOMIC MOBILE ROBOTS USING A BIOINSPIRED NEURODYNAMIC BASED APPROACH

2.6.2	Validation for Leader-Follower Formation Control Based on Bioinspired Neurodynamics	58
2.7	Conclusion	64

2.1 Introduction

Note from the discussions in Chapter 1 that, in some applications the formation control problem can be essentially viewed as a natural extension of the traditional trajectory tracking problem. To the best of my knowledge, just few researchers have considered the trajectory tracking problem when dealing with the multi-robot formation problem. In this chapter, we will extent the traditional trajectory tracking control problem for single robot to formation control problem for multiple mobile robots.

In the literature, the trajectory tracking control problem for a single mobile robot has been studied in recent years (Blažič 2011; Boukattaya *et al.* 2012; Gu & Hu 2006; Jiang & Nijmeijer 1997; Kanayama *et al.* 1990; Yang *et al.* 2012). Kanayama *et al.* (1990) proposed an classic error-based tracking model and designed a stable tracking controller for a single nonholonomic mobile robot. Jiang & Nijmeijer (1997) proposed a backstepping approach to the trajectory tracking control, and studied tracking problems locally and globally trajectory. Fierro & Lewis (1998) introduced a novel torque controller for a mobile robot, and integrated a kinematic controller and a neural network torque controller for non-holonomic mobile robot. However, this method must consider the dynamics of the mobile robot, which is complicated. Gu & Hu (2006) proposed the receding horizon tracking control on the wheeled mobile robots, which uses the optimized method to accelerate the convergence speed of errors.

Various tracking control methods for mobile robot have been mentioned in the literature, such as sliding mode, linearization, neural networks, fuzzy systems and backstepping. Among the above methods, the backstepping method is preferred. By using the backstepping technique, the tracking controllers can be simple, and the system stability can be guaranteed by Lyapunov stability theory. Moreover, some of the backstepping based controllers can deal with arbitrarily large initial errors.

2.2 Mathematical Model of a Nonholonomic Mobile Robot

In this Chapter, we further investigate the leader-follower formation control problem for nonholonomic mobile robots using a bioinspired neurodynamic based approach. The contribution of this chapter is threefold. First, note from the literatures (Blažič 2011; Boukattaya *et al.* 2012; Fierro & Lewis 1998; Gu & Hu 2006; Jiang & Nijmeijer 1997; Kanayama *et al.* 1990; Yang *et al.* 2012) that, in tracking problem for a single robot, the robot tracks the desired trajectory which has been predefined. However, in the leader-follower formation system, the trajectories of the followers are usually not predefined, which are decided by its real-time leader. Inspired by the above literatures, this chapter extends the trajectory tracking control for a single nonholonomic mobile robot to the formation control for multiple nonholonomic mobile robots based on backstepping technique, in which follower can track its real-time leader by the proposed kinematic controller. Second, due to the nonholonomic constraint of each robot and the leader-follower formation control objective, an auxiliary angular velocity control law is developed to guarantee the global asymptotic stability of the followers and to further guarantee the local asymptotic stability of the entire formation. Finally, it is well known that mobile robot will start with a very large velocity value by using the backstepping technique, and can suffer from impractical velocity jumps when tracking errors suddenly occur. Therefore, a bioinspired neurodynamics based approach according to the backstepping technique is developed to control the leader-follower formation to solve the impractical velocity jumps problem. In comparison to the previous backstepping control technique, the proposed neurodynamics based tracking controller in this chapter is simple and efficient. It is not necessary to use the torque controllers for resolving the velocity jumps.

2.2 Mathematical Model of a Nonholonomic Mobile Robot

Consider a group of n nonholonomic mobile robots. For simplicity, we assume that each robot has the same mechanical structure as shown in Fig. 2.1. The posture of the i -th ($1 \leq i \leq n$) robot (named robot R_i) in a cartesian frame OXY is specified by $p_i = [x_i, y_i, \theta_i]^T$, where (x_i, y_i) denotes the front coordinate of the robot R_i , θ_i is the heading angle.

2. LEADER-FOLLOWER FORMATION CONTROL OF MULTIPLE NONHOLONOMIC MOBILE ROBOTS USING A BIOINSPIRED NEURODYNAMIC BASED APPROACH

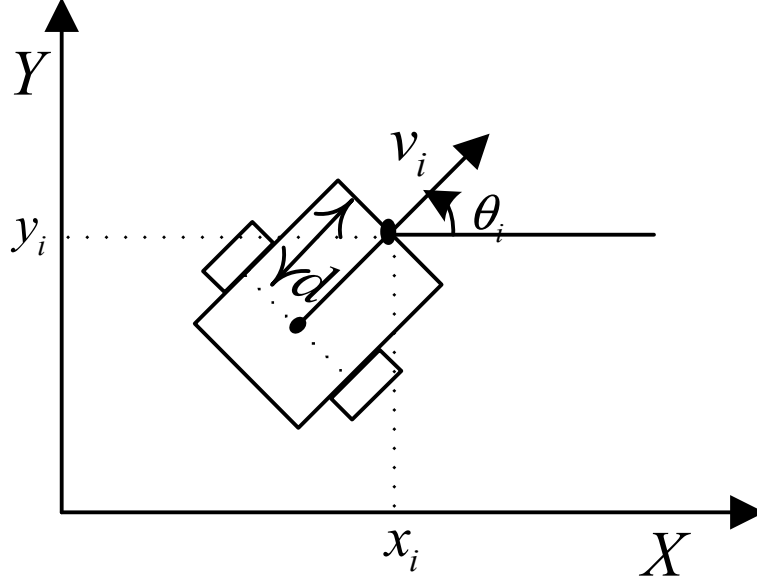


Figure 2.1: A nonholonomic mobile robot.

The mobile robot with two driven wheels shown in Fig. 2.1 is a typical example of nonholonomic mechanical systems. Under the hypothesis of pure rolling and nonslipping [Fierro & Lewis \(1998\)](#), the kinematic constraint of the nonholonomic mobile robot R_i is given as

$$\dot{y}_i \cos \theta_i - \dot{x}_i \sin \theta_i = d \dot{\theta}_i, \quad (2.1)$$

where d is the distance from the rear axle to the front of the robot.

From the kinematic constraint (2.1), the kinematics model of the nonholonomic mobile robot R_i can be written as

$$\dot{p}_i = \begin{bmatrix} \dot{x}_i \\ \dot{y}_i \\ \dot{\theta}_i \end{bmatrix} = \begin{bmatrix} \cos \theta_i & -d \sin \theta_i \\ \sin \theta_i & d \cos \theta_i \\ 0 & 1 \end{bmatrix} \begin{bmatrix} v_i \\ w_i \end{bmatrix}, \quad (2.2)$$

where v_i and w_i are the linear velocity and the angular velocity.

2.3 Leader-Follower Formation Control

2.3.1 A Leader-Follower Formation Model

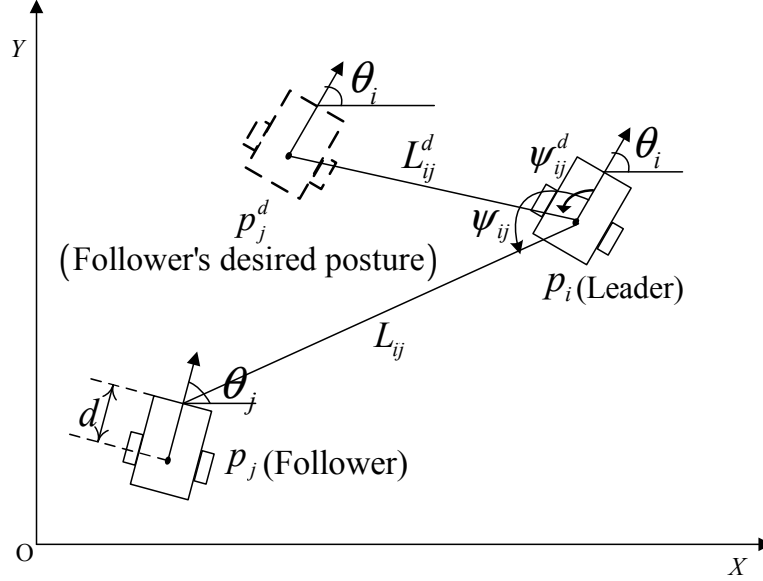


Figure 2.2: A leader-follower formation scheme.

From the formation control scheme shown in Fig. 2.2, the robot R_j follows its leader R_i with desired separation L_{ij}^d , desired bearing ψ_{ij}^d and desired orientation θ_j^d . Here $\theta_j^d = \theta_i$. Note that $p_i = [x_i, y_i, \theta_i]^T$ is the actual posture of leader robot R_i , $p_j = [x_j, y_j, \theta_j]^T$ is the actual posture of follower robot R_j , $p_j^d = [x_j^d, y_j^d, \theta_j^d]^T$ is the desired posture of follower robot R_j , L_{ij} and ψ_{ij} are the actual separation and the actual bearing between follower R_j and its leader R_i , and L_{ij}^d and ψ_{ij}^d represent the desired separation and the desired relative bearing respectively,

Through the geometrical relation between robots, it is easy to obtain that the desired posture p_j^d of the follower robot satisfies

$$\begin{aligned} p_j^d &= [x_j^d, y_j^d, \theta_j^d]^T \\ &= \begin{bmatrix} x_i - d \cos \theta_i + L_{ij}^d \cos (\psi_{ij}^d + \theta_i) \\ y_i - d \sin \theta_i + L_{ij}^d \sin (\psi_{ij}^d + \theta_i) \\ \theta_i \end{bmatrix}, \end{aligned} \quad (2.3)$$

2. LEADER-FOLLOWER FORMATION CONTROL OF MULTIPLE NONHOLONOMIC MOBILE ROBOTS USING A BIOINSPIRED NEURODYNAMIC BASED APPROACH

The actual posture p_j of the follower R_j satisfies

$$\begin{aligned} p_j &= [x_j, y_j, \theta_j]^T \\ &= \begin{bmatrix} x_i - d \cos \theta_i + L_{ij} \cos(\psi_{ij} + \theta_i) \\ y_i - d \sin \theta_i + L_{ij} \sin(\psi_{ij} + \theta_i) \\ \theta_j \end{bmatrix}. \end{aligned} \quad (2.4)$$

Project the relative distance L_{ij} along the X and Y directions by cartesian coordinates as

$$L_{ij} = \sqrt{L_{ijx}^2 + L_{ijy}^2}, \quad (2.5)$$

where $L_{ijx}(t)$ and $L_{ijy}(t)$ denote that the actual relative separations between leader and follower project along X and Y direction by cartesian coordinates respectively, and satisfy

$$\begin{aligned} L_{ijx} &= x_i - x_j - d \cos \theta_i = -L_{ij} \cos(\psi_{ij} + \theta_i), \\ L_{ijy} &= y_i - y_j - d \sin \theta_i = -L_{ij} \sin(\psi_{ij} + \theta_i). \end{aligned} \quad (2.6)$$

Taking the derivative of (2.6) along (2.2) gives

$$\begin{aligned} \dot{L}_{ijx} &= \dot{x}_i - \dot{x}_j + d\dot{\theta}_i \sin \theta_i \\ &= v_i \cos \theta_i - v_j \cos \theta_j + dw_j \sin \theta_j, \\ \dot{L}_{ijy} &= \dot{y}_i - \dot{y}_j - d\dot{\theta}_i \cos \theta_i \\ &= v_i \sin \theta_i - v_j \sin \theta_j - dw_j \cos \theta_j, \end{aligned}$$

where v_i and w_i denote the linear velocity and angular velocity of the leader R_i , v_j and w_j denote the linear velocity and angular velocity of the follower R_j .

Taking the derivative of (2.5) along (2.2) yields

$$\begin{aligned} \dot{L}_{ij} &= \frac{1}{\sqrt{L_{ijx}^2 + L_{ijy}^2}} \left(L_{ijx} \cdot \dot{L}_{ijx} + L_{ijy} \cdot \dot{L}_{ijy} \right) \\ &= \frac{1}{L_{ij}} \{ v_i (L_{ijx} \cos \theta_i + L_{ijy} \sin \theta_i) \} \\ &\quad - \frac{1}{L_{ij}} \{ v_j (L_{ijx} \cos \theta_j + L_{ijy} \sin \theta_j) \} \\ &\quad + \frac{1}{L_{ij}} \{ -dw_j (-L_{ijx} \sin \theta_j + L_{ijy} \cos \theta_j) \} \\ &= -v_i \cos \psi_{ij} + v_j \cos \gamma_{ij} + dw_j \sin \gamma_{ij}, \end{aligned} \quad (2.7)$$

where $\gamma_{ij} = \psi_{ij} + \theta_i - \theta_j$, and

$$\begin{aligned} L_{ijx} \cos \theta_i + L_{ijy} \sin \theta_i &= -L_{ij} \cos \psi_{ij}, \\ -L_{ijx} \sin \theta_i + L_{ijy} \cos \theta_i &= -L_{ij} \sin \psi_{ij}, \\ L_{ijx} \cos \theta_j + L_{ijy} \sin \theta_j &= -L_{ij} \cos \gamma_{ij}, \\ -L_{ijx} \sin \theta_j + L_{ijy} \cos \theta_j &= -L_{ij} \sin \gamma_{ij}. \end{aligned}$$

From Fig. 2.2, $\psi_{ij} = \arctan(L_{ijy}/L_{ijx}) - \theta_i + \pi$. Let's take the derivative of the relative bearing,

$$\begin{aligned} \dot{\psi}_{ij} &= \left[\arctan \left(\frac{L_{ijy}}{L_{ijx}} \right) - \theta_i + \pi \right]' \\ &= \frac{1}{L_{ij}} \{v_i \sin \psi_{ij} - v_j \sin \gamma_{ij} + dw_j \cos \gamma_{ij}\} - w_i. \end{aligned} \quad (2.8)$$

Hence, the kinematic model of the leader-follower formation is

$$\dot{L}_{ij} = -v_i \cos \psi_{ij} + v_j \cos \gamma_{ij} + dw_j \sin \gamma_{ij}, \quad (2.9)$$

$$\dot{\psi}_{ij} = \frac{1}{L_{ij}} \{v_i \sin \psi_{ij} - v_j \sin \gamma_{ij} + dw_j \cos \gamma_{ij}\} - w_i. \quad (2.10)$$

2.3.2 Formation Control Objective

Our objective is to achieve and maintain the desired leader-follower formation, i.e. maintaining the desired separation-separation and separation-bearing between the leader and follower. Therefore, the control task is to design the control inputs v_j and w_j for the follower robot R_j ($1 \leq j \leq n$) such that

$$\lim_{t \rightarrow \infty} (L_{ij}^d - L_{ij}) = 0 \quad \lim_{t \rightarrow \infty} (\psi_{ij}^d - \psi_{ij}) = 0, \quad (2.11)$$

i.e.

$$\lim_{t \rightarrow \infty} (p_j^d - p_j) = 0.$$

Before proceeding, the following assumptions are needed.

Assumption 2.1 *Assume that the separation distance L_{ij} and bearing ψ_{ij} are available. The linear velocity and angular velocity and its orientations of each robot are also available.*

2. LEADER-FOLLOWER FORMATION CONTROL OF MULTIPLE NONHOLONOMIC MOBILE ROBOTS USING A BIOINSPIRED NEURODYNAMIC BASED APPROACH

Assumption 2.2 *The angular velocity of the robot are bounded for all t , and $-w_{max} \leq w_j \leq w_{max}$, where w_{max} is a positive constant.*

Assumption 2.3 *The perfect velocity tracking holds.*

2.3.3 The Error Dynamics of Leader-Follower Formation

In the leader-follower approach, the angular and linear velocity of the leader are given, we will only need to control the follower's angular and linear velocity to keep the relative separation and relative bearing between them to make the desired formation satisfied. Therefore, the leader following based multiple mobile robots formation control can be considered as an extension of tracking problem of nonholonomic mobile robot [Li et al. \(2005\)](#).

Using the equations (2.3), (2.4) and applying simple trigonometric identities, the tracking error for leader-follower formation is obtained as

$$\begin{aligned}
 e_j &= \begin{bmatrix} x_{je} \\ y_{je} \\ \theta_{je} \end{bmatrix} \\
 &= \begin{bmatrix} \cos \theta_j & \sin \theta_j & 0 \\ -\sin \theta_j & \cos \theta_j & 0 \\ 0 & 0 & 1 \end{bmatrix} \begin{bmatrix} x_j^d - x_j \\ y_j^d - y_j \\ \theta_j^d - \theta_j \end{bmatrix} \\
 &= \begin{bmatrix} L_{ij}^d \cos(\psi_{ij}^d + \theta_{ij}) - L_{ij} \cos(\psi_{ij} + \theta_{ij}) \\ L_{ij}^d \sin(\psi_{ij}^d + \theta_{ij}) - L_{ij} \sin(\psi_{ij} + \theta_{ij}) \\ \theta_j^d - \theta_j \end{bmatrix}, \tag{2.12}
 \end{aligned}$$

where $\theta_{ij} = \theta_i - \theta_j$.

Assume that the desired separation L_{ij}^d and the desired bearing ψ_{ij}^d are constants. It then follows that $\dot{L}_{ij}^d = 0, \dot{\psi}_{ij}^d = 0$. Taking the time derivative of (2.12)

2.3 Leader-Follower Formation Control

along (2.3) and (2.4) have

$$\begin{aligned}
\dot{x}_{je} &= -L_{ij}^d \sin(\psi_{ij}^d + \theta_{ij}) \dot{\theta}_{ij} - \dot{L}_{ij} \cos(\psi_{ij} + \theta_{ij}) + L_{ij} \sin(\psi_{ij} + \theta_{ij}) (\dot{\psi}_{ij} + \dot{\theta}_{ij}) \\
&= -L_{ij}^d \sin(\psi_{ij}^d + \theta_{ij}) (w_i - w_j) - \dot{L}_{ij} \cos(\psi_{ij} + \theta_{ij}) \\
&\quad + L_{ij} \sin(\psi_{ij} + \theta_{ij}) (\dot{\psi}_{ij} + w_i - w_j) \\
&= -L_{ij}^d \sin(\psi_{ij}^d + \theta_{ij}) (w_i - w_j) - \cos(\psi_{ij} + \theta_{ij}) \{-v_i \cos \psi_{ij} + v_j \cos \gamma_{ij} + dw_j \sin \gamma_{ij}\} \\
&\quad + L_{ij} \sin(\psi_{ij} + \theta_{ij}) \cdot \left\{ \frac{1}{L_{ij}} (v_i \sin \psi_{ij} - v_j \sin \gamma_{ij} + dw_j \cos \gamma_{ij}) - w_i \right\} \\
&= -L_{ij}^d w_i \sin(\psi_{ij}^d + \theta_{ij}) + L_{ij}^d w_j \sin(\psi_{ij}^d + \theta_{ij}) + v_i \cos \gamma_{ij} \cos \psi_{ij} - v_j \cos^2 \gamma_{ij} \\
&\quad - dw_j \cos \gamma_{ij} \sin \gamma_{ij} + v_i \sin \gamma_{ij} \sin \psi_{ij} - v_j \sin^2 \gamma_{ij} \\
&\quad - L_{ij} w_i \sin \gamma_{ij} + dw_j \cos \gamma_{ij} \sin \gamma_{ij} + L_{ij} \sin \gamma_{ij} (w_i - w_j) \\
&= -v_j - L_{ij}^d w_i \sin(\psi_{ij}^d + \theta_{ij}) + v_i \cos \gamma_{ij} \cos \psi_{ij} + v_i \sin \gamma_{ij} \sin \psi_{ij} \\
&\quad + L_{ij}^d w_j \sin(\psi_{ij}^d + \theta_{ij}) - L_{ij} w_j \sin \gamma_{ij} \\
&= v_i \cos \theta_{ij} + w_j y_{je} - v_j - L_{ij}^d w_i \sin(\psi_{ij}^d + \theta_{ij}),
\end{aligned}$$

and

$$\begin{aligned}
\dot{y}_{je} &= L_{ij}^d \cos(\psi_{ij}^d + \theta_{ij}) \dot{\theta}_{ij} - \dot{L}_{ij} \sin \gamma_{ij} - L_{ij} \cos \gamma_{ij} (\dot{\psi}_{ij} + w_i - w_j) \\
&= L_{ij}^d \cos(\psi_{ij}^d + \theta_{ij}) (w_i - w_j) - \sin \gamma_{ij} \{-v_i \cos \psi_{ij} + v_j \cos \gamma_{ij} + dw_j \sin \gamma_{ij}\} \\
&\quad - L_{ij} \cos \gamma_{ij} \cdot \left\{ \frac{1}{L_{ij}} (v_i \sin \psi_{ij} - v_j \sin \gamma_{ij} + dw_j \cos \gamma_{ij}) - w_i \right\} \\
&\quad + L_{ij} \cos \gamma_{ij} (w_i - w_j) \\
&= L_{ij}^d w_i \cos(\psi_{ij}^d + \theta_{ij}) - L_{ij}^d w_j \sin(\psi_{ij}^d + \theta_{ij}) + v_i \sin \gamma_{ij} \cos \psi_{ij} - v_j \sin \gamma_{ij} \cos \gamma_{ij} \\
&\quad - dw_j \sin^2 \gamma_{ij} - v_i \cos \gamma_{ij} \sin \psi_{ij} + v_j \cos \gamma_{ij} \sin \gamma_{ij} \\
&\quad - dw_j \cos^2 \gamma_{ij} + L_{ij} w_i \cos \gamma_{ij} - L_{ij} \cos \gamma_{ij} w_i + L_{ij} \cos \gamma_{ij} w_j \\
&= L_{ij}^d w_i \cos(\psi_{ij}^d + \theta_{ij}) + v_i \sin \gamma_{ij} \cos \psi_{ij} - v_i \cos \gamma_{ij} \sin \psi_{ij} - dw_j \\
&\quad - L_{ij}^d w_j \sin(\psi_{ij}^d + \theta_{ij}) + L_{ij} w_j \cos \gamma_{ij} \\
&= v_i \sin \theta_{ij} - w_j x_{je} - dw_j + L_{ij}^d w_i \cos(\psi_{ij}^d + \theta_{ij}).
\end{aligned}$$

Thus, one can obtain the error dynamics of mobile robot can be described as

$$\begin{aligned}
\dot{x}_{je} &= v_i \cos \theta_{ij} + w_j y_{je} - v_j - L_{ij}^d w_i \sin(\psi_{ij}^d + \theta_{ij}), \\
\dot{y}_{je} &= v_i \sin \theta_{ij} - w_j x_{je} - dw_j + L_{ij}^d w_i \cos(\psi_{ij}^d + \theta_{ij}), \\
\dot{\theta}_{je} &= w_j^d - w_j.
\end{aligned} \tag{2.13}$$

2. LEADER-FOLLOWER FORMATION CONTROL OF MULTIPLE NONHOLONOMIC MOBILE ROBOTS USING A BIOINSPIRED NEURODYNAMIC BASED APPROACH

2.4 Backstepping Control Algorithm

Due to the characteristics of the error dynamic system (2.13), the input-output feedback control cannot be used to tackle this model (2.13). Also due to the nonholonomic constraint of each robot and the leader-follower formation control objective, the orientations of each follower will not be equal while the formation is turning, and thus, the reference orientation cannot be chosen as $\theta_j^d = \theta_i$. Here, we choose the derivative of the reference orientation as follows

$$\dot{\theta}_j^d = (v_i \sin \theta_{ij} + L_{ij}^d w_i \cos (\psi_{ij}^d + \theta_{ij}) + 2k_2 y_{je}) / d. \quad (2.14)$$

By choosing (2.14), the asymptotic stability of all error states can be found. Hence, the error dynamic system becomes

$$\begin{aligned} \dot{x}_{je} &= w_j y_{je} - v_j + v_i \cos \theta_{ij} - L_{ij}^d w_i \sin (\psi_{ij}^d + \theta_{ij}), \\ \dot{y}_{je} &= -w_j x_{je} - d w_j + v_i \sin \theta_{ij} + L_{ij}^d w_i \cos (\psi_{ij}^d + \theta_{ij}), \\ \dot{\theta}_{je} &= (v_i \sin \theta_{ij} + L_{ij}^d w_i \cos (\psi_{ij}^d + \theta_{ij}) + 2k_2 y_{je}) / d - w_j. \end{aligned} \quad (2.15)$$

Consider the following backstepping control inputs (2.16),

$$\begin{aligned} v_j &= k_1 x_{je} + v_i \cos \theta_{ij} - L_{ij}^d w_i \sin (\psi_{ij}^d + \theta_{ij}), \\ w_j &= (v_i \sin \theta_{ij} + L_{ij}^d w_i \cos (\psi_{ij}^d + \theta_{ij}) + k_2 y_{je} + k_3 \theta_{je}) / d, \end{aligned} \quad (2.16)$$

where $k_1 > 0$, $k_2 > 0$, $k_3 > 0$. Hence, the closed-loop kinematics error dynamic becomes

$$\begin{aligned} \dot{x}_{je} &= w_j y_{je} - k_1 x_{je}, \\ \dot{y}_{je} &= -w_j x_{je} - k_2 y_{je} - k_3 \theta_{je}, \\ \dot{\theta}_{je} &= (-k_3 \theta_{je} + k_2 y_{je}) / d. \end{aligned} \quad (2.17)$$

To prove that the trajectory tracking control system (2.17) under the controller laws (2.16) is asymptotically stable and the tracking errors converge to zeros, we choose the following Lyapunov function candidate as

$$V(t) = \frac{1}{2} (x_{je}^2 + y_{je}^2) + \frac{dk_3 \theta_{je}^2}{2k_2}. \quad (2.18)$$

It's obvious that $V(t) \geq 0$, and $V(t) = 0$ if and only if $x_{je} = 0$, $y_{je} = 0$, $\theta_{je} = 0$.

2.5 The Bioinspired Neurodynamics Applying to Backstepping Control Algorithm

The derivative of the Lyapunov function (2.18) is given by

$$\dot{V}(t) = x_{je}\dot{x}_{je} + y_{je}\dot{y}_{je} + \frac{dk_3\theta_{je}\dot{\theta}_{je}}{k_2}. \quad (2.19)$$

Substituting (2.17) into (2.19), we have

$$\begin{aligned} \dot{V}(t) &= -k_1x_{je}^2 - k_2y_{je}^2 - k_3\theta_{je}y_{je} - k_3^2\theta_{je}^2/k_2 + k_3\theta_{je}y_{je} \\ &= -k_1x_{je}^2 - k_2y_{je}^2 - k_3\theta_{je}^2 \leq 0. \end{aligned}$$

Since $\dot{V}(t) \leq 0$ and $V(t) \geq 0$, the tracking controller (2.16) for the follower R_j is stable. It then infers that x_{je} , y_{je} and θ_{je} are bounded. Therefore, we have $\|\ddot{V}(t)\| < \infty$. Thus it then follows that $V(t)$ is uniformly continuous. From $\dot{V}(t) \leq 0$ and $V(t) \geq 0$, it also follows that $V(t)$ does not increase, i.e., $V(t) \leq V(0)$. By Barbalat's Lemma, $\dot{V} \rightarrow 0$ as $t \rightarrow \infty$, from which it can be deduced that $x_{je} \rightarrow 0$, $y_{je} \rightarrow 0$ and $\theta_{je} \rightarrow 0$ as $t \rightarrow \infty$. Therefore, the tracking controller (2.16) can guarantee the closed-loop dynamics system (2.17) to be globally asymptotically stable. Hence, the closed-loop error dynamic system is asymptotically stable, and the tracking errors converge to zero.

2.5 The Bioinspired Neurodynamics Applying to Backstepping Control Algorithm

It is well known that various tracking control methods have been used for mobile robot tracking control, such as sliding mode, linearization, neural networks, fuzzy systems and backstepping. Among the above methods, the backstepping method is preferred. By using the backstepping technique, the tracking controllers can be stable and simple. Moreover, some of the backstepping based controllers can deal with arbitrarily large initial errors. However, the disadvantage is quite obvious (Fierro & Lewis (1998); Yang *et al.* (2012)): The velocity control law is directly related to the state errors, so large velocities can be generated in large initial error conditions, and it will suffer from impractical velocity jumps when the tracking errors suddenly change. This implies that the initial linear acceleration and angular acceleration are very large, that is to say, the force and torque of follower are very large, which does not hold in practice. To resolve the impractical

2. LEADER-FOLLOWER FORMATION CONTROL OF MULTIPLE NONHOLONOMIC MOBILE ROBOTS USING A BIOINSPIRED NEURODYNAMIC BASED APPROACH

velocity jump problem, a novel tracking controller will be proposed in this section by incorporating the bioinspired neurodynamics into the backstepping technique.

2.5.1 The Bioinspired Neurodynamics Model

A typical biological neural model is the shunting model [Ogmen & Gagné \(1990\)](#), which is derived from Hodgkin and Huxley's membrane model [Hodgkin & Huxley \(1952\)](#), and can be used to solve the problem of sudden speed jumps. The Shunting Neural Dynamic Model is described as

$$\frac{dx_j}{dt} = -A_j x_j + (B_j - x_j) S_j^+(t) - (D_j + x_j) S_j^-(t), \quad (2.20)$$

where x_j is the neural activity of the j -th neuron in the neural network, the parameters A_j, B_j , and D_j are nonnegative constants representing the passive decay rate, the upper and lower bounds of the neural activity respectively, and the variables S_j^+ and S_j^- are the excitatory and inhibitory inputs to the neuron.

By analyzing the backstepping technology based tracking controller proposed in [Dierks & Jagannathan 2007](#); [Fierro & Lewis 1998](#); [Tsai *et al.* 2004](#); [Zhang *et al.* 1999](#), it is well known that the velocity-jumps are caused by the suddenly changes in tracking error, particular x_{je} and y_{je} . Inspired by the smooth neural dynamics of the shunting neural model, a biological tracking controller is proposed to solve the velocity-jumps problem.

Substituting $A_j = A$, $B_j = B$, $D_j = D$, $x_j = \alpha_j$, $S_j^+(t) = f_{1j}(x_{je})$, $S_j^-(t) = g_{1j}(x_{je})$ into (2.20), a velocity dynamic equation with the error in longitudinal direction is obtained as

$$d\alpha_j/dt = -A\alpha_j + (B - \alpha_j) f_{1j}(x_{je}) - (D + \alpha_j) g_{1j}(x_{je}). \quad (2.21)$$

Similarly, substituting $x_j = \beta_j$, $S_j^+(t) = f_{2j}(y_{je})$, $S_j^-(t) = g_{2j}(y_{je})$ into (2.20), a velocity dynamic equation with the error in traverse direction is obtained as

$$d\beta_j/dt = -A\beta_j + (B - \beta_j) f_{2j}(y_{je}) - (D + \beta_j) g_{2j}(y_{je}), \quad (2.22)$$

2.5 The Bioinspired Neurodynamics Applying to Backstepping Control Algorithm

where the functions f_{1j} , g_{1j} , f_{2j} and g_{2j} are defined as

$$f_{1j}(x_{je}) = \max\{k_1 x_{je}, 0\}, \quad g_{1j}(x_{je}) = \max\{-k_1 x_{je}, 0\}, \quad (2.23)$$

$$f_{2j}(y_{je}) = \max\{k_2 y_{je}, 0\}, \quad g_{2j}(y_{je}) = \max\{-k_2 y_{je}, 0\}. \quad (2.24)$$

where k_1 and k_2 are positive constants.

2.5.2 Backstepping-based Algorithm with a Bioinspired Neurodynamics Model

Using α_j and β_j to replace the tracking error x_{je} and y_{je} in the backstepping model (2.16), the tracking controller for the follower R_j can be obtained as follows

$$\begin{aligned} v_j &= k_1 \alpha_j + v_i \cos \theta_{ij} - L_{ij}^d w_i \sin(\psi_{ij}^d + \theta_{ij}), \\ w_j &= (v_i \sin \theta_{ij} + L_{ij}^d w_i \cos(\psi_{ij}^d + \theta_{ij}) + k_2 \beta_j + k_3 \theta_{je}) / d. \end{aligned} \quad (2.25)$$

The differentiation of the reference orientation of the follower R_j relative to its leader is redefined as

$$\dot{\theta}_j^d = (v_i \sin \theta_{ij} + L_{ij}^d w_i \cos(\psi_{ij}^d + \theta_{ij}) + k_2 y_{je} + k_3 \theta_{je}) / d. \quad (2.26)$$

From (2.21) and (2.22), α_j and β_j are the function of the tracking errors x_{je} and y_{je} respectively, and the output of the shunting model is chosen as the input of tracking controller, i.e., the outputs α_j and β_j of the shunting model change as the inputs x_{je} and y_{je} change. Due to the dynamics behavior of the shunting model, the new proposed tracking controller (2.25) become a smooth function of the position errors, and the outputs of the shunting model will change smoothly without any jumps even when sudden sharp change in the inputs occur.

Substituting the (2.25) into (2.13), the closed-loop error dynamic can be rewritten as

$$\begin{aligned} \dot{x}_{je} &= w_j y_{je} - k_1 \alpha_j, \\ \dot{y}_{je} &= -w_j x_{je} - k_2 \beta_j - k_3 \theta_{je}, \\ \dot{\theta}_{je} &= (-k_3 \theta_{je} + k_2 y_{je}) / d. \end{aligned} \quad (2.27)$$

A Lyapunov function candidate is chosen as

$$V(t) = \frac{1}{2} \left(x_{je}^2 + y_{je}^2 + \frac{dk_3}{k_2} \theta_{je}^2 \right) + \frac{1}{2B} (\alpha_j^2 + \beta_j^2). \quad (2.28)$$

2. LEADER-FOLLOWER FORMATION CONTROL OF MULTIPLE NONHOLONOMIC MOBILE ROBOTS USING A BIOINSPIRED NEURODYNAMIC BASED APPROACH

It's obvious that $V(t) \geq 0$ and $V(t) = 0$ if and only if $\alpha_j = 0, \beta_j = 0, e_j = 0$.

Taking the derivative of the Lyapunov function (2.28) along (2.27) gives

$$\begin{aligned}
 \dot{V}(t) &= x_{je}\dot{x}_{je} + y_{je}\dot{y}_{je} + \frac{dk_3}{k_2}\dot{\theta}_{je}\theta_{je} + \frac{1}{B}(\alpha_j\dot{\alpha}_j + \beta_j\dot{\beta}_j) \\
 &= -k_1x_{je}\alpha_j - k_2y_{je}\beta_j - \frac{k_3^2}{k_2}\theta_{je}^2 \\
 &\quad + \frac{1}{B}\{-A\alpha_j^2 - f_{1j}(x_{je})\alpha_j^2 - g_{1j}(x_{je})\alpha_j^2 + Bf_{1j}(x_{je})\alpha_j - Dg_{1j}(x_{je})\alpha_j\} \\
 &\quad + \frac{1}{B}\{-A\beta_j^2 - f_{2j}(y_{je})\beta_j^2 - g_{2j}(y_{je})\beta_j^2 + Bf_{2j}(y_{je})\beta_j - Dg_{2j}(y_{je})\beta_j\} \\
 &= -\frac{k_3^2}{k_2}\theta_{je}^2 + \frac{1}{B}\{-A - f_{1j}(x_{je}) - g_{1j}(x_{je})\}\alpha_j^2 \\
 &\quad + \frac{1}{B}\{Bf_{1j}(x_{je}) - Dg_{1j}(x_{je}) - Bk_1x_{je}\}\alpha_j \\
 &\quad + \frac{1}{B}\{-A - f_{2j}(y_{je}) - g_{2j}(y_{je})\}\beta_j^2 \\
 &\quad + \frac{1}{B}\{Bf_{2j}(y_{je}) - Dg_{2j}(y_{je}) - Bk_2y_{je}\}\beta_j.
 \end{aligned}$$

Choosing the constant $B = D$ in the shunting equations (2.21) and (2.22), we have

$$\begin{aligned}
 \dot{V}(t) &= -\frac{k_3^2}{k_2}\theta_{je}^2 + \frac{1}{B}\{-A - f_{1j}(x_{je}) - g_{1j}(x_{je})\}\alpha_j^2 \\
 &\quad + \{f_{1j}(x_{je}) - g_{1j}(x_{je}) - k_1x_{je}\}\alpha_j \\
 &\quad + \frac{1}{B}\{-A - f_{2j}(y_{je}) - g_{2j}(y_{je})\}\beta_j^2 + \{f_{2j}(y_{je}) - g_{2j}(y_{je}) - k_2y_{je}\}\beta_j.
 \end{aligned}$$

Based on the definitions of $f_{1j}(x_{je})$ and $g_{1j}(x_{je})$ in (2.23), whatever $x_{je} \geq 0$ or $x_{je} < 0$, we have

$$f_{1j}(x_{je}) - g_{1j}(x_{je}) - k_1x_{je} = 0. \quad (2.29)$$

Similarly, it is easy to obtain that

$$f_{2j}(y_{je}) - g_{2j}(y_{je}) - k_2y_{je} = 0. \quad (2.30)$$

From the definitions of the functions of $f_{1j}(x_{je})$ and $g_{1j}(x_{je})$ in (2.23), $f_{1j}(x_{je}) \geq 0$ and $g_{1j}(x_{je}) \geq 0$. Also since A and B are nonnegative constants, it follows that

$$\{-A - f_{1j}(x_{je}) - g_{1j}(x_{je})\}/B \leq 0 \quad (2.31)$$

Similarly, we have $f_{2j}(x_{je}) \geq 0$ and $g_{2j}(x_{je}) \geq 0$, and

$$\{-A - f_{2j}(y_{je}) - g_{2j}(y_{je})\}/B \leq 0. \quad (2.32)$$

Hence, the Lyapunov function becomes

$$\begin{aligned} \dot{V}(t) = & -\frac{k_3^2}{k_2}\theta_{je}^2 + \frac{1}{B}\{-A - f_{1j}(x_{je}) - g_{1j}(x_{je})\}\alpha_j^2 \\ & + \frac{1}{B}\{-A - f_{2j}(y_{je}) - g_{2j}(y_{je})\}\beta_j^2 \leq 0. \end{aligned}$$

Since $\dot{V}(t) \leq 0$ and $V(t) \geq 0$, the biological tracking controller (2.25) for the follower R_j is stable. It then infers that $\|e_j\|$, $\|\alpha_j\|$, and $\|\beta_j\|$ are bounded. Therefore, we have $\|\ddot{V}(t)\| < \infty$. Thus, $V(t)$ is uniformly continuous. From $\dot{V}(t) \leq 0$ and $V(t) \geq 0$, it follows that $V(t)$ does not increase, i.e., $V(t) \leq V(0)$. By Barbalat's Lemma, $\dot{V} \rightarrow 0$ as $t \rightarrow \infty$, from which it can be deduced that $\alpha_j \rightarrow 0$, $\beta_j \rightarrow 0$ and $\theta_{je} \rightarrow 0$ as $t \rightarrow \infty$. By using (2.21), (2.22) and the input-output property of the shunting model, it infers that if the output converges to certain constant values (zero), the input is supposed to go to a constant value (zero), that is to say, $x_{je} \rightarrow 0$ and $y_{je} \rightarrow 0$ while $\alpha_j \rightarrow 0$ and $\beta_j \rightarrow 0$. Therefore, the tracking controller (2.25) can guarantee the closed-loop dynamics system (2.27) to be globally asymptotically stable.

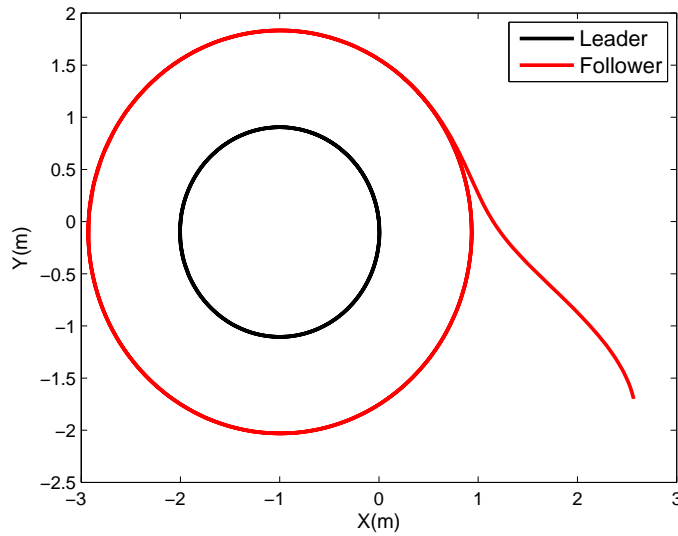
2.6 Simulations Results

2.6.1 Validation and Comparison of the Proposed Backstepping Controllers (2.16) and (2.25)

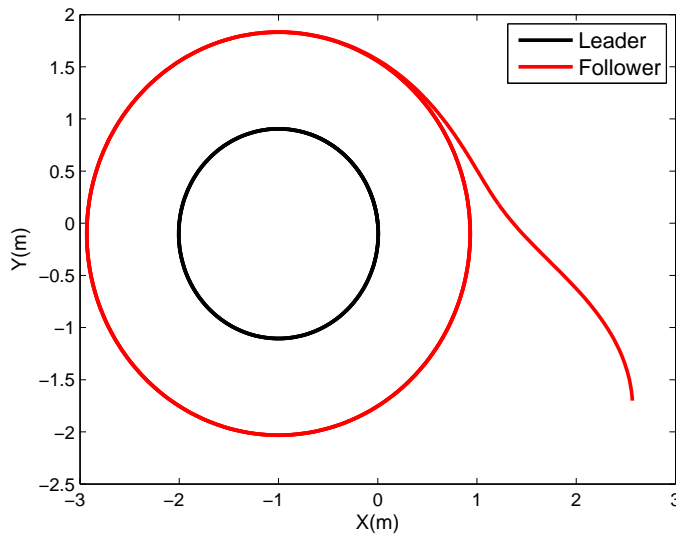
In this simulation, the effectiveness of the proposed tracking controllers (2.16) and (2.25) will be verified, a comparison of this two tracking controllers will also be given. Consider one leader and one follower. Assume that the distance d from the rear axle to the front of robot is 0.1, the linear velocity and the angular velocity of the leader robot are 1 and 1 respectively, and the initial posture of the leader robot is at $(0, 0, \pi/2)$. In order to keep the leader-follower formation, the follower must keep the desired separation $l_0 = 1$ and the desired bearing $\psi_{ij}^d = 4\pi/3$ with its leader. By calculation, it is easy to obtain that the desired posture of

2. LEADER-FOLLOWER FORMATION CONTROL OF MULTIPLE NONHOLONOMIC MOBILE ROBOTS USING A BIOINSPIRED NEURODYNAMIC BASED APPROACH

the follower is at $(0.866, -0.6, \pi/2)$. Assume that the initial actual posture of the follower is at $(2.566, -1.7, \pi/2)$. Then, the initial error is $(1.1, 1.7, 0)$. The control gains for the robot are selected as $k_1 = 10$, $k_2 = 2$, $k_3 = 1$, $A = 50$, and $B = D = 5$.



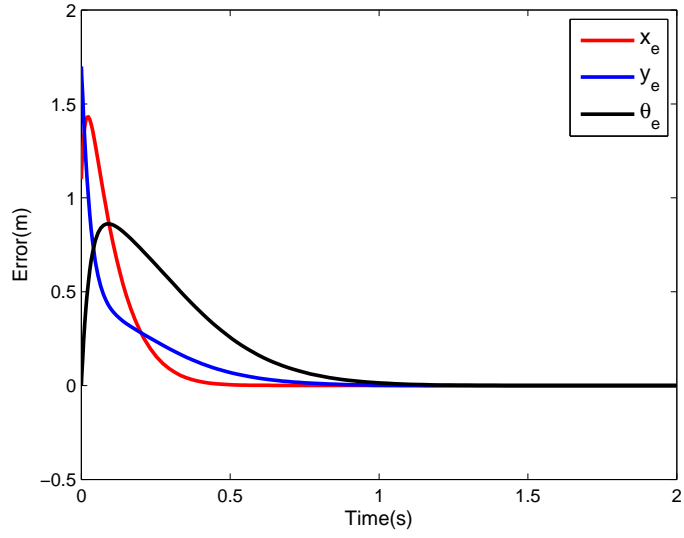
(a)



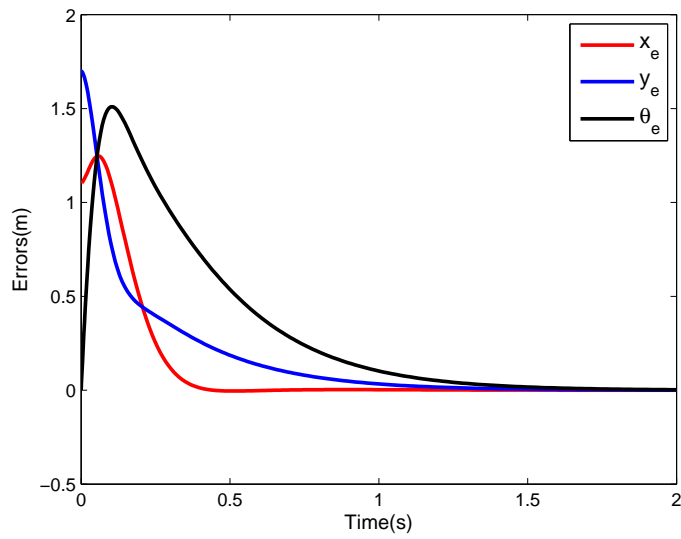
(b)

Figure 2.3: The real-time trajectories of robots: (a) by using the controller(2.16); (b) by using the controller (2.25).

2.6 Simulations Results



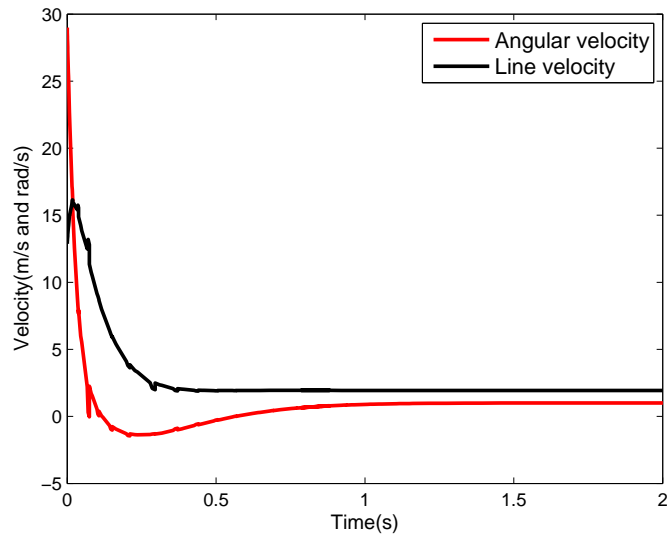
(a)



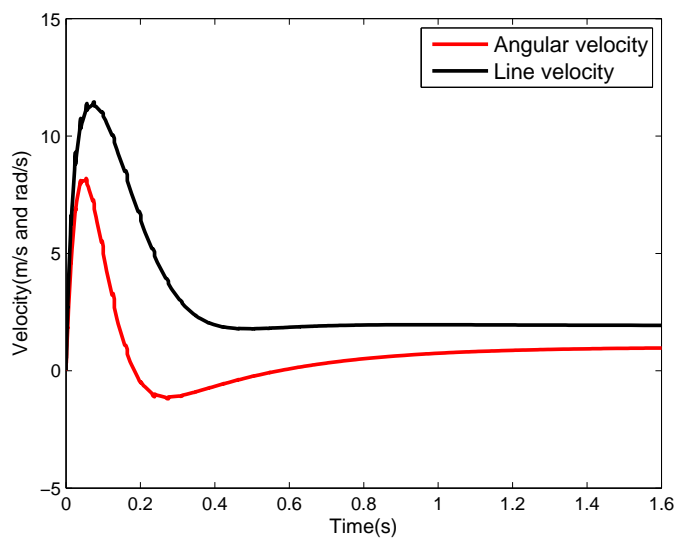
(b)

Figure 2.4: The tracking errors of the follower: (a) by using the controller(2.16); (b) by using the controller (2.25).

2. LEADER-FOLLOWER FORMATION CONTROL OF MULTIPLE NONHOLONOMIC MOBILE ROBOTS USING A BIOINSPIRED NEURODYNAMIC BASED APPROACH



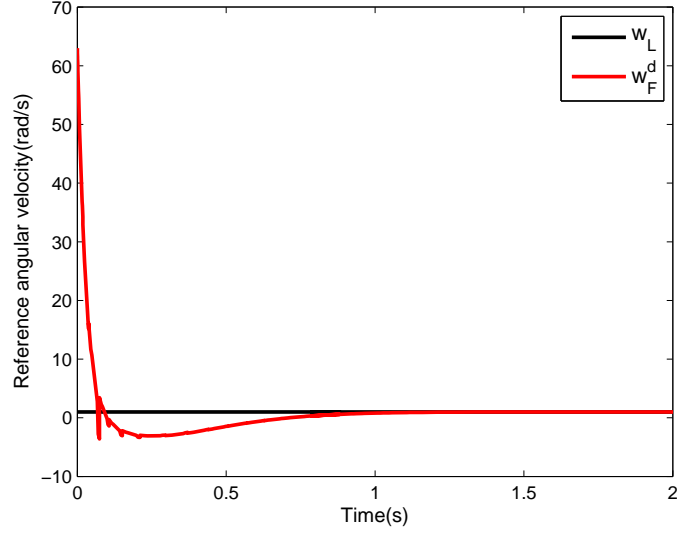
(a)



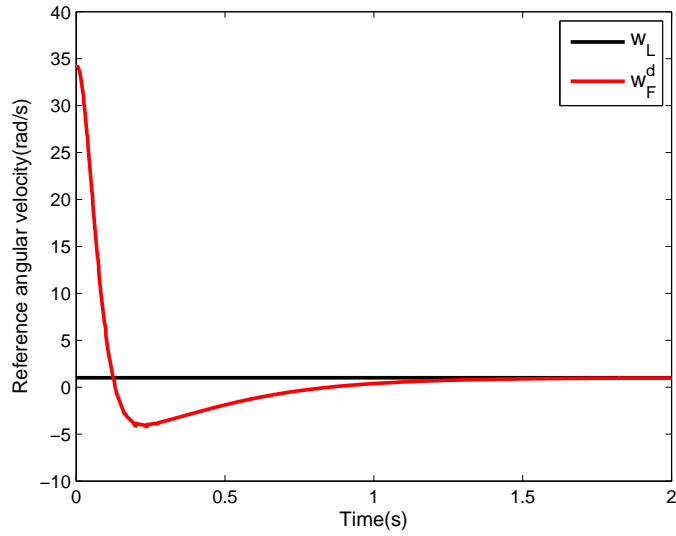
(b)

Figure 2.5: The linear velocities and angular velocities of follower: (a) by using the controller(2.16); (b) by using the controller (2.25).

2.6 Simulations Results



(a)



(b)

Figure 2.6: The reference angular velocities of follower and the angular velocities of the leader: (a) by using the controller(2.16); (b) by using the controller (2.25).

Figs. 2.3(a) and 2.3(b) are the real-time trajectories of robots by using the controllers (2.16) and (2.25) respectively. Fig. 2.3 shows that the follower can well track the leader, and maintain the desired separation and the desired bearing with the leader. Figs. 2.4(a) and 2.4(b) are the tracking errors of follower by using

2. LEADER-FOLLOWER FORMATION CONTROL OF MULTIPLE NONHOLONOMIC MOBILE ROBOTS USING A BIOINSPIRED NEURODYNAMIC BASED APPROACH

the controllers (2.16) and (2.25) respectively. Fig. 2.4 shows that the tracking errors of follower converge to zero over time. Figs. 2.5(a) and 2.5(b) are the angular velocity and linear velocity of follower by using the controllers (2.16) and (2.25) respectively. From Fig. 2.5(a), the follower starts with a large linear velocity and a large angular velocity, and change suddenly. This implies that the initial linear acceleration and angular acceleration are very large, that is to say, the force and torque of follower are very large, which is impractical. From Fig. 2.5(b), the velocity commands are smooth and reasonable by using the bioinspired neurodynamics technique, and change gradually from zero at initial time $t = 0$. Fig. 2.6(a) is the reference angular velocity w_j^d of follower and the angle velocity of the leader by using the controllers (2.16), and Fig. 2.6(b) is the reference angular velocity w_j^d of follower and the angular velocity of the leader by using the controller (2.25). It shows from Fig. 2.6 that the defined reference angular velocities for follower can converge to the angular velocity of leader over time.

2.6.2 Validation for Leader-Follower Formation Control Based on Bioinspired Neurodynamics

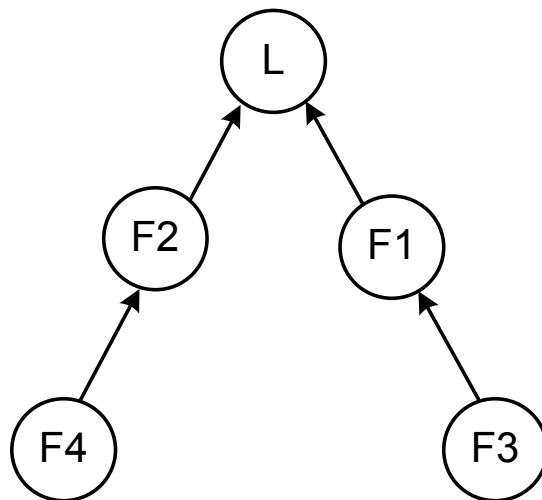


Figure 2.7: Leader-follower formation with five mobile robots.

2.6 Simulations Results

In the Fig.2.7, $F1$ and $F2$ follow the leader L , $F4$ follows $F2$, $F3$ follows $F1$, that is to say, $F2$ is the leader of $F4$, $F1$ is the leader of $F3$. Suppose that the robot axle $d = 0.1$. The control gains for the robots $F1$, $F2$, $F3$ and $F4$ are selected as $k_1 = 8$, $k_2 = 1$, $k_3 = 0.25$, $A = 10$, and $B = D = 1$. Suppose that the trajectory of the leader L is

$$\begin{aligned} x &= t^3/1000 \\ y &= t. \end{aligned} \tag{2.33}$$

and the initial posture of the leader is at $(0, 0, \pi/2)$. The follower $F1$ keeps the desired separation $l_{i1}^d = 2$ and the desired bearing $\psi_{i1}^d = 4\pi/3$ with the leader L . Hence, the initial desired posture of $F1$ is at $(1.7321, -1.1, \pi/2)$. Suppose that the actual posture of $F1$ is at $(2, 1, \pi/4)$. It then follows that the initial error of $F1$ is $(-1.6744, -1.2955, \pi/4)$. The follower $F2$ keeps the desired separation $l_{i2}^d = 2$ and bearing $\psi_{i2}^d = 2\pi/3$ with the leader L . Then, the initial desired posture of $F2$ is at $(-1.7321, -1.1, \pi/2)$. Suppose that the initial actual posture of the $F2$ is $(-1.5, -3, 0)$. Hence, the initial error of $F2$ is $(1.5294, 1.1510, \pi/2)$. The follower $F3$ keeps the desired separation $l_{i3}^d = 2$ and bearing $\psi_{i3}^d = 4\pi/3$ with its leader $F1$. Then, the initial desired posture of $F3$ is at $(2.4469, -1.0026, \pi/4)$. The initial actual posture of $F3$ is $(3, 1.5, 0)$. The initial error of $F3$ is $(-0.5531, -2.5026, \pi/4)$. The follower $F4$ keeps the desired separation $l_{i3}^d = 2$ and bearing $\psi_{i3}^d = 2\pi/3$ with its leader $F2$. Then, the initial desired posture of $F4$ is at $(-3.5500, -3.0866, \pi/3)$. The initial actual posture of $F4$ is at $(-2, -3.5, \pi/6)$. The initial error of $F4$ is $(-1.1356, 1.133, \pi/6)$.

2. LEADER-FOLLOWER FORMATION CONTROL OF MULTIPLE NONHOLONOMIC MOBILE ROBOTS USING A BIOINSPIRED NEURODYNAMIC BASED APPROACH

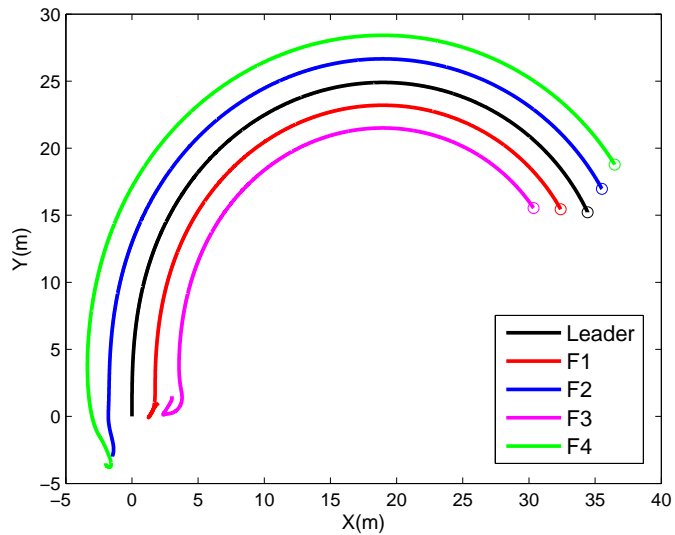


Figure 2.8: The trajectory of Leader-Follower formation.

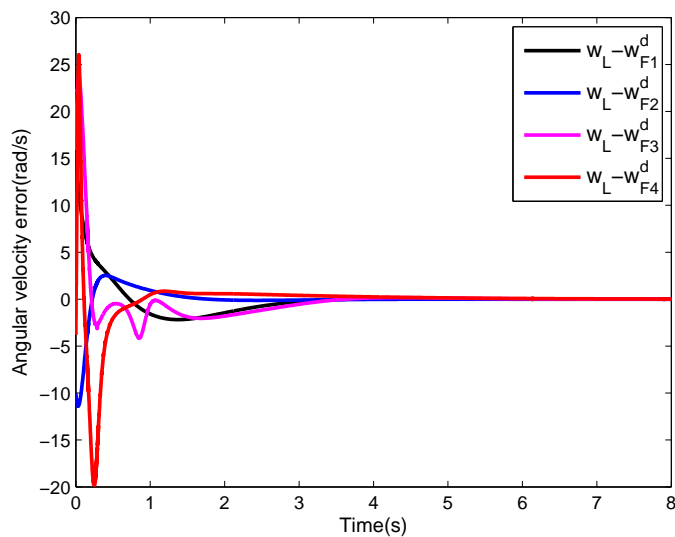
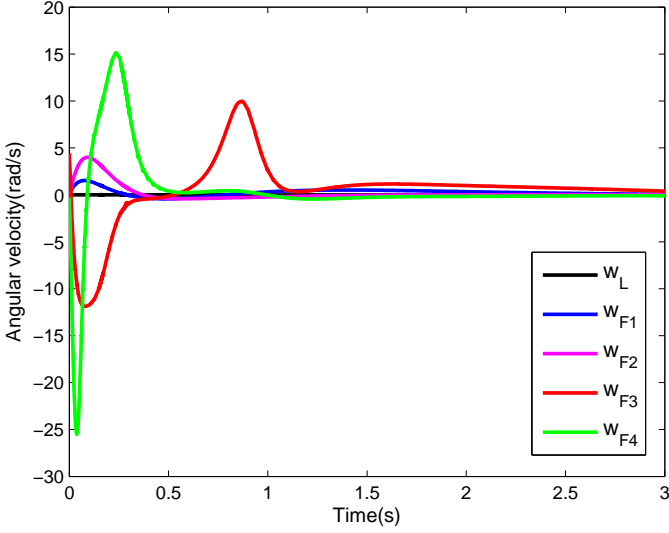
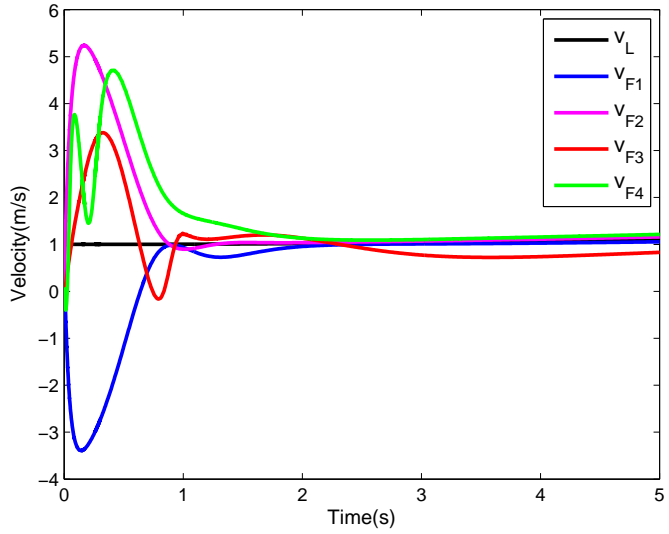


Figure 2.9: The errors between the angular velocity of leader L and the reference angular velocity w_j^d of each follower F_j .

2.6 Simulations Results



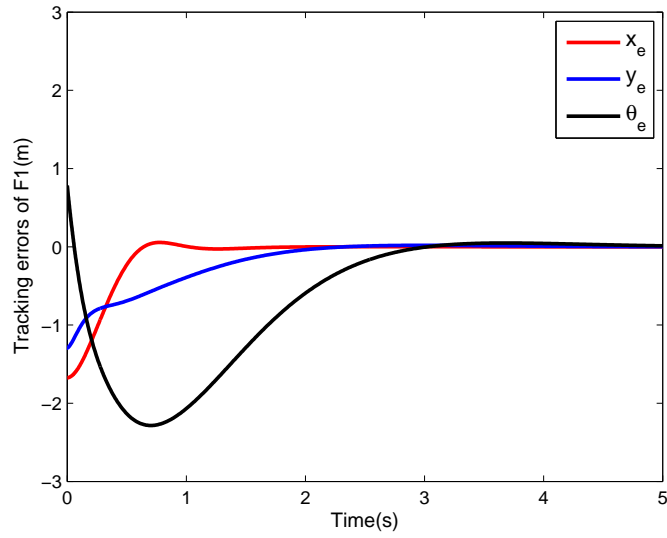
(a)



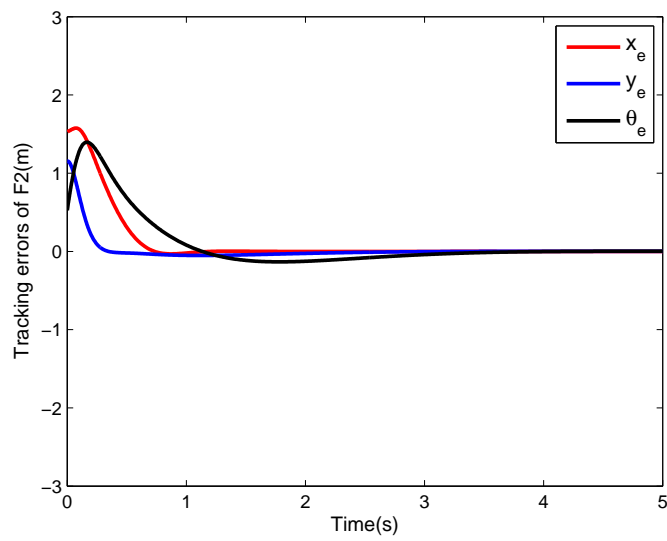
(b)

Figure 2.10: The angular velocities and linear velocities of robots.

2. LEADER-FOLLOWER FORMATION CONTROL OF MULTIPLE NONHOLONOMIC MOBILE ROBOTS USING A BIOINSPIRED NEURODYNAMIC BASED APPROACH

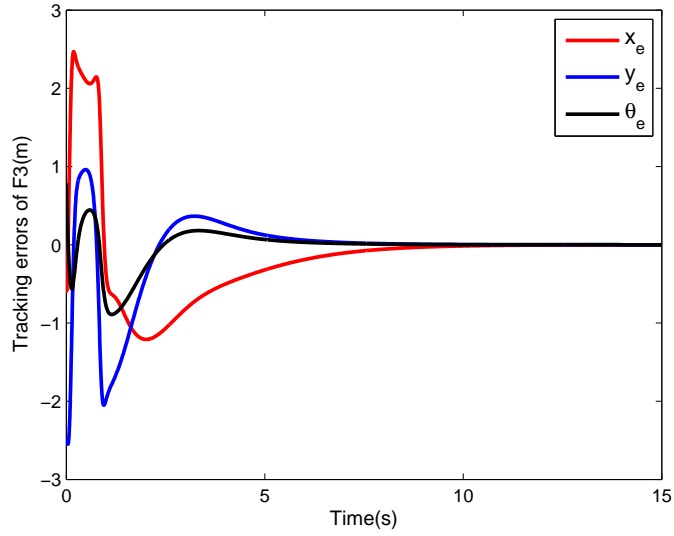


(a)

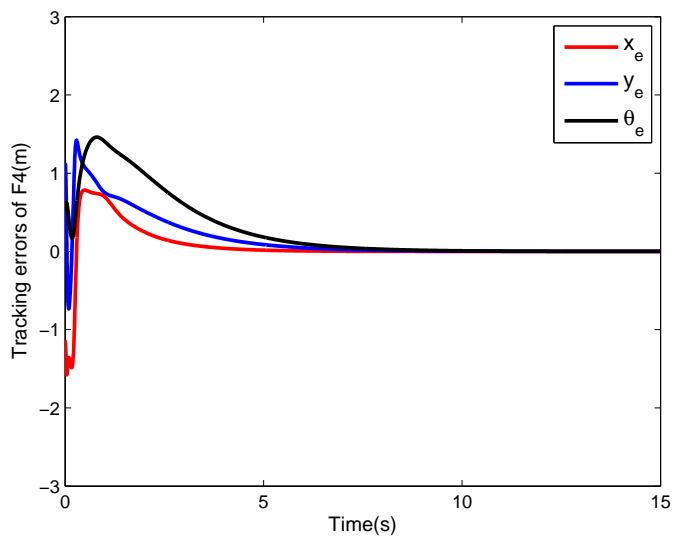


(b)

2.6 Simulations Results



(c)



(d)

Figure 2.11: The tracking errors of the follower in Leader-follower Formation .

Fig. 2.8 shows the trajectory of the Leader-Follower formation. It is shown that the desired leader-follower formation is maintained. Fig. 2.9 shows the errors between the angular velocity of leader L and the reference angular velocity w_j^d of each follower F_j . It shows that the defined reference angular velocities of each follower can converge to the angular velocity of leader over time. Fig. 2.10(a)

2. LEADER-FOLLOWER FORMATION CONTROL OF MULTIPLE NONHOLONOMIC MOBILE ROBOTS USING A BIOINSPIRED NEURODYNAMIC BASED APPROACH

shows the angular velocities of robots, and Fig. 2.10(b) shows the linear velocities of robots. It is shown from Fig. 2.10 that the velocity commands are smooth and reasonable, and change gradually from zero at initial time $t = 0$. Figs. 2.11(a), 2.11(b), 2.11(c) and 2.11(d) are tracking errors of the followers $F1$, $F2$, $F3$ and $F4$, respectively. It is shown that the tracking errors of followers converge to zero over time.

2.7 Conclusion

In this chapter, the leader-follower formation control problem for nonholonomic mobile robots based on the backstepping approach has been investigated. The trajectory tracking control for a single nonholonomic mobile robot has been extended to the formation control for multiple nonholonomic mobile robots based on backstepping technique, in which follower can track its real-time leader by the proposed kinematic controller. Due to the nonholonomic constraint of each robot and the leader-follower formation control objective, an auxiliary angular velocity control law has been developed to guarantee the global asymptotic stability of the followers and to further guarantee the local asymptotic stability of the entire formation. Then an asymptotically stable control law for the formation control of multiple mobile robots has been developed by using backstepping technology, which not only guarantee all mobile robots achieve and maintain the desired formation, but also guarantee all follower robots track the time-varying trajectory of the leader robot. Finally, a bioinspired neurodynamics based approach has been developed to solve the impractical velocity jumps problem. It is shown that each robot has smooth and continuous velocities with zero initial value by using the bioinspired neurodynamics based approach. Stability analysis has been provided by using Lyapunov theory. The effectiveness of the proposed control scheme has been demonstrated by simulation results.

Chapter 3

Distributed Consensus-Based Formation Control for Multiple Nonholonomic Mobile Robots with A Specified Reference Trajectory

Contents

3.1	Introduction	65
3.2	Mathematical Model of a Nonholonomic Mobile Robot	67
3.3	Problem Statement	68
3.4	Distributed Control Algorithm	70
3.5	Simulation Results	76
3.6	Conclusion	83

3.1 Introduction

Numerous of previous works assume that multiple mobile robot systems have tree sensing structures. The tree sensing structures generally lead to cascade interconnections of the closed-loop systems(Desai *et al.* 1998). Some researchers have attempted to relax the assumption of tree sensing structures at the cost of using global position measurements. However, in some application scenarios, robots

3. DISTRIBUTED CONSENSUS-BASED FORMATION CONTROL FOR MULTIPLE NONHOLONOMIC MOBILE ROBOTS WITH A SPECIFIED REFERENCE TRAJECTORY

can have limited communication ability. Generally speaking, it is very difficult to get all the global information to be available for each robot. A centralized controller usually is not assumed to exist. The design of the controller for each robot has to be based on the local information. Therefore, from a practical point of view, using relative local positions make the control laws more realistic.

In recent years, due to the development of consensus theory in the dynamical network system, consensus strategies have been applied to achieve the formation control of multiple mobile robots, which focus on driving the kinematics of all mobile robots to a common value. In [Jadbabaie *et al.* \(2003\)](#), a formal mathematical analysis for consensus is first presented. Lately, the research on consensus problems for multiple systems was also extended to the case of directed topology ([Lu & Chen 2009](#); [Ren & Beard 2005](#); [Wen *et al.* 2013](#); [Wu *et al.* 2012](#); [Yu & Wang 2012](#)). However, the robot system models in these papers are all linear. In practice, many robot system models are nonlinear and have nonholonomic constraints. Therefore, it is natural to study the formation control problem for nonholonomic mobile robots. [Dong & Farrell \(2008, 2009\)](#) proposed some formation control laws to nonholonomic mobile robot systems. [Dong \(2012\)](#) studied the tracking control problem for nonholonomic mobile robots with limited information of a desired trajectory. However, in [Dong & Farrell \(2008, 2009\)](#)'s papers, each robot is assumed to know a desired trajectory.

This chapter investigates the distributed formation control problem for multiple nonholonomic mobile robots using consensus-based approach. The contributions of this chapter are fourfold. First, a transformation is given to convert the formation control problem for multiple nonholonomic mobile robots into a state consensus problem. Second, the control laws are established using the result from graph theory and Lyapunov techniques for accomplishing our formation control objectives: a group of nonholonomic mobile robots converge to a desired geometric pattern with its centroid moving along the specified reference trajectory. In this chapter, the specified reference trajectory is represented by the state of a virtual leader whose outputs is only its position information that is available to only a subset of a group of followers, which differs with existing results in [Dong & Farrell \(2008, 2009\)](#). Third, in our previous Chapter, we use the leader-follower approach([Consolini *et al.* 2008](#); [Das *et al.* 2002](#); [Desai *et al.* 1998, 2001](#); [Mariottini *et al.* 2007](#)) to research formation control problem, the communication topology

3.2 Mathematical Model of a Nonholonomic Mobile Robot

is tree information sensing structure. The relative separation and relative bearing for each robot with its leader is need for design the controller, However, in this Chapter, the control laws proposed are distributed. It is not necessary to know the global information for each robot. In fact, each robot can obtain information only from its neighbors. The informations about relative separation and relative bearing of the robot with its leader don't need. Fourth, different with existing results given in [Dong & Farrell \(2008, 2009\)](#) and [Dong \(2012\)](#), our control laws guaranty that the nonholonomic mobile robots can at least exponentially converge to the desired geometric pattern, as well as the geometric centroid of the formation at least exponentially converges to the trajectory of virtual leader.

3.2 Mathematical Model of a Nonholonomic Mobile Robot

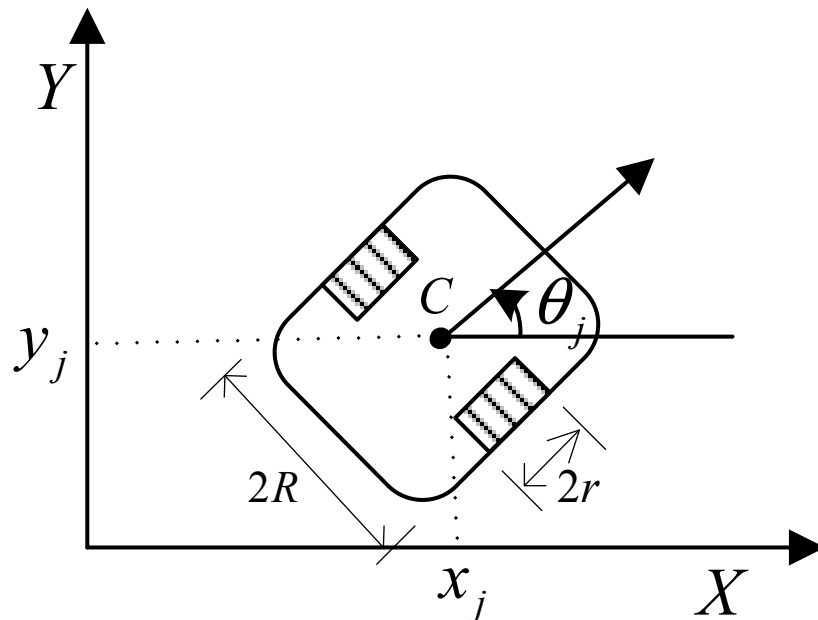


Figure 3.1: Differential wheel mobile robot.

Consider a unicycle mobile robot in Fig.3.1, It is assumed that the mobile robot moves without side slip, which means that the mobile robot satisfies the nonholo-

3. DISTRIBUTED CONSENSUS-BASED FORMATION CONTROL FOR MULTIPLE NONHOLONOMIC MOBILE ROBOTS WITH A SPECIFIED REFERENCE TRAJECTORY

nonic constraint,

$$\dot{x}_j \sin \theta_j - \dot{y}_j \cos \theta_j = 0. \quad (3.1)$$

Hence, the kinematics of the j th robot can be described by

$$\dot{q}_j = \begin{bmatrix} \dot{x}_j \\ \dot{y}_j \\ \dot{\theta}_j \end{bmatrix} = \begin{bmatrix} \cos \theta_j & 0 \\ \sin \theta_j & 0 \\ 0 & 1 \end{bmatrix} \begin{bmatrix} v_j \\ w_j \end{bmatrix}, \quad (3.2)$$

where $q_j = (x_j, y_j, \theta_j)^T$ is the posture of the j th robot in a cartesian frame, (x_j, y_j) is the coordinate C of the center of mass, v_j , w_j and θ_j are the linear velocity, the angular velocity, and the heading angle of the j th robot.

3.3 Problem Statement

Consider a multi-robot system with m nonholonomic mobile robots, labeled as $1, 2, \dots, m$, moving on a horizontal plane. For simplicity, we assume that all robots have the same mechanical structure shown in Fig. 3.1, and the kinematics of the i th robot can be described by (3.2). Suppose that the desired geometric pattern \mathcal{F} of m mobile robots is defined by orthogonal coordinates (p_{jx}, p_{jy}) , which satisfies

$$\sum_{j=1}^m p_{jx} = p_{0x}, \quad \sum_{j=1}^m p_{jy} = p_{0y}. \quad (3.3)$$

where (p_{0x}, p_{0y}) is the center of the geometric pattern \mathcal{F} . Without loss of generality, we assume that $p_{0x} = 0, p_{0y} = 0$.

In this chapter, our objective is to design the control inputs v_j and w_j for the robot j based on its states (q_j, \dot{q}_j) , (p_{jx}, p_{jy}) , and its neighbors's states (q_i, \dot{q}_i) and (p_{ix}, p_{iy}) for $i \in \mathcal{N}_j$, such that a group of mobile robots converge to the desired formation pattern \mathcal{F} , the orientation of each robot converges to a desired value θ_0 , and the geometric centroid of the formation converges to the desired trajectory

3.3 Problem Statement

(x_0, y_0) , that is to say,

$$\lim_{t \rightarrow \infty} \begin{bmatrix} x_j - x_i \\ y_j - y_i \end{bmatrix} = \begin{bmatrix} p_{jx} - p_{ix} \\ p_{jy} - p_{iy} \end{bmatrix}, \quad (3.4)$$

$$\lim_{t \rightarrow \infty} (\theta_j - \theta_0) = 0, \quad (3.5)$$

$$\lim_{t \rightarrow \infty} \left(\sum_{j=1}^m \frac{x_j}{m} - x_0 \right) = 0, \quad \lim_{t \rightarrow \infty} \left(\sum_{j=1}^m \frac{y_j}{m} - y_0 \right) = 0. \quad (3.6)$$

Here, the geometric centroid (x_0, y_0) and the desired value θ_0 can be considered as the posture of a virtual leader 0, which does not have to be an actual robot but is specified by

$$\dot{x}_0 = v_0 \cos \theta_0, \quad \dot{y}_0 = v_0 \sin \theta_0, \quad \dot{\theta}_0 = w_0. \quad (3.7)$$

Hence, we hereafter call the m robots in system (3.2) as followers.

The connection weight between robot j ($1 \leq j \leq m$) and the virtual leader 0 is denoted by B , where $B = \text{diag}\{b_1, b_2, \dots, b_j, \dots, b_m\}$, such that

$$b_j = \begin{cases} b_j > 0, & \text{if robot } j \text{ can obtain information of the virtual leader 0} \\ 0, & \text{otherwise.} \end{cases}$$

To make the control objective solvable, the following assumptions and preliminaries are given.

Assumption 3.1 *The θ_j for $(0 \leq j \leq m)$ is bounded, w_j for $(0 \leq j \leq m)$ is persistently exciting and $|w_j| \leq w_{max}$.*

Remark 3.2 *w_j is persistently exciting, which means w_j does not converge to 0. The assumption is because of the fact that the wheeled mobile robot system is nonholonomic.*

Assumption 3.3 *There exists at least one follower which can obtain information from the virtual leader.*

Remark 3.4 *From the Assumption 3.3, it is not required that each robot knows virtual leader's information, that is to say, the desired trajectory is not required to available to each robot, that is different from existing results in [Dong & Farrell \(2008, 2009\)](#).*

3. DISTRIBUTED CONSENSUS-BASED FORMATION CONTROL FOR MULTIPLE NONHOLONOMIC MOBILE ROBOTS WITH A SPECIFIED REFERENCE TRAJECTORY

3.4 Distributed Control Algorithm

Let's define the following transformation:

$$\begin{aligned}
 z_{1j} &= \theta_j, \\
 z_{2j} &= (x_j - p_{jx}) \cos \theta_j + (y_j - p_{jy}) \sin \theta_j + k_0 \text{sign}(u_{1j}) z_{3j}, \\
 z_{3j} &= (x_j - p_{jx}) \sin \theta_j - (y_j - p_{jy}) \cos \theta_j, \\
 u_{1j} &= w_j, \\
 u_{2j} &= v_j - (1 + k_0^2) u_{1j} z_{3j},
 \end{aligned} \tag{3.8}$$

with the inputs u_{1j} and u_{2j} , where $0 \leq j \leq m$, $k_0 > 0$, and $\text{sign}(\cdot)$ is the signum function. Hence, the dynamic system of (3.8) is given as follows

$$\dot{z}_{1j} = u_{1j}, \tag{3.9}$$

$$\dot{z}_{2j} = u_{2j} + k_0 |u_{1j}| z_{2j}, \tag{3.10}$$

$$\dot{z}_{3j} = u_{1j} z_{2j} - k_0 |u_{1j}| z_{3j}. \tag{3.11}$$

Using (3.8)-(3.11), the control objective (3.4-3.6) becomes

$$\lim_{t \rightarrow \infty} (z_{1j} - z_{10}) = 0, \tag{3.12}$$

$$\lim_{t \rightarrow \infty} (z_{2j} - z_{20}) = 0, \tag{3.13}$$

$$\lim_{t \rightarrow \infty} (z_{3j} - z_{30}) = 0, \tag{3.14}$$

$$\lim_{t \rightarrow \infty} (u_{1j} - u_{10}) = 0. \tag{3.15}$$

Lemma 3.5 *If the equations (3.12)-(3.15) hold for $0 \leq j \leq m$, then the m mobile robots can converge to the formation pattern \mathcal{F} , i.e., the equations (3.4)-(3.6) can be satisfied.*

Proof: From (3.8), it can be easily obtained that

$$\begin{bmatrix} x_j - p_{jx} \\ y_j - p_{jy} \end{bmatrix} = \begin{bmatrix} \cos \theta_j & \sin \theta_j \\ \sin \theta_j & -\cos \theta_j \end{bmatrix} \begin{bmatrix} z_{2j} - k_0 \text{sign}(u_{1j}) z_{3j} \\ z_{3j} \end{bmatrix}.$$

3.4 Distributed Control Algorithm

Since (3.12)-(3.15) are satisfied, it then follows that

$$\begin{aligned} \lim_{t \rightarrow \infty} \begin{bmatrix} x_j - p_{jx} \\ y_j - p_{jy} \end{bmatrix} &= \lim_{t \rightarrow \infty} \begin{bmatrix} \cos \theta_j & \sin \theta_j \\ \sin \theta_j & -\cos \theta_j \end{bmatrix} \begin{bmatrix} z_{2j} - k_0 \text{sign}(u_{1j}) z_{3j} \\ z_{3j} \end{bmatrix} \\ &= \begin{bmatrix} \cos \theta_0 & \sin \theta_0 \\ \sin \theta_0 & -\cos \theta_0 \end{bmatrix} \begin{bmatrix} z_{20} - k_0 \text{sign}(u_{10}) z_{30} \\ z_{30} \end{bmatrix} \\ &= \begin{bmatrix} x_0 \\ y_0 \end{bmatrix}. \end{aligned}$$

This proof is completed.

Remark 3.6 *Based on our proposed transformation (3.8) and above proof, the formation control problem for multiple nonholonomic mobile robots becomes into a consensus problem. In the following part of this chapter, we will propose the distributed control protocols according to the consensus theory. The controller for the mobile robot will be proposed according the communication graph \mathcal{G} .*

According to its neighbors' information based on the communication graph \mathcal{G} , the controller for the mobile robot j , ($1 \leq j \leq m$) can be given as follows

$$\begin{aligned} u_{1j} = & u_{10} - \alpha \sum_{i \in \mathcal{N}_j} a_{ji} (z_{1j} - z_{1i}) - \alpha b_j (z_{1j} - z_{10}) \\ & - \beta \text{sign} \left(\sum_{i \in \mathcal{N}_j} a_{ji} (z_{1j} - z_{1i}) + b_j (z_{1j} - z_{10}) \right), \end{aligned} \quad (3.16)$$

$$\begin{aligned} u_{2j} = & -\alpha \sum_{i \in \mathcal{N}_j} a_{ji} (z_{2j} - z_{2i}) - \alpha b_j (z_{2j} - z_{20}) \\ & - \beta \text{sign} \left(\sum_{i \in \mathcal{N}_j} a_{ji} (z_{2j} - z_{2i}) + b_j (z_{2j} - z_{20}) \right) - k_0 |u_{1j}| z_{2j}, \end{aligned} \quad (3.17)$$

where $j = 1, \dots, m$, b_j is a positive constant if the virtual leader's position is available to the follower j , and $b_j = 0$ otherwise, $|\dot{z}_{20}| \leq \kappa$, κ is a positive constant, α is a nonnegative constant, β is a positive constant and satisfies $\beta > \kappa$.

Since the undirected graph \mathcal{G} is connected, it follows that $L + B = L + \text{diag}\{b_1, \dots, b_m\}$ is a symmetric positive definite matrix, where $B = \text{diag}(b_1, \dots, b_m)$ and $b_j \geq 0$, ($j = 1, \dots, m$). Furthermore, it is easy to verify that the matrix $\mathcal{M} = \text{diag}\{L + B, L + B\}$ is also a symmetric positive definite.

3. DISTRIBUTED CONSENSUS-BASED FORMATION CONTROL FOR MULTIPLE NONHOLONOMIC MOBILE ROBOTS WITH A SPECIFIED REFERENCE TRAJECTORY

Substituting (3.16) and (3.17) into the questions (3.9) and (3.10), we have

$$\begin{aligned}\dot{z}_{1*} &= -\alpha(L+B)z_{1*} + \alpha B\mathbf{1}_m z_{10} - \beta \text{sign}((L+B)z_{1*} - B\mathbf{1}_m z_{10}) + \mathbf{1}_m u_{10} \\ \dot{z}_{2*} &= -\alpha(L+B)z_{2*} + \alpha B\mathbf{1}_m z_{20} - \beta \text{sign}((L+B)z_{2*} - B\mathbf{1}_m z_{20}),\end{aligned}\quad (3.18)$$

where $z_{1*} = [z_{11}, \dots, z_{1m}]^T$ and $z_{2*} = [z_{21}, \dots, z_{2m}]^T$. Let $\tilde{z}_{1*} = z_{1*} - \mathbf{1}_m z_{10}$ and $\tilde{z}_{2*} = z_{2*} - \mathbf{1}_m z_{20}$. From (3.18), the closed-loop error dynamic system can be obtained as

$$\begin{aligned}\dot{\tilde{z}}_{1*} &= -\alpha(L+B)\tilde{z}_{1*} - \beta \text{sign}((L+B)\tilde{z}_{1*}), \\ \dot{\tilde{z}}_{2*} &= -\alpha(L+B)\tilde{z}_{1*} - \beta \text{sign}((L+B)\tilde{z}_{2*}) - \mathbf{1}_m \dot{z}_{20},\end{aligned}\quad (3.19)$$

where the fact $L\mathbf{1}_m z_{10} = 0$ has been applied according to (1.2). Let $Z =$

$$[z_{1*}, z_{2*}]^T = [Z_1, \dots, Z_{2m}]^T, \tilde{Z} = [\tilde{z}_{1*}, \tilde{z}_{2*}]^T = [\tilde{Z}_1, \dots, \tilde{Z}_{2m}]^T \text{ and } \mathbf{f}_0 = \begin{bmatrix} \underbrace{0, \dots, 0}_m, \underbrace{z_{20}, \dots, z_{20}}_m \end{bmatrix}^T.$$

Hence, the error dynamic system can be rewritten into a vector form as

$$\dot{\tilde{Z}} = -\alpha\mathcal{M}\tilde{Z} - \beta \text{sign}(\mathcal{M}\tilde{Z}) - \dot{\mathbf{f}}_0. \quad (3.20)$$

Note that the right-hand side of (3.20) is discontinuous. Therefore, the stability of (3.20) will be analyzed by using differential inclusions and nonsmooth analysis Paden & Sastry (1987). Because the signum function is measurable and locally essentially bounded, the Filippov solution for (3.20) exists Paden & Sastry (1987). Equation (3.20) is written in terms of differential inclusions as

$$\dot{\tilde{Z}} \in^{a.e.} \mathcal{K}[-\alpha\mathcal{M}\tilde{Z} - \beta \text{sign}(\mathcal{M}\tilde{Z}) - \dot{\mathbf{f}}_0]. \quad (3.21)$$

Theorem 3.7 *For the systems in (3.9) and (3.10), if the communication graph \mathcal{G} is connected and the Assumption 3.3 is satisfied, then $\lim_{t \rightarrow \infty} (z_{1j} - z_{10}) = 0$, $\lim_{t \rightarrow \infty} (z_{2j} - z_{20}) = 0$ and $\lim_{t \rightarrow \infty} (u_{1j} - u_{10}) = 0$ in finite time under the control laws (3.16) and (3.17), in particular, $z_{1j} = z_{10}$, $u_{1j} = u_{10}$ and $z_{2j} = z_{20}$ for any $t \geq T$, where*

$$T = \frac{\sqrt{\tilde{Z}^T(0)\mathcal{M}\tilde{Z}(0)}\sqrt{\lambda_{\max}(\mathcal{M})}}{(\beta - \kappa)\lambda_{\min}(\mathcal{M})}. \quad (3.22)$$

3.4 Distributed Control Algorithm

Proof: Choose the Lyapunov function candidate as

$$V = \frac{1}{2} \tilde{Z}^T \mathcal{M} \tilde{Z}. \quad (3.23)$$

Using the Properties of $\mathcal{K}[\cdot]$, the set-valued Lie derivative of V can be obtained as follows

$$\dot{V} \doteq \bigcap_{\xi \in \partial V(\tilde{Z})} \xi^T \mathcal{K}[-\alpha \mathcal{M} \tilde{Z} - \beta \text{sign}(\mathcal{M} \tilde{Z}) - \dot{\mathbf{f}}_0].$$

where $\partial V(\tilde{Z})$ is the generalized gradient of V at \tilde{Z} . Because V is continuously differentiable with respect to \tilde{Z} , $\partial V(\tilde{Z}) = \{M\tilde{Z}\}$, which is a singleton. Therefore, it follows that

$$\begin{aligned} \dot{V}(\tilde{Z}) &= \mathcal{K}[-\alpha \tilde{Z}^T \mathcal{M}^2 \tilde{Z} - \beta \tilde{Z}^T \mathcal{M} \text{sign}(\mathcal{M} \tilde{Z}) - \tilde{Z}^T \mathcal{M} \dot{\mathbf{f}}_0] \\ &= \{-\alpha \tilde{Z}^T \mathcal{M}^2 \tilde{Z} - \beta \|\tilde{Z}^T \mathcal{M}\|_1 - \tilde{Z}^T \mathcal{M} \dot{\mathbf{f}}_0\}, \end{aligned} \quad (3.24)$$

where the fact that $x^T \text{sign}(x) = \|x\|_1$ has been used. By Lemma 1.7 and Paden & Sastry (1987), if f is continuous, then $\mathcal{K}[f] = \{f\}$. Note that the set-valued Lie derivative \dot{V} is a singleton, whose only element is actually \dot{V} . Therefore, it follows that

$$\max \dot{V} = \dot{V} = -\alpha \tilde{Z}^T \mathcal{M}^2 \tilde{Z} - \beta \|\tilde{Z}^T \mathcal{M}\|_1 - \tilde{Z}^T \mathcal{M} \dot{\mathbf{f}}_0 \quad (3.25)$$

$$\begin{aligned} &\leq -\alpha \tilde{Z}^T \mathcal{M}^2 \tilde{Z} - \beta \|\tilde{Z}^T \mathcal{M}\|_1 - \tilde{Z}^T \mathcal{M} \mathbf{1}_{2m} \dot{z}_{20} \\ &\leq -\alpha \tilde{Z}^T \mathcal{M}^2 \tilde{Z} - (\beta - \kappa) \|\tilde{Z}^T \mathcal{M}\|_1, \end{aligned} \quad (3.26)$$

where $|\dot{z}_{20}| \leq \kappa$. Note that \mathcal{M}^2 is symmetric positive definite, $\alpha \geq 0$ and $\beta > \kappa$. Therefore, it follows that $\max \dot{V}$ is negative definite. It then follows from Lemma 1.10 that $\|\tilde{Z}(t)\| \rightarrow 0$ as $t \rightarrow \infty$.

Next, we show that V will decrease to zero in finite time. Note that

$$\begin{aligned} V &= \frac{1}{2} \tilde{Z}^T \mathcal{M} \tilde{Z} \\ &\leq \frac{1}{2} \lambda_{\max}(\mathcal{M}) \|\tilde{Z}\|_2^2. \end{aligned}$$

3. DISTRIBUTED CONSENSUS-BASED FORMATION CONTROL FOR MULTIPLE NONHOLONOMIC MOBILE ROBOTS WITH A SPECIFIED REFERENCE TRAJECTORY

It then follows from (3.25) that the derivative of V satisfies

$$\begin{aligned}
\dot{V} &\leq -\alpha \tilde{Z}^T \mathcal{M}^2 \tilde{Z} - (\beta - \kappa) \|\tilde{Z}^T \mathcal{M}\|_1 \\
&\leq -(\beta - \kappa) \|\tilde{Z}^T \mathcal{M}\|_2 \\
&= -(\beta - \kappa) \sqrt{\tilde{Z}^T \mathcal{M}^2 \tilde{Z}} \\
&\leq -(\beta - \kappa) \sqrt{\lambda_{\min}^2(\mathcal{M}) \|\tilde{Z}\|_2^2} \\
&= \frac{-(\beta - \kappa) \lambda_{\min}(\mathcal{M}) \sqrt{\lambda_{\max}(\mathcal{M}) \|\tilde{Z}\|_2^2}}{\sqrt{\lambda_{\max}(\mathcal{M})}} \\
&\leq \frac{-(\beta - \kappa) \sqrt{2} \lambda_{\min}(\mathcal{M})}{\sqrt{\lambda_{\max}(\mathcal{M})}} \sqrt{V}.
\end{aligned}$$

After some manipulation, we get

$$2\sqrt{V(t)} \leq 2\sqrt{V(0)} - \frac{(\beta - \kappa) \sqrt{2} \lambda_{\min}(\mathcal{M})}{\sqrt{\lambda_{\max}(\mathcal{M})}} t.$$

Therefore, $V(t) = 0$ when $t \geq T = \frac{\sqrt{\tilde{Z}^T(0) \mathcal{M} \tilde{Z}(0)} \sqrt{\lambda_{\max}(\mathcal{M})}}{(\beta - \kappa) \lambda_{\min}(\mathcal{M})}$.

Hence, z_{1j} ($1 \leq j \leq m$) and z_{2j} ($1 \leq j \leq m$) converge to z_{10} and z_{20} in finite time, respectively. Also it is obvious from (3.16) that u_{1j} ($1 \leq j \leq m$) can converge to u_{10} in finite time. This proof is completed.

Remark 3.8 *From the Theorem 3.7, we have proved that the variables z_{1j} ($1 \leq j \leq m$), z_{2j} ($1 \leq j \leq m$) and u_{1j} respectively converge to z_{10} , z_{20} and u_{10} in finite time under the proposed control laws (3.16), (3.17). In Theorem 3.9, we will prove that z_{3j} exponentially converges to z_{30} under the control laws (3.16) and (3.17).*

Theorem 3.9 *For the systems in (3.11), if the communication graph \mathcal{G} is connected and the Assumption 3.3 is satisfied, then z_{3j} exponentially converges to z_{30} under the control laws (3.16) and (3.17).*

Proof: Let $\tilde{z}_{3j} = z_{3j} - z_{30}$. Taking the derivative of \tilde{z}_{3j} gives

$$\begin{aligned}
\dot{\tilde{z}}_{3j} &= \dot{z}_{3j} - \dot{z}_{30} \\
&= -k_0 |u_{1j}| \tilde{z}_{3j} + u_{1j} \tilde{z}_{2j} + (u_{1j} - u_{10}) z_{20} - k_0 (|u_{1j}| - |u_{10}|) z_{30} \\
&= -k_0 |u_{1j}| \tilde{z}_{3j} + x_2(t).
\end{aligned} \tag{3.27}$$

3.4 Distributed Control Algorithm

where $x_2(t) = u_{1j}\tilde{z}_{2j} + (u_{1j} - u_{10})z_{20} - k_0(|u_{1j}| - |u_{10}|)z_{30}$.

Consider the following Lyapunov function candidate as

$$V_2 = \frac{1}{2}\tilde{z}_{3j}^2. \quad (3.28)$$

Step 1: we prove that the state \tilde{z}_{3j} is bounded when $t \leq T$, that means for \tilde{z}_{3j} large disturbance will not occur during the period of $z_{1*} \rightarrow z_{10}$ and $z_{2*} \rightarrow z_{20}$.

The derivative of V_2 along the trajectory (3.27) gives

$$\dot{V}_2 = \tilde{z}_{3j}\dot{\tilde{z}}_{3j} = -k_0|u_{1j}|\tilde{z}_{3j}^2 + x_2(t)\tilde{z}_{3j}. \quad (3.29)$$

Note from Theorem 3.7, $\tilde{Z} \rightarrow 0$ in finite time. It follows that there exists a positive constant σ , such that

$$|x_2(t)| = |u_{1j}\tilde{z}_{2j} + (u_{1j} - u_{10})z_{20} - k_0(|u_{1j}| - |u_{10}|)z_{30}| \leq \sigma. \quad (3.30)$$

Since \tilde{z}_{1j} and \tilde{z}_{2j} converge to zero in finite time T , it follows that \tilde{z}_{1j} and \tilde{z}_{2j} are bounded for all t , i.e. there exists a positive constant $C_1 > 0$, such that $|u_{1j}| < C_1, |z_{1j}| < C_1$ and $|z_{2j}| < C_1$. In the following, we will first verify that, when $|\tilde{z}_{3j}| \geq 1$, there exists a positive constant L_1 , such that

$$\dot{V}_2 \leq L_1 V_2. \quad (3.31)$$

In fact, from (3.29), we have

$$\begin{aligned} \dot{V}_2 &= -k_0|u_{1j}|\tilde{z}_{3j}^2 + x_2(t)\tilde{z}_{3j} \\ &\leq k_0|u_{1j}|\tilde{z}_{3j}^2 + |x_2(t)|\tilde{z}_{3j}^2 = 2\{k_0|u_{1j}| + |x_2(t)|\}V_2 \\ &\leq 2\{k_0C_1^2 + \sigma\}V_2 = L_1V_2, \end{aligned} \quad (3.32)$$

where $L_1 = 2\{k_0C_1^2 + \sigma\}$. Next, we will prove that when $|\tilde{z}_{3j}| < 1$, there exists a positive constant L_2 , such that

$$\dot{V}_2 < L_2. \quad (3.33)$$

3. DISTRIBUTED CONSENSUS-BASED FORMATION CONTROL FOR MULTIPLE NONHOLONOMIC MOBILE ROBOTS WITH A SPECIFIED REFERENCE TRAJECTORY

In fact, since $|u_{1j}| < C_1$ and $|x_2(t)| \leq \sigma$, it follows from (3.29) that

$$\begin{aligned}\dot{V}_2 &< k_0|u_{1j}||\tilde{z}_{3j}|^2 + |x_2(t)||\tilde{z}_{3j}| \\ &< k_0C_1 + \sigma = L_2.\end{aligned}\tag{3.34}$$

where $L_2 = k_0C_1 + \sigma$. From the inequalities (3.31) and (3.33), whatever $|\tilde{z}_{3j}| \geq 1$ or $|\tilde{z}_{3j}| < 1$, we have

$$\dot{V}_2 \leq L_1V_2 + L_2.$$

After some manipulation, we can further get that

$$V_2(t) \leq \left\{V_2(0) + \frac{L_2}{L_1}\right\}e^{L_1t} + \frac{L_2}{L_1}.$$

Hence, from (3.28), \tilde{z}_{3j} is bounded when $t \leq T$.

Step 2: we prove that \tilde{z}_{3j} is converged to zero when $t \geq T$.

From the Theorem 3.1, when $t \geq T$, the $\tilde{Z} = 0$, i.e. $z_{1j} = z_{10}$, $z_{2j} = z_{20}$ and $u_{1j} = u_{10}$, then the system (3.27) becomes

$$\dot{\tilde{z}}_{3j} = -k_0|u_{10}|\tilde{z}_{3j}.\tag{3.35}$$

Then, we have

$$\tilde{z}_{3j}(t) = e^{\int_T^t -k_0|u_{10}|d\tau} \tilde{z}_{3j}(T) = e^{-k_0|u_{10}|(t-T)} \tilde{z}_{3j}.$$

Hence, $\tilde{z}_{3j}(t)$ exponentially converges to zero.

Remark 3.10 *From the Theorems 3.7 and 3.9, our control objectives (3.12)-(3.15) are hold. Therefore from the Lemma 3.5, the m mobile robots converge to the formation pattern \mathcal{F} , i.e., the equations (3.4)-(3.6) are satisfied.*

3.5 Simulation Results

In this section, some simulation results are presented to demonstrate the effectiveness of the theoretical results obtained in the previous sections. Let's consider a multiple mobile robot system with six followers denoted by F_1 - F_6 and one vir-

tual leader denoted by L , respectively. The communication graph of the multiple mobile robot system is shown in Figure 3.2.

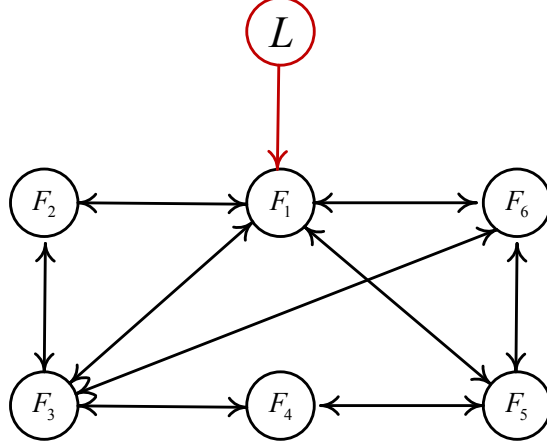


Figure 3.2: Communication graph of a group of six followers and one virtual leader.

For simplicity, suppose that $\mathcal{A} = [a_{ij}]_{6 \times 6}$, $a_{ij} = 1$ if robot i can receive information from robot j , $a_{ij} = 0$ otherwise; $B = \text{diag}\{b_1, b_2, \dots, b_6\}$, $b_j = 1$ if the virtual leader's information is available to the follower j , and $b_j = 0$ otherwise, where $i \in \{1, \dots, 6\}$ and $j \in \{1, \dots, 6\}$. And the adjacency matrix \mathcal{A} , the degree matrix and the Laplacian matrix of the graph shown in Fig.3.2 can be written as:

$$\mathcal{A} = \begin{bmatrix} 0 & 1 & 1 & 0 & 1 & 1 \\ 1 & 0 & 1 & 0 & 0 & 0 \\ 1 & 1 & 0 & 1 & 0 & 1 \\ 0 & 0 & 1 & 0 & 1 & 0 \\ 1 & 0 & 0 & 1 & 0 & 0 \\ 1 & 0 & 1 & 0 & 0 & 0 \end{bmatrix}, \quad \mathcal{D} = \begin{bmatrix} 4 & & & & & \\ & 2 & & & & \\ & & 4 & & & \\ & & & 2 & & \\ & & & & 2 & \\ & & & & & 2 \end{bmatrix},$$

$$L = \mathcal{D} - \mathcal{A} = \begin{bmatrix} 4 & -1 & -1 & 0 & -1 & -1 \\ -1 & 2 & -1 & 0 & 0 & 0 \\ -1 & -1 & 4 & -1 & 0 & -1 \\ 0 & 0 & -1 & 2 & -1 & 0 \\ -1 & 0 & 0 & -1 & 2 & 0 \\ -1 & 0 & -1 & 0 & 0 & 2 \end{bmatrix},$$

3. DISTRIBUTED CONSENSUS-BASED FORMATION CONTROL FOR MULTIPLE NONHOLONOMIC MOBILE ROBOTS WITH A SPECIFIED REFERENCE TRAJECTORY

and $B = \text{diag}\{1, 0, 0, 0, 0, 0\}$. Hence,

$$L + B = \begin{bmatrix} 5 & -1 & -1 & 0 & -1 & -1 \\ -1 & 2 & -1 & 0 & 0 & 0 \\ -1 & -1 & 4 & -1 & 0 & -1 \\ 0 & 0 & -1 & 2 & -1 & 0 \\ -1 & 0 & 0 & -1 & 2 & 0 \\ -1 & 0 & -1 & 0 & 0 & 2 \end{bmatrix}, \quad \mathcal{M} = \begin{bmatrix} L + B & 0 \\ 0 & L + B \end{bmatrix}. \quad (3.36)$$

The desired formation geometric pattern \mathcal{F} is defined by orthogonal coordinates as $(p_{1x}, p_{1y}) = (2, 0)$, $(p_{2x}, p_{2y}) = (1, \sqrt{3})$, $(p_{3x}, p_{3y}) = (-1, \sqrt{3})$, $(p_{4x}, p_{4y}) = (-2, 0)$, $(p_{5x}, p_{5y}) = (-1, -\sqrt{3})$, and $(p_{6x}, p_{6y}) = (1, -\sqrt{3})$ shown in Fig. 3.3. The reference trajectory of the virtual leader is chosen as $x_0 = 12 \sin(t/3)$, $y_0 = -12 \cos(t/3)$.

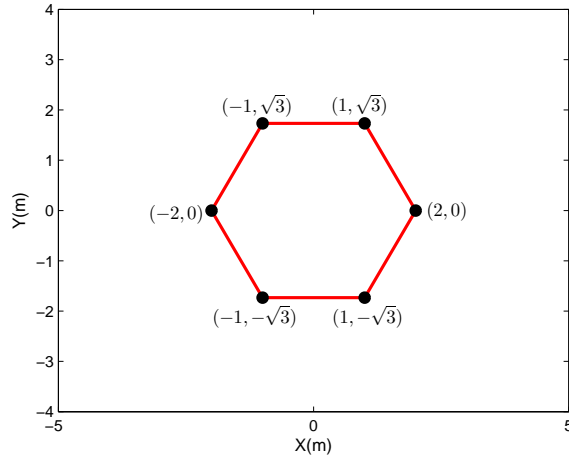


Figure 3.3: Desired geometric pattern of formation.

From the coordinate transformation (3.8), it can be obtained that $z_{20} = 12k_0$, thus, $\dot{z}_{20} = 0 < \kappa$. The gain parameters for each robot are chosen as $\alpha = 23$, $\beta = 0.65 \geq \kappa$ and $k_0 = 2$. It is easy to verify that these parameters satisfy the constraints in Theorem 3.7.

Fig. 3.4 shows the formation pattern of the six follower robots at some time, the trajectory of virtual leader (black line), and the trajectory of the six follower robots' centroid (blue line). Fig. 3.5 shows the trajectories of x_0 (blue line) and the centroid of x_i ($1 \leq i \leq 6$) (red line); and the position error between x_0 and the

3.5 Simulation Results

centroid of x_i . Fig. 3.6 shows the trajectories of y_0 (blue line) and the centroid of y_i ($1 \leq i \leq 6$)(red line); and the position error between y_0 and the centroid of y_i . Fig. 3.7(a) shows the tracking errors between the orientation w_i of follower F_i ($1 \leq i \leq 6$) and the orientation w_0 of virtual leader. Fig. 3.7(b) shows the tracking errors between the orientation θ_i of follower F_i ($1 \leq i \leq 6$) and the orientation θ_0 of virtual leader.

It is shown from Fig. 3.4 that the desired geometry pattern of the six robots is formed under the proposed distributed controllers (3.17) and (3.16), i.e., the equation (3.4) is verified. From Fig. 3.5 and Fig. 3.6, the geometric centroid of the formation converges to the trajectory of virtual leader, that is to say, the equation (3.6) is verified. From Fig. 3.7, the angular velocity and orientation of each follower robot converge to the angular velocity and orientation of virtual leader, i.e., the equation (3.5) and (3.15) are verified.

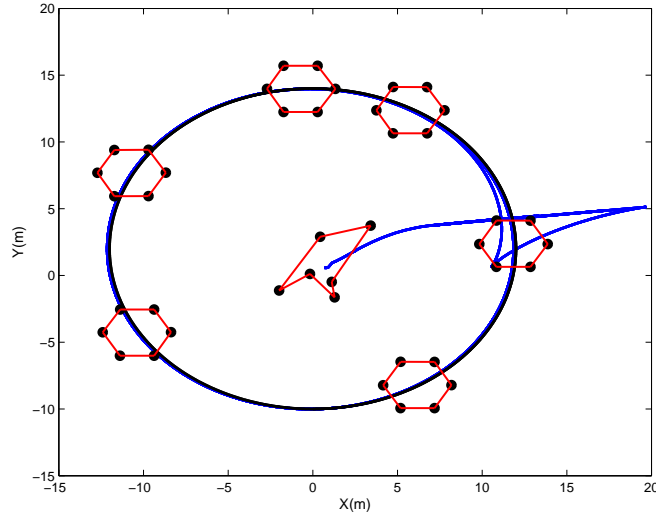
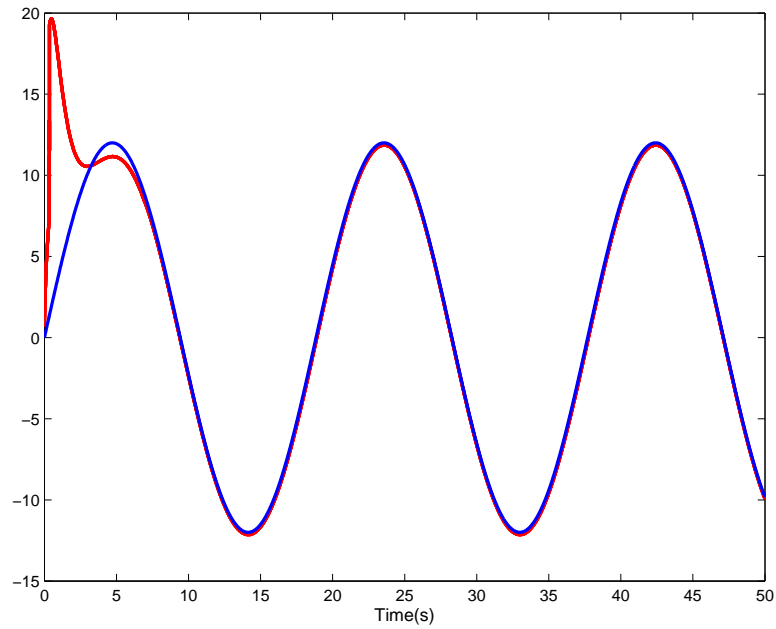
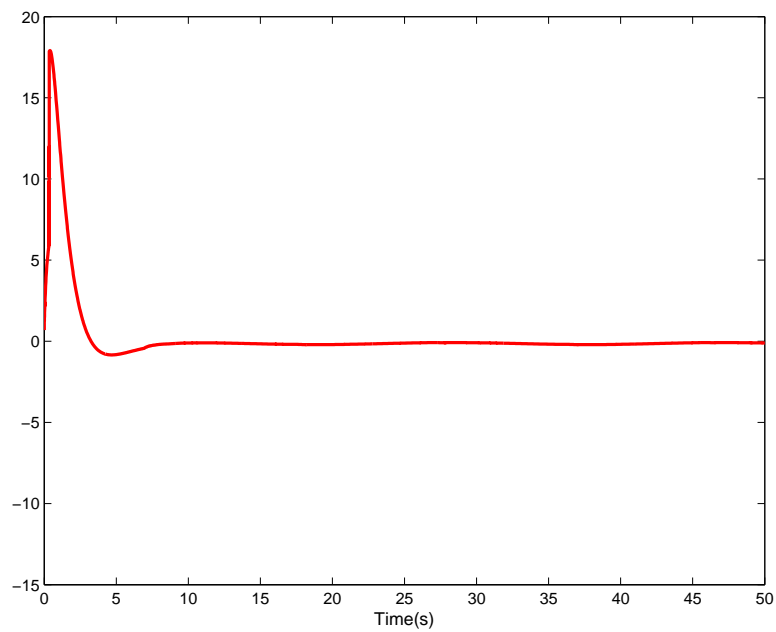


Figure 3.4: Formation pattern of the six follower robots at some time, the trajectory of virtual leader(black line), and the trajectory of the six follower robots' centroid (blue line).

3. DISTRIBUTED CONSENSUS-BASED FORMATION CONTROL FOR MULTIPLE NONHOLONOMIC MOBILE ROBOTS WITH A SPECIFIED REFERENCE TRAJECTORY



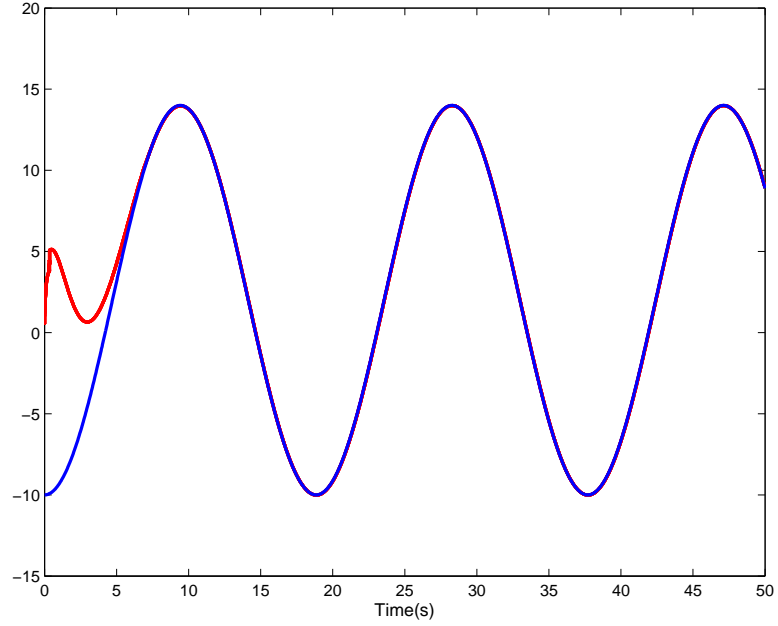
(a)



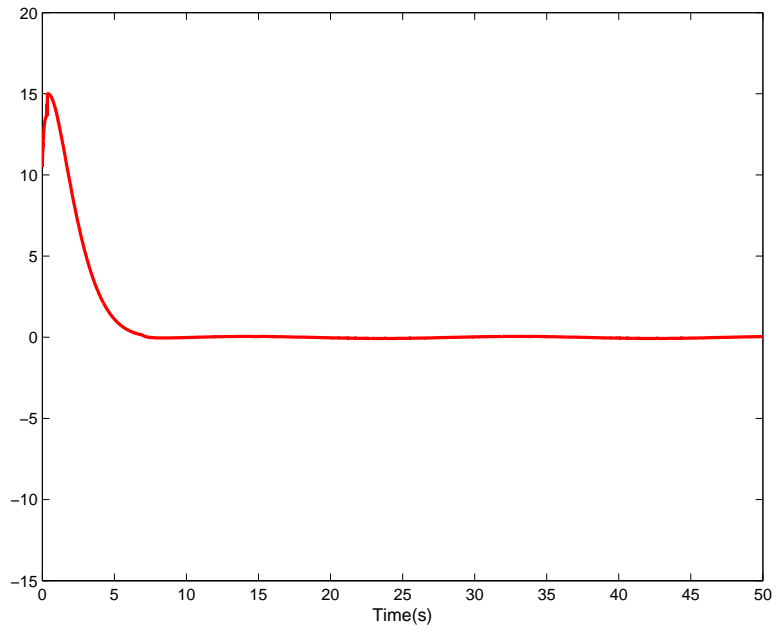
(b)

Figure 3.5: (a) The trajectories of x_0 (blue line) and the centroid of x_i ($1 \leq i \leq 6$) (red line); (b) The position error between x_0 and the centroid of x_i .

3.5 Simulation Results



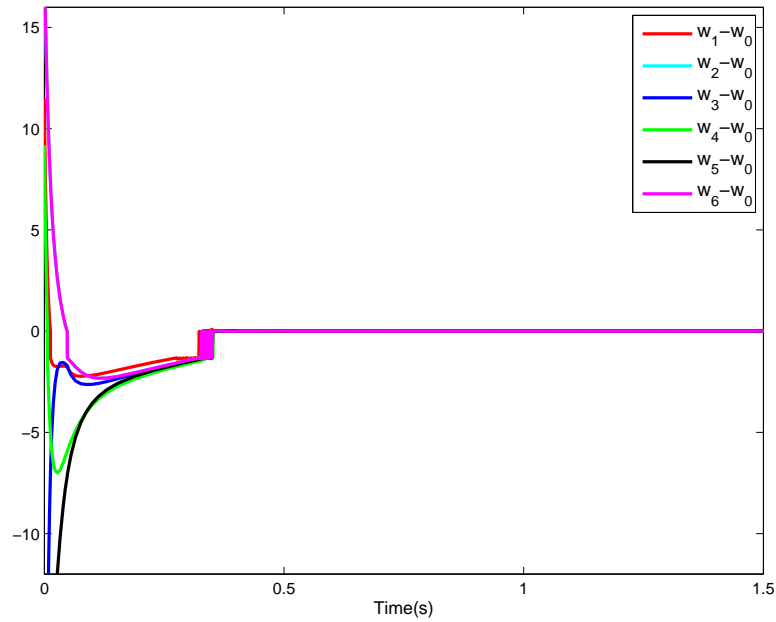
(a)



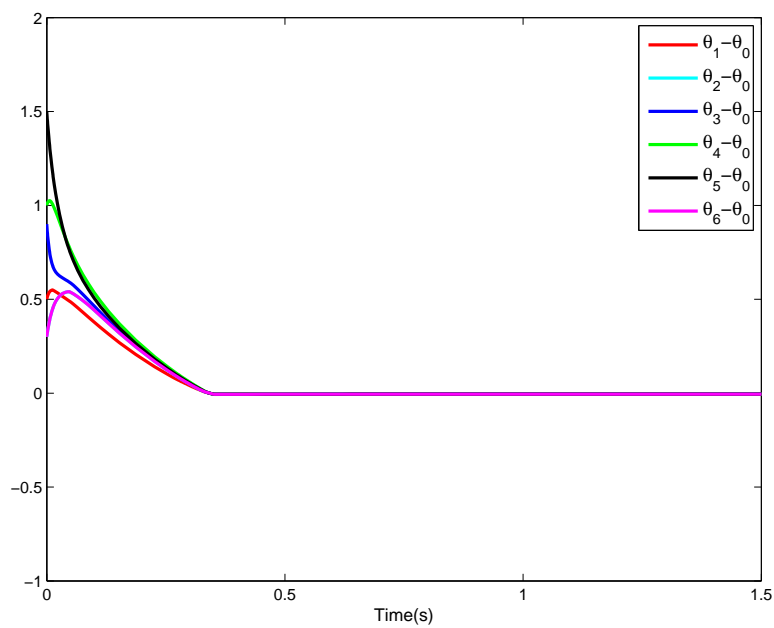
(b)

Figure 3.6: (a)The trajectories of y_0 (blue line) and the centroid of y_i ($1 \leq i \leq 6$)(red line); (b)The position error between y_0 and the centroid of y_i .

3. DISTRIBUTED CONSENSUS-BASED FORMATION CONTROL FOR MULTIPLE NONHOLONOMIC MOBILE ROBOTS WITH A SPECIFIED REFERENCE TRAJECTORY



(a)



(b)

Figure 3.7: The tracking errors: (a) between w_i ($1 \leq i \leq 6$) and w_0 ; (b) between θ_i ($1 \leq i \leq 6$) and θ_0 .

3.6 Conclusion

In this chapter, the distributed formation control problem for multiple nonholonomic mobile robots using consensus-based approach has been studied. Some distributed control laws have been proposed based on the some results from graph theory and Lyapunov techniques. Some simulation results have been obtained to verify the effectiveness of the distributed control algorithm proposed for the formation control.

**3. DISTRIBUTED CONSENSUS-BASED FORMATION CONTROL
FOR MULTIPLE NONHOLONOMIC MOBILE ROBOTS WITH A
SPECIFIED REFERENCE TRAJECTORY**

Chapter 4

Distributed Adaptive Formation Control for Multiple Nonholonomic Wheeled Mobile Robots

Contents

4.1	Introduction	85
4.2	Problem Formulation and Preliminaries	87
4.2.1	Dynamics of Nonholonomic Wheeled Mobile Robot	87
4.2.2	Problem Description	89
4.3	Distributed Control Algorithm	90
4.4	Adaptive Dynamic Controller Design	95
4.4.1	Robot Model and Its Properties	95
4.4.2	Controller Design	96
4.5	Simulation	101
4.6	Conclusion	106

4.1 Introduction

In the previous Chapter, the formation control of nonholonomic wheeled mobile robots is based on kinematic models, which requires “perfect velocity tracking”.

4. DISTRIBUTED ADAPTIVE FORMATION CONTROL FOR MULTIPLE NONHOLONOMIC WHEELED MOBILE ROBOTS

However, in many practical situations, the dynamics of robot should not be ignored and practical control strategies accounting for both the kinematic and dynamic effect should be implemented (Fierro & Lewis 1998; Fukao *et al.* 2000; Zohar *et al.* 2011).

This chapter investigates the distributed adaptive formation control problem for multiple nonholonomic wheeled mobile robots. The objective is to develop the distributed controllers based on the combination both kinematic model and dynamics systems with unknown parameters, such that a group of nonholonomic wheeled mobile robots asymptotically converge to a desired geometric pattern with its centroid moving along the specified reference trajectory. To achieve this goal, a variable transformation is first given to convert the formation control problem into a state consensus problem. Then, the distributed kinematic controllers are developed. We assume that the specified reference trajectory can be considered as the trajectory of a virtual leader whose information is available to only a subset of the followers. Also the followers are assumed to have only local interaction. In practice, it is well known that the dynamics model of the wheel mobile robot has unknown dynamic parameters, which will affect the robust trajectory tracking of the system. Therefore, adaptive computed-torque controllers for mobile robots are developed, and sufficient conditions are derived for accomplishing the asymptotically stability of the systems based on algebraic graph theory, matrix theory, and Lyapunov control approach. Finally, simulation examples illustrate the effectiveness of the proposed controllers.

Compared with existing works in the literature, the current work has the following advantages. Firstly, in contrast to the traditional leader-follower approach (Consolini *et al.* 2008; Das *et al.* 2002; Desai *et al.* 1998; Liu & Tian 2009; Mariottini *et al.* 2007), the communication topology is not required to have tree information sensing structure. Moreover, the relative separation and bearing for each robot with its leader is not required to be known. Secondly, in contrast to that only kinematic control models are considered (Chen *et al.* 2010; Dierks & Jagannathan 2009a,b; Dong 2012; Dong & Farrell 2008, 2009; Park *et al.* 2011), we design the controllers based on both the kinematic and dynamic models of robots. Thirdly, the control laws proposed in this chapter are distributed. It is not necessary to know the global information for each robot. In fact, each robot can obtain information only from its neighbors.

4.2 Problem Formulation and Preliminaries

4.2.1 Dynamics of Nonholonomic Wheeled Mobile Robot

Consider a multi-robot system consisting of m nonholonomic wheeled mobile robots indexed by $1, 2, \dots, m$. The nonholonomic dynamics model of the mobile robot j can be described by the Euler-Lagrange equation as follows

$$M_j(q_j)\ddot{q}_j + C_j(q_j, \dot{q}_j)\dot{q}_j + G_j(q_j) = B_j(q_j)\tau_j - A_j^T(q_j)\lambda_j, \quad j = 1, \dots, m, \quad (4.1)$$

where $q_j = (x_j, y_j, \theta_j)^T$ is the posture of the mobile robot j , (x_j, y_j) are coordinates, θ_j is the heading angle of the robot, $M_j(q_j) \in \mathbb{R}^{3 \times 3}$ is a symmetric positive definite inertia matrix, $C_j(q_j, \dot{q}_j) \in \mathbb{R}^{3 \times 3}$ is the bounded centripetal and coriolis matrix, $G_j(q_j) \in \mathbb{R}^{3 \times 1}$ is the gravitations vector, $B_j(q_j) \in \mathbb{R}^{3 \times 2}$ is the input transformation matrix, $\tau_j \in \mathbb{R}^{2 \times 1}$ is the control torque vector, $A_j(q) \in \mathbb{R}^{1 \times 3}$ is the matrix associated with the constraints, and $\lambda_j \in \mathbb{R}^{1 \times 1}$ is the vector of constraint forces.

Suppose that all kinematic equality constraints are independent of time, and can be expressed as follows:

$$A(q_j)\dot{q}_j = 0. \quad (4.2)$$

It is well know that the wheeled mobile robot is a typical example of a nonholonomic mechanical system. The wheeled mobile robot satisfies the nonholonomic constraint 3.1, which means the robot can only move in the direction normal to the axis of the driving wheels, i.e. the wheeled mobile robot satisfies pure rolling and nonslipping. Then, the kinematics model of the mobile robot $j \in \{1, \dots, m\}$ can be written as

$$\dot{q}_j = \begin{bmatrix} \dot{x}_j \\ \dot{y}_j \\ \dot{\theta}_j \end{bmatrix} = \begin{bmatrix} \cos \theta_j & 0 \\ \sin \theta_j & 0 \\ 0 & 1 \end{bmatrix} \begin{bmatrix} v_j \\ w_j \end{bmatrix} = S(q_j)\bar{v}_j, \quad (4.3)$$

where $\bar{v}_j = [v_j, w_j]^T$, and v_j and w_j are the linear velocity and angular velocity respectively.

From (4.2) and (4.3), it is easily obtained that

$$S^T(q_j)A^T(q_j) = 0. \quad (4.4)$$

4. DISTRIBUTED ADAPTIVE FORMATION CONTROL FOR MULTIPLE NONHOLONOMIC WHEELED MOBILE ROBOTS

We consider the wheeled mobile robot with two driving wheels, which is shown in Fig. 3.1. The geometrical center of robot is C , which is the center of mass of the robot. The trajectory of the mobile robot is constrained to the horizontal plain, i.e. $G_j(q_j) = 0$. The dynamical equations of the mobile robot in Fig. 3.1 can be expressed in matrix form (4.1) where

$$\begin{aligned} M_j(q_j) &= \begin{bmatrix} \hat{m} & 0 & 0 \\ 0 & \hat{m} & 0 \\ 0 & 0 & I \end{bmatrix}, & C_j(q_j, \dot{q}_j) &= \begin{bmatrix} 0 & 0 & 0 \\ 0 & 0 & 0 \\ 0 & 0 & 0 \end{bmatrix}, & G_j(q) &= \begin{bmatrix} 0 \\ 0 \\ 0 \end{bmatrix}, \\ B_j(q_j) &= \frac{1}{r} \begin{bmatrix} \cos \theta_j & \cos \theta_j \\ \sin \theta_j & \sin \theta_j \\ R & -R \end{bmatrix}, & A_j(q)^T &= \begin{bmatrix} -\sin \theta_j \\ \cos \theta_j \\ 0 \end{bmatrix}, & \tau_j &= \begin{bmatrix} \tau_{rj} \\ \tau_{lj} \end{bmatrix}, \\ \lambda_j &= -\hat{m}(\dot{x}_j \cos \theta_j + \dot{y}_j \sin \theta_j)\dot{\theta}_j. \end{aligned}$$

where \hat{m} is the mass of the wheel mobile robot. I is the inertia moment of the robot. $2R$ is the width of the mobile robot and r is the radius of the wheel. The equation (4.1) has the following properties (Lewis *et al.* (1993)).

Property 4.1 *The inertia matrix $M_j(q_j)$ is symmetric positive definite, and satisfies the following inequality*

$$m_1 \|q_j\|^2 \leq q_j^T M_j(q_j) q_j \leq m_2 \|q_j\|^2, q_j \in \mathbb{R}^3, \quad (4.5)$$

where m_1, m_2 are positive constants, and $\|\cdot\|$ is the standard Euclidean norm.

Property 4.2 *$\dot{M}_j(q_j) - 2C_j(q_j, \dot{q}_j)$ is skew symmetric, that is to say,*

$$\xi^T \left[\frac{1}{2} \dot{M}_j(q_j) - C_j(q_j, \dot{q}_j) \right] \xi = 0. \quad \forall \xi \in \mathbb{R}^3. \quad (4.6)$$

Property 4.3 *For any differentiable vector ξ ,*

$$M_j \dot{\xi} + C_j \xi + G_j = Y_j \Theta_j, \quad j = 1, \dots, m, \quad (4.7)$$

where Y_j is regression vector, and Θ_j is the constant parameter vector associated with the j th robot.

4.2.2 Problem Description

Similar to Chapter 3, in this chapter the desired geometric pattern \mathcal{F} of m mobile robots is still defined by using orthogonal coordinates (p_{jx}, p_{jy}) , which satisfies

$$\sum_{j=1}^m p_{jx} = p_{0x}, \quad \sum_{j=1}^m p_{jy} = p_{0y}. \quad (4.8)$$

where (p_{0x}, p_{0y}) is the center of the geometric pattern \mathcal{F} . Without loss of generality, we also assume that $p_{0x} = 0, p_{0y} = 0$.

In this chapter, we will still design the control inputs v_j and w_j for the wheeled nonholonomic mobile robot j using its states (q_j, \dot{q}_j) , (p_{jx}, p_{jy}) , and its neighbors' states (q_i, \dot{q}_i) and (p_{ix}, p_{iy}) for $i \in \mathcal{N}_j$, to achieve our control objective (1): a group of such robots converge to the desired formation pattern \mathcal{F} , (2): the orientation of each robot converges to a desired value θ_0 , and (3): the geometric centroid of the formation converges to the desired reference trajectory (x_0, y_0) , that is to say,

$$\lim_{t \rightarrow \infty} \begin{bmatrix} x_j - x_i \\ y_j - y_i \end{bmatrix} = \begin{bmatrix} p_{jx} - p_{ix} \\ p_{jy} - p_{iy} \end{bmatrix}, \quad (4.9)$$

$$\lim_{t \rightarrow \infty} (\theta_j - \theta_0) = 0, \quad (4.10)$$

$$\lim_{t \rightarrow \infty} \left(\sum_{j=1}^m \frac{x_j}{m} - x_0 \right) = 0, \quad \lim_{t \rightarrow \infty} \left(\sum_{j=1}^m \frac{y_j}{m} - y_0 \right) = 0. \quad (4.11)$$

Similarly, the geometric centroid (x_0, y_0) and the desired value θ_0 are considered as the posture of a virtual leader 0,

$$\dot{x}_0 = v_0 \cos \theta_0, \quad \dot{y}_0 = v_0 \sin \theta_0, \quad \dot{\theta}_0 = w_0. \quad (4.12)$$

To achieve our control objective, the same assumptions Assumption 3.1 and Assumption 3.3 in Section 3.3 are needed.

4. DISTRIBUTED ADAPTIVE FORMATION CONTROL FOR MULTIPLE NONHOLONOMIC WHEELED MOBILE ROBOTS

4.3 Distributed Control Algorithm

To achieve our control objective (3.4)-(3.6) based on the combination both kinematic model and dynamics model, the following transformation is defined:

$$\begin{aligned}
 z_{1j} &= \theta_j, \\
 z_{2j} &= (x_j - p_{jx}) \cos \theta_j + (y_j - p_{jy}) \sin \theta_j + k_0 \text{sign}(u_{1j}) z_{3j}, \\
 z_{3j} &= (x_j - p_{jx}) \sin \theta_j - (y_j - p_{jy}) \cos \theta_j, \\
 u_{1j} &= w_j, \\
 u_{2j} &= v_j - (1 + k_0^2) u_{1j} z_{3j} + k_0 |u_{1j}| z_{2j},
 \end{aligned} \tag{4.13}$$

with the inputs u_{1j} and u_{2j} , where $0 \leq j \leq m$, $k_0 > 0$, and $\text{sign}(\cdot)$ is the signum function. Hence, the dynamic system of (4.13) is given as follows

$$\dot{z}_{1j} = u_{1j}, \tag{4.14}$$

$$\dot{z}_{2j} = u_{2j}, \tag{4.15}$$

$$\dot{z}_{3j} = u_{1j} z_{2j} - k_0 |u_{1j}| z_{3j}. \tag{4.16}$$

According to (4.13)-(4.16), the control objective (4.9)-(4.11) becomes

$$\lim_{t \rightarrow \infty} (z_{1j} - z_{10}) = 0, \tag{4.17}$$

$$\lim_{t \rightarrow \infty} (z_{2j} - z_{20}) = 0, \tag{4.18}$$

$$\lim_{t \rightarrow \infty} (z_{3j} - z_{30}) = 0, \tag{4.19}$$

$$\lim_{t \rightarrow \infty} (u_{1j} - u_{10}) = 0. \tag{4.20}$$

Lemma 4.4 *If the equations (4.17)-(4.20) are hold for $0 \leq j \leq m$, then the m mobile robots can converge to the formation pattern \mathcal{F} , i.e., the equations (3.4)-(3.6) can be satisfied.*

Proof: The proof is similar to that of Lemma 3.5 and is therefore omitted here.

Note that the undirected graph \mathcal{G} is connected, it follows that the matrix $L + B = L + \text{diag}\{b_1, \dots, b_m\}$ and the matrix $\mathcal{M} = \text{diag}\{L + B, L + B\}$ are symmetric positive definite, where $B = \text{diag}(b_1, \dots, b_m)$ and $b_j \geq 0$, ($j = 1, \dots, m$).

It is well known that the "perfect velocity tracking" for robot may not hold

4.3 Distributed Control Algorithm

in practice. In fact, the dynamics model of the wheel mobile robot has unknown dynamical parameters, which will affect the robust tracking of the system. Hence, in this chapter, according to the mobile robot j 's neighbors' information, the following desired control inputs for the mobile robot j are proposed by

$$\begin{aligned} u_{1jr} = & u_{10} - \alpha \sum_{i \in \mathcal{N}_j} a_{ji}(z_{1j} - z_{1i}) - \alpha b_j(z_{1j} - z_{10}) \\ & - \beta \text{sign}\left(\sum_{i \in \mathcal{N}_j} a_{ji}(z_{1j} - z_{1i}) + b_j(z_{1j} - z_{10})\right), \end{aligned} \quad (4.21)$$

$$\begin{aligned} u_{2jr} = & -\alpha \sum_{i \in \mathcal{N}_j} a_{ji}(z_{2j} - z_{2i}) - \alpha b_j(z_{2j} - z_{20}) \\ & - \beta \text{sign}\left(\sum_{i \in \mathcal{N}_j} a_{ji}(z_{2j} - z_{2i}) + b_j(z_{2j} - z_{20})\right), \end{aligned} \quad (4.22)$$

where $j = 1, \dots, m$, b_j is a positive constant if the virtual leader's position is available to the follower j , and $b_j = 0$ otherwise, $|\dot{z}_{20}| \leq \kappa$, κ is a positive constant, α is a nonnegative constant, β is a positive constant and satisfies $\beta > \kappa$.

Remark 4.5 *If we only consider the kinematic model of the nonholonomic wheeled mobile robot with the velocity input (4.21) and (4.22), and assume that there is "perfect velocity tracking", i.e.*

$$\begin{bmatrix} u_{1j} \\ u_{2j} \end{bmatrix} = \begin{bmatrix} u_{1jr} \\ u_{2jr} \end{bmatrix}, \quad (4.23)$$

then the kinematic model (4.14)-(4.16) is at least exponentially stable under the control law (4.21) and (4.22). However, the perfect velocity tracking does not hold in practice. In fact, the dynamics model of the wheel mobile robot has unknown dynamical parameters, which will affect the robust tracking of the system.

Define the auxiliary velocity tracking error as

$$\tilde{u}_j = \begin{bmatrix} \tilde{u}_{wj} \\ \tilde{u}_{vj} \end{bmatrix} = u_{jr} - u_j = \begin{bmatrix} u_{1jr} \\ u_{2jr} \end{bmatrix} - \begin{bmatrix} u_{1j} \\ u_{2j} \end{bmatrix}. \quad (4.24)$$

where $u_{jr} = [u_{1jr}, u_{2jr}]^T$ and $u_j = [u_{1j}, u_{2j}]^T$. Then the dynamic system (4.14)-

4. DISTRIBUTED ADAPTIVE FORMATION CONTROL FOR MULTIPLE NONHOLONOMIC WHEELED MOBILE ROBOTS

(4.16) become

$$\dot{z}_{1j} = u_{1jr} - \tilde{u}_{wj}, \quad (4.25)$$

$$\dot{z}_{2j} = u_{2jr} - \tilde{u}_{vj}, \quad (4.26)$$

$$\dot{z}_{3j} = (u_{1jr} - \tilde{u}_{wj})z_{2j} - k_0|(u_{1jr} - \tilde{u}_{wj})|z_{3j}. \quad (4.27)$$

Substituting (4.21) and (4.22) into the dynamic system (4.25) and (4.26), and rewriting the closed-loop system (4.25) and (4.26) in a vector form gives

$$\begin{aligned} \dot{z}_{1*} &= -\alpha(L+B)z_{1*} + \alpha B\mathbf{1}_m z_{10} - \beta \text{sign}((L+B)z_{1*} - B\mathbf{1}_m z_{10}) + \mathbf{1}_m u_{10} - \hat{u}_w, \\ \dot{z}_{2*} &= -\alpha(L+B)z_{2*} + \alpha B\mathbf{1}_m z_{20} - \beta \text{sign}((L+B)z_{2*} - B\mathbf{1}_m z_{20}) - \hat{u}_v, \end{aligned} \quad (4.28)$$

where $z_{1*} = [z_{11}, \dots, z_{1m}]^T$ and $z_{2*} = [z_{21}, \dots, z_{2m}]^T$, $\hat{u}_w = [\tilde{u}_{w1}, \dots, \tilde{u}_{wm}]^T$ and $\hat{u}_v = [\tilde{u}_{v1}, \dots, \tilde{u}_{vm}]^T$. Let $\tilde{z}_{1*} = z_{1*} - \mathbf{1}_m z_{10}$ and $\tilde{z}_{2*} = z_{2*} - \mathbf{1}_m z_{20}$. From (4.28), the closed-loop error dynamic system can be obtained as

$$\begin{aligned} \dot{\tilde{z}}_{1*} &= -\alpha(L+B)\tilde{z}_{1*} - \beta \text{sign}((L+B)\tilde{z}_{1*}) - \hat{u}_w, \\ \dot{\tilde{z}}_{2*} &= -\alpha(L+B)\tilde{z}_{2*} - \beta \text{sign}((L+B)\tilde{z}_{2*}) - \mathbf{1}_m \dot{z}_{20} - \hat{u}_v, \end{aligned} \quad (4.29)$$

where the fact that $L\mathbf{1}_m z_{10} = 0$ has been applied according to (1.2). Let $Z = [z_{1*}, z_{2*}]^T = [Z_1, \dots, Z_{2m}]^T$, $\tilde{Z} = [\tilde{z}_{1*}, \tilde{z}_{2*}]^T = [\tilde{Z}_1, \dots, \tilde{Z}_{2m}]^T$ and $f_0 = \begin{bmatrix} \underbrace{0, \dots, 0}_m, \underbrace{z_{20}, \dots, z_{20}}_m \end{bmatrix}^T$. Hence, the error dynamic system can be rewritten in a vector form as

$$\dot{\tilde{Z}} = -\alpha\mathcal{M}\tilde{Z} - \beta \text{sign}(\mathcal{M}\tilde{Z}) - \dot{f}_0 - \hat{u} \quad (4.30)$$

where $\hat{u} = [\hat{u}_w, \hat{u}_v]^T = [\tilde{u}_{w1}, \dots, \tilde{u}_{wm}, \tilde{u}_{v1}, \dots, \tilde{u}_{vm}]^T$.

Note that the right-hand side of (5.37) is discontinuous. Therefore, the stability of (5.37) will be analyzed by using differential inclusions and nonsmooth analysis Paden & Sastry (1987). Because the signum function is measurable and locally essentially bounded, the Filippov solution for (5.37) exists Paden & Sastry (1987). Equation (5.37) is written in terms of differential inclusions as

$$\dot{\tilde{Z}} \in^{a.e.} \mathcal{K}[-\alpha\mathcal{M}\tilde{Z} - \beta \text{sign}(\mathcal{M}\tilde{Z}) - \dot{f}_0 - \hat{u}]. \quad (4.31)$$

4.3 Distributed Control Algorithm

Remark 4.6 Note that the stability of the kinematic error system (4.30) is now dependent on the error \tilde{Z} and the velocity tracking error \hat{u} . The following Theorem 4.7 is given to prove that when $\hat{u} = 0$ (i.e., perfect velocity tracking (4.23)) the state \tilde{Z} of system (4.30) converge to zero in finite time under the kinematic controller (4.21) and (4.22).

Theorem 4.7 Suppose that the communication graph \mathcal{G} is connected, Assumption 3.3 is satisfied, and the kinematic controller for the system (4.30) is chosen by (4.21) and (4.22), if the auxiliary velocity tracking error $\hat{u} = 0$, then the state \tilde{Z} of system (4.30) can converge to zero in finite time, that is to say, $z_{1j} - z_{10}$, $u_{1j} - u_{10}$ and $z_{2j} - z_{20}$ converge to zero in finite time.

Proof: If it is assumed that the dynamics system of the mobile robot satisfies perfect velocity tracking, i.e. $\hat{u} = 0$, then the error dynamic system (4.30) becomes

$$\dot{\tilde{Z}} \in^{a.e.} \mathcal{K}[-\alpha \mathcal{M}\tilde{Z} - \beta \text{sign}(\mathcal{M}\tilde{Z}) - \dot{\mathbf{f}}_0]. \quad (4.32)$$

Consider the following Lyapunov function candidate as

$$V = \frac{1}{2} \tilde{Z}^T \mathcal{M} \tilde{Z}. \quad (4.33)$$

Using the Properties of $\mathcal{K}[\cdot]$, the set-valued Lie derivative of V can be obtained as follows

$$\dot{V} \doteq \bigcap_{\xi \in \partial V(\tilde{Z})} \xi^T \mathcal{K}[-\alpha \mathcal{M}\tilde{Z} - \beta \text{sign}(\mathcal{M}\tilde{Z}) - \dot{\mathbf{f}}_0].$$

where $\partial V(\tilde{Z})$ is the generalized gradient of V at \tilde{Z} . Because V is continuously differentiable with respect to \tilde{Z} , $\partial V(\tilde{Z}) = \{M\tilde{Z}\}$, which is a singleton. Therefore, it follows that

$$\begin{aligned} \dot{V}(\tilde{Z}) &= \mathcal{K}[-\alpha \tilde{Z}^T \mathcal{M}^2 \tilde{Z} - \beta \tilde{Z}^T \mathcal{M} \text{sign}(\mathcal{M}\tilde{Z}) - \tilde{Z}^T \mathcal{M} \dot{\mathbf{f}}_0] \\ &= \{-\alpha \tilde{Z}^T \mathcal{M}^2 \tilde{Z} - \beta \|\tilde{Z}^T \mathcal{M}\|_1 - \tilde{Z}^T \mathcal{M} \dot{\mathbf{f}}_0\}, \end{aligned} \quad (4.34)$$

where the fact that $x^T \text{sign}(x) = \|x\|_1$ has been used. By Lemma 1.7 and Paden & Sastry (1987), if f is continuous, then $\mathcal{K}[f] = \{f\}$. Note that the set-valued Lie derivative \dot{V} is a singleton, whose only element is actually \dot{V} . Therefore, it

4. DISTRIBUTED ADAPTIVE FORMATION CONTROL FOR MULTIPLE NONHOLONOMIC WHEELED MOBILE ROBOTS

follows that

$$\max \dot{V} = \dot{V} \leq -\alpha \tilde{Z}^T \mathcal{M}^2 \tilde{Z} - (\beta - \kappa) \|\tilde{Z}^T \mathcal{M}\|_1, \quad (4.35)$$

where $|\dot{z}_{20}| \leq \kappa$. Note that \mathcal{M}^2 is symmetric positive definite, $\alpha \geq 0$ and $\beta > \kappa$. Therefore, it follows that $\max \dot{V}$ is negative definite. It then follows from Lemma 1.10 that $\|\tilde{Z}(t)\| \rightarrow 0$ as $t \rightarrow \infty$.

Next, we show that V will decrease to zero in finite time. Note that

$$V = \frac{1}{2} \tilde{Z}^T \mathcal{M} \tilde{Z} \leq \frac{1}{2} \lambda_{\max}(\mathcal{M}) \|\tilde{Z}\|_2^2.$$

It then follows from (4.35) that the derivative of V satisfies

$$\begin{aligned} \dot{V} &\leq -\alpha \tilde{Z}^T \mathcal{M}^2 \tilde{Z} - (\beta - \kappa) \|\tilde{Z}^T \mathcal{M}\|_1 \\ &\leq -(\beta - \kappa) \|\tilde{Z}^T \mathcal{M}\|_2 \\ &= -(\beta - \kappa) \sqrt{\tilde{Z}^T \mathcal{M}^2 \tilde{Z}} \\ &\leq -(\beta - \kappa) \sqrt{\lambda_{\min}^2(\mathcal{M}) \|\tilde{Z}\|_2^2} \\ &= \frac{-(\beta - \kappa) \lambda_{\min}(\mathcal{M}) \sqrt{\lambda_{\max}(\mathcal{M}) \|\tilde{Z}\|_2^2}}{\sqrt{\lambda_{\max}(\mathcal{M})}} \\ &\leq \frac{-(\beta - \kappa) \sqrt{2} \lambda_{\min}(\mathcal{M})}{\sqrt{\lambda_{\max}(\mathcal{M})}} \sqrt{V}. \end{aligned}$$

After some manipulations, we get

$$2\sqrt{V(t)} \leq 2\sqrt{V(0)} - \frac{(\beta - \kappa) \sqrt{2} \lambda_{\min}(\mathcal{M})}{\sqrt{\lambda_{\max}(\mathcal{M})}} t.$$

Therefore, $V(t) = 0$ when $t \geq T = \frac{\sqrt{\tilde{Z}^T(0) \mathcal{M} \tilde{Z}(0)} \sqrt{\lambda_{\max}(\mathcal{M})}}{(\beta - \kappa) \lambda_{\min}(\mathcal{M})}$.

Hence, $z_{1j}(1 \leq j \leq m)$ and $z_{2j}(1 \leq j \leq m)$ converge to z_{10} and z_{20} in finite time, respectively. Also it is obvious from (4.21) that $u_{1j}(1 \leq j \leq m)$ can converge to u_{10} in finite time. This proof is completed.

Remark 4.8 From Theorem 4.7, when $\hat{u} = 0$ (i.e., perfect velocity tracking), the state \tilde{Z} of system (4.30) can converge to zero in finite time. As in our previous discussion, the "perfect velocity tracking" for mobile robot may not hold in practice, due to the fact that the dynamics model of the wheel mobile robot has

unknown dynamic parameters, which will affect the robust tracking of the system. In the next section, we will consider that "perfect velocity tracking" assumption doesn't hold in practice. Hence, it is necessary to design a suitable torque controller τ_j based on the controller 4.21 and 4.22, guaranteeing the stability of the kinematic error system (4.30).

4.4 Adaptive Dynamic Controller Design

4.4.1 Robot Model and Its Properties

From (4.3) and (4.13), the new kinematic model of the mobile robot j is obtained as follows

$$\dot{q}_j = \begin{bmatrix} (1 + k_0^2)z_{3j} \cos \theta_j - k_0 \text{sign}(u_{1j})z_{2j} \cos \theta_j & \cos \theta_j \\ (1 + k_0^2)z_{3j} \sin \theta_j - k_0 \text{sign}(u_{1j})z_{2j} \sin \theta_j & \sin \theta_j \\ 1 & 0 \end{bmatrix} \begin{bmatrix} u_{1j} \\ u_{2j} \end{bmatrix} = \bar{S}(q_j)u_j. \quad (4.36)$$

Differentiating (4.36), substituting it into the (4.1) and multiplying both sides by $\bar{S}^T(q_j)$, the following dynamic equation is obtained

$$\bar{M}_j \dot{u}_j + \bar{C}_j u_j + \bar{G}_j = \bar{\tau}_j, \quad j = 1, \dots, m, \quad (4.37)$$

where $\bar{M}_j = \bar{S}^T M_j \bar{S}$ is a symmetric positive definite inertia matrix, $\bar{C}_j = \bar{S}^T (M_j \dot{\bar{S}} + C_j \bar{S})$ is the centripetal and coriolis matrix, $\bar{\tau}_j = \bar{S}^T B \tau_j$ denotes input vector. Let $A = (1 + k_0^2)z_{3j} - k_0 \text{sign}(u_{1j})z_{2j}$. The matrices in the dynamic equation (5.39) are given as follows

$$\bar{M}(q_j) = \begin{bmatrix} A^2 \hat{m} + I & A \hat{m} \\ A \hat{m} & \hat{m} \end{bmatrix}, \quad \bar{C}(q_j, \dot{q}_j) = \begin{bmatrix} A \dot{A} \hat{m} & 0 \\ \dot{A} \hat{m} & 0 \end{bmatrix},$$

$$\bar{G}_j(q) = 0, \quad \bar{B}(q_j) = \frac{1}{r} \begin{bmatrix} A + R & A + R \\ 1 & 1 \end{bmatrix},$$

where \hat{m} and I are respectively the mass and inertia moment of the mobile robot.

Similar to the properties 4.1- 4.3, the equation (5.39) has the following properties.

Property 4.9 *The inertia matrix $\bar{M}_j(q_j)$ is symmetric positive definite.*

Proof: It is easy to verify, and is therefore omitted here.

4. DISTRIBUTED ADAPTIVE FORMATION CONTROL FOR MULTIPLE NONHOLONOMIC WHEELED MOBILE ROBOTS

Property 4.10 *The matrix $\dot{M}_j - 2\bar{C}_j$ is skew symmetric.*

Proof: The derivative of the inertia matrix, and the centripetal and coriolis matrix are given by

$$\begin{aligned}\dot{M}_j(q_j) &= \dot{S}^T M_j \bar{S} + \bar{S}^T \dot{M}_j \bar{S} + \bar{S}^T M_j \dot{S}, \\ 2\bar{C}_j &= 2\bar{S}^T (M_j \dot{S} + C_j \bar{S}).\end{aligned}$$

Since $\dot{M}_j - 2C_j$ is skew symmetric and M_j is symmetric positive definite, it follows that

$$\begin{aligned}\dot{M}_j - 2\bar{C}_j &= \dot{S}^T M_j \bar{S} + \bar{S}^T \dot{M}_j \bar{S} + \bar{S}^T M_j \dot{S} - 2\bar{S}^T (M_j \dot{S} + C_j \bar{S}) \\ &= \dot{S}^T M_j \bar{S} - \bar{S}^T M_j \dot{S} + \bar{S}^T (\dot{M}_j - 2C_j) \bar{S} \\ &= \bar{S}^T (\dot{M}_j - 2C_j) \bar{S}.\end{aligned}$$

Hence, the matrix $\dot{M}_j - 2\bar{C}_j$ is skew symmetric.

Property 4.11 *For any differentiable vector ξ , the following equation (4.11) is satisfied*

$$\bar{M}_j \dot{\xi} + \bar{C}_j \xi + \bar{G}_j = Y_j \Theta_j, \quad j = 1, \dots, m, \quad (4.38)$$

where Y_j is regression vector and Θ_j is the constant parameter vector associated with the follower robot j .

Proof: It is easy to verify, and is therefore omitted here.

4.4.2 Controller Design

Taking the derivative of (4.24), and multiplying the inertia matrix \bar{M}_j to both sides of equation gives

$$\begin{aligned}\bar{M}_j \dot{\dot{u}}_j &= \bar{M}_j \dot{u}_{jr} - \bar{M}_j \dot{u}_j \\ &= \bar{M}_j \dot{u}_{jr} + \bar{C}_j u_j + \bar{G}_j - \bar{\tau}_j \\ &= -\bar{C}_j \tilde{u}_j - \bar{\tau}_j + \bar{M}_j \dot{u}_{jr} + \bar{C}_j u_{jr} + \bar{G}_j, \quad j = 1, \dots, m.\end{aligned} \quad (4.39)$$

From the property 4.11, it follows that

$$\bar{M}_j \dot{u}_{jr} + \bar{C}_j u_{jr} + \bar{G}_j = Y_j \Theta_j, \quad j = 1, \dots, m. \quad (4.40)$$

4.4 Adaptive Dynamic Controller Design

Then, the equation (4.39) can be rewritten as

$$\bar{M}_j \dot{\tilde{u}}_j = -\bar{C}_j \tilde{u}_j - \bar{\tau}_j + Y_j \Theta_j, \quad j = 1, \dots, m. \quad (4.41)$$

It is easy to obtain that Y_j and Θ_j satisfy

$$Y_j = \begin{bmatrix} A^2 \dot{u}_{1jr} + A \dot{u}_{2jr} + A \dot{A} u_{1jr} & \dot{A} u_{1jr} \\ A \dot{u}_{1jr} + \dot{u}_{2jr} + \dot{A} u_{1jr} & 0 \end{bmatrix}, \quad \Theta_j = \begin{bmatrix} \hat{m} \\ I \end{bmatrix}. \quad (4.42)$$

Next, we design an adaptive controller for the system (4.41) as follows

$$\bar{\tau}_j = K_j \tilde{u}_j + Y_j \hat{\Theta}_j, \quad (4.43)$$

where K_j is a symmetric positive-definite matrix defined by $K_j = k_j I_2$ with k_j being a positive gain constant and $I_2 \in \mathbb{R}^{2 \times 2}$ being the identity matrix. $\hat{\Theta}_j$ is the estimate of Θ_j and satisfies

$$\dot{\hat{\Theta}}_j = \Gamma_j Y_j^T \tilde{u}_j, \quad (4.44)$$

and Γ_j is a symmetric positive definite matrix. Let $\tilde{\Theta}_j$ be the estimation error of the parameter vector, and $\tilde{\Theta}_j = \Theta_j - \hat{\Theta}_j$. It then follows from (4.42) that $\dot{\tilde{\Theta}}_j = -\dot{\hat{\Theta}}_j$.

Substituting (4.43) into (4.41), the dynamics system of the robot j can be written as

$$\begin{aligned} \bar{M}_j \dot{\tilde{u}}_j &= -\bar{C}_j \tilde{u}_j - \bar{\tau}_j + Y_j \Theta_j \\ &= -\bar{C}_j \tilde{u}_j - K_j \tilde{u}_j - Y_j \hat{\Theta}_j + Y_j \Theta_j \\ &= -(\bar{C}_j + K_j) \tilde{u}_j + Y_j \tilde{\Theta}_j, \quad j = 1, \dots, m. \end{aligned} \quad (4.45)$$

Hence, the dynamics systems of all the follower robots can be written in a vector form as

$$\bar{M}(q) \dot{\tilde{u}} + \bar{C}(q, \dot{q}) \tilde{u} = -K \tilde{u} + Y \tilde{\Theta}, \quad (4.46)$$

where $\bar{M}(q)$, $\bar{C}(q, \dot{q})$ and K are respectively the block diagonal matrices of $\bar{M}_j(q_j)$, $\bar{C}_j(q_j, \dot{q}_j)$ and K_j , and $\tilde{u} = [\tilde{u}_{w1}, \tilde{u}_{v1}, \tilde{u}_{w2}, \tilde{u}_{v2}, \dots, \tilde{u}_{wm}, \tilde{u}_{vm}]^T$, it is easily obtained from (4.30) that $\|\tilde{u}\|_2 = \|\hat{u}\|_2$.

4. DISTRIBUTED ADAPTIVE FORMATION CONTROL FOR MULTIPLE NONHOLONOMIC WHEELED MOBILE ROBOTS

Theorem 4.12 *Suppose that the communication graph \mathcal{G} is connected. Assumption 3.3 is satisfied, the velocity controllers for (4.25) and (4.26) are respectively designed by (4.21) and (4.22), and the torque control input for (4.39) is designed by (4.43), if the control gains are chosen as $\alpha > \frac{1}{2\lambda_{max}(\mathcal{M})}$, $\beta > \kappa$ and $k_{max} > \frac{\lambda_{max}(\mathcal{M})}{2}$, where $k_{max} = \max\{k_1, k_2, \dots, k_m\}$, then, for $1 \leq j \leq m$, the errors $\tilde{z}_{1j} = 0$, $\tilde{z}_{2j} = 0$, $\tilde{u}_{wj} = 0$ and $\tilde{u}_{vj} = 0$ are globally asymptotically stable.*

Proof: Define the Lyapunov function candidate as

$$V = V_1 + V_2, \quad (4.47)$$

where

$$V_1 = \frac{1}{2} \tilde{Z}^T \mathcal{M} \tilde{Z}, \quad (4.48)$$

$$V_2 = \frac{1}{2} \tilde{u}^T \bar{M} \tilde{u} + \frac{1}{2} \tilde{\Theta}^T \Gamma^{-1} \tilde{\Theta}, \quad (4.49)$$

with $\tilde{\Theta} = [\tilde{\Theta}_1, \dots, \tilde{\Theta}_m]^T$, and Γ is the block diagonal matrices of Γ_j . Using the properties of $\mathcal{K}[\cdot]$, the set-valued Lie derivative of V can be obtained as follows

$$\begin{aligned} \dot{V} &= \mathcal{K}[V_1 + V_2] \subseteq \mathcal{K}[V_1] + \mathcal{K}[V_2] \\ &= \dot{V}_1 + \dot{V}_2. \end{aligned} \quad (4.50)$$

Since V_2 is continuous, according to Lemma 1.7, the equality (5.69) holds. First, let us compute the set-valued Lie derivative of V_1 ,

$$\begin{aligned} \dot{V}_1(\tilde{Z}) &= \mathcal{K}[-\alpha \tilde{Z}^T \mathcal{M}^2 \tilde{Z} - \beta \tilde{Z}^T \mathcal{M} \text{sign}(\mathcal{M} \tilde{Z}) - \tilde{Z}^T \mathcal{M} \dot{\mathbf{f}}_0 - \tilde{Z}^T \mathcal{M} \dot{\mathbf{u}}] \\ &= \{-\alpha \tilde{Z}^T \mathcal{M}^2 \tilde{Z} - \beta \|\tilde{Z}^T \mathcal{M}\|_1 - \tilde{Z}^T \mathcal{M} \dot{\mathbf{f}}_0 - \tilde{Z}^T \mathcal{M} \dot{\mathbf{u}}\}. \end{aligned} \quad (4.51)$$

Similar to the proof process in Theorem 5.10, the set-valued Lie derivative \dot{V}_1 is a singleton. By using the Hölder's inequality, it then follows from (4.51) that

$$\begin{aligned} \dot{V}_1 &\leq -\alpha \tilde{Z}^T \mathcal{M}^2 \tilde{Z} - \beta \|\tilde{Z}^T \mathcal{M}\|_1 - \tilde{Z}^T \mathcal{M} \mathbf{1}_{2m} \dot{z}_{20} - \tilde{Z}^T \mathcal{M} \dot{\mathbf{u}} \\ &\leq -\alpha \tilde{Z}^T \mathcal{M}^2 \tilde{Z} - (\beta - \kappa) \|\tilde{Z}^T \mathcal{M}\|_1 - \tilde{Z}^T \mathcal{M} \dot{\mathbf{u}} \\ &\leq -\alpha \tilde{Z}^T \mathcal{M}^2 \tilde{Z} - (\beta - \kappa) \|\tilde{Z}^T \mathcal{M}\|_1 + \frac{\lambda_{max}(\mathcal{M})}{2} (\|\tilde{Z}\|_2^2 + \|\dot{\mathbf{u}}\|_2^2), \end{aligned} \quad (4.52)$$

4.4 Adaptive Dynamic Controller Design

where the fact $|\dot{z}_{20}| \leq \kappa$ has been used. Since the matrix \mathcal{M} is symmetric positive definite, it then follows that \mathcal{M}^2 is also symmetric positive definite. Since V_2 is continuous, it follows that the set-valued Lie derivative of V_2 satisfies $\max \dot{V}_2 = \dot{V}_2$. Hence, we have

$$\begin{aligned}
\dot{V}_2 &= \tilde{u}^T \bar{M} \dot{\tilde{u}} + \frac{1}{2} \tilde{u}^T \dot{\bar{M}} \tilde{u} + \tilde{\Theta}^T \Gamma^{-1} \dot{\tilde{\Theta}} \\
&= \tilde{u}^T \{-\bar{C} \tilde{u} - K \tilde{u} + Y \tilde{\Theta}\} + \frac{1}{2} \tilde{u}^T \dot{\bar{M}} \tilde{u} + \tilde{\Theta}^T \Gamma^{-1} \dot{\tilde{\Theta}} \\
&= -\tilde{u}^T K \tilde{u} + \tilde{u}^T \{-\bar{C} + \frac{1}{2} \dot{\bar{M}}\} \tilde{u} + \tilde{u}^T Y \tilde{\Theta} + (-Y^T \tilde{u})^T \Gamma^T \Gamma^{-1} \dot{\tilde{\Theta}} \\
&= -\tilde{u}^T K \tilde{u},
\end{aligned} \tag{4.53}$$

where the fact that $\dot{\bar{M}}_j - 2\bar{C}_j$ is skew symmetric has been used .

Now, Substituting (4.52) and (4.53) into the Lie derivative \dot{V} gives

$$\begin{aligned}
\max \dot{V} = \dot{V} &\leq -\alpha \tilde{Z}^T \mathcal{M}^2 \tilde{Z} - (\beta - \kappa) \|\tilde{Z}^T \mathcal{M}\|_1 + \frac{\lambda_{max}(\mathcal{M})}{2} (\|\tilde{Z}\|_2^2 + \|\hat{u}\|_2^2) - \tilde{u}^T K \tilde{u} \\
&= -\alpha \tilde{Z}^T \mathcal{M}^2 \tilde{Z} - (\beta - \kappa) \|\tilde{Z}^T \mathcal{M}\|_1 + \frac{\lambda_{max}(\mathcal{M})}{2} (\|\tilde{Z}\|_2^2 + \|\tilde{u}\|_2^2) - \tilde{u}^T K \tilde{u} \\
&\leq -\alpha \lambda_{max}^2(\mathcal{M}) \|\tilde{Z}\|_2^2 - (\beta - \kappa) \|\tilde{Z}^T \mathcal{M}\|_1 + \frac{\lambda_{max}(\mathcal{M})}{2} (\|\tilde{Z}\|_2^2 + \|\tilde{u}\|_2^2) \\
&\quad - k_{max} \|\tilde{u}\|_2^2 \\
&\leq -(\alpha \lambda_{max}^2(\mathcal{M}) - \frac{\lambda_{max}(\mathcal{M})}{2}) \|\tilde{Z}\|_2^2 - (\beta - \kappa) \|\tilde{Z}^T \mathcal{M}\|_1 \\
&\quad - (k_{max} - \frac{\lambda_{max}(\mathcal{M})}{2}) \|\tilde{u}\|_2^2,
\end{aligned}$$

and it is clear that $\max \dot{V} < 0$ provided by $\dot{z}_{20} \leq \kappa$, $\alpha > \frac{1}{2\lambda_{max}(\mathcal{M})}$, $\beta > \kappa$ and $k_{max} > \frac{\lambda_{max}(\mathcal{M})}{2}$. It then from Lemma 1.10 that, $\tilde{u} \rightarrow 0$ and $\tilde{Z} \rightarrow 0$ as $t \rightarrow \infty$, i.e., $\tilde{z}_{1j} \rightarrow 0$, $\tilde{z}_{2j} \rightarrow 0$, $\tilde{u}_{wj} \rightarrow 0$ and $\tilde{u}_{vj} \rightarrow 0$ as $t \rightarrow \infty$. Therefore, the errors $\tilde{z}_{1j} = 0$, $\tilde{z}_{2j} = 0$, $\tilde{u}_{wj} = 0$ and $\tilde{u}_{vj} = 0$ are globally asymptotically stable. This proof is completed.

Remark 4.13 *From the Theorem 4.12, we have proved that the variables z_{1j} ($1 \leq j \leq m$) and z_{2j} ($1 \leq j \leq m$) respectively converge to z_{10} and z_{20} globally asymptotically under the proposed control laws (4.21), (4.22) and (4.43). In the following Theorem 4.14, we will prove that z_{3j} exponentially converges to z_{30} under the control laws (4.21), (4.22) and (4.43).*

4. DISTRIBUTED ADAPTIVE FORMATION CONTROL FOR MULTIPLE NONHOLONOMIC WHEELED MOBILE ROBOTS

Theorem 4.14 *Suppose that the communication graph \mathcal{G} is connected, Assumption 3.3 is satisfied, the velocity controllers for (4.25) and (4.26) are respectively designed by (4.21) and (4.22), and the torque control input for (4.39) is designed by (4.43), If z_{1j} and z_{2j} asymptotically converge to z_{10} and z_{20} , then z_{3j} also asymptotically converges to z_{30} .*

Proof: Let $\tilde{z}_{3j} = z_{3j} - z_{30}$. Take the derivative of \tilde{z}_{3j} as

$$\begin{aligned}\dot{\tilde{z}}_{3j} &= \dot{z}_{3j} - \dot{z}_{30} \\ &= -k_0|u_{1j}|\tilde{z}_{3j} + u_{1j}\tilde{z}_{2j} + (u_{1j} - u_{10})z_{20} - k_0(|u_{1j}| - |u_{10}|)z_{30} \\ &= -k_0|u_{1j}|\tilde{z}_{3j} + x_2(t).\end{aligned}\tag{4.54}$$

where $x_2(t) = u_{1j}\tilde{z}_{2j} + (u_{1j} - u_{10})z_{20} - k_0(|u_{1j}| - |u_{10}|)z_{30}$. The solution of the differential equation (4.54) is given as follows

$$\tilde{z}_{3j}(t) = e^{\int_0^t -k_0|u_{1j}|d\tau}\tilde{z}_{3j}(0) + \int_0^t e^{\int_\tau^t -k_0|u_{1j}|d\nu}x_2(\tau)d\tau.\tag{4.55}$$

According to Theorem 4.12, \tilde{z}_{2j} asymptotically converges to zero, and u_{1j} asymptotically converges to u_{10} . It then follows the definition of $x_2(t)$ that $x_2(t)$ also asymptotically converges to zero. Hence, according to the definition of asymptotic stability, for a arbitrary positive value $\sigma > 0$, it exists $o > 0$, when the $|x_2(0)| < o$, it has $|x_2(t)| < \sigma$.

From the Assumption (3.1), the u_{1j} is bounded, and $u_{1j} = w_j$, Hence, $|u_{1j}| \leq w_{max}$.

The solution of the differential equation (4.55) satisfies the inequality

$$\begin{aligned}\tilde{z}_{3j}(t) &= e^{\int_0^t -k_0|u_{1j}|d\tau}\tilde{z}_{3j}(0) + \int_0^t e^{\int_\tau^t -k_0|u_{1j}|d\nu}x_2(\tau)d\tau \\ &\leq e^{-k_0w_{max}t}\tilde{z}_{3j}(0) + \int_0^t e^{-k_0w_{max}(t-\tau)}x_2(\tau)d\tau \\ &\leq e^{-k_0w_{max}t}\tilde{z}_{3j}(0) + e^{-k_0w_{max}t} \int_0^t e^{k_0w_{max}\tau}x_2(\tau)d\tau \\ &\leq e^{-k_0w_{max}t}\tilde{z}_{3j}(0) + \frac{\sigma k_0w_{max} - \sigma k_0w_{max}e^{-k_0w_{max}t}}{k_0w_{max}} \\ &= \sigma + e^{-k_0w_{max}t}(\tilde{z}_{3j}(0) - \sigma).\end{aligned}$$

Hence, when $t \rightarrow +\infty$, $|\tilde{z}_{3j}(t)| \leq \sigma$. Since σ is a arbitrary positive values, from

the definition of asymptotic stability, the $\tilde{z}_{3j}(t)$ is asymptotically stable at the neighborhood of origin. This proof is completed.

Remark 4.15 *From the Theorems 4.12 and 4.14, our control objectives (4.17)-(4.20) are hold. Therefore from the Lemma 4.4, the m mobile robots converge to the formation pattern \mathcal{F} , i.e., the equations (4.9)-(4.11) are satisfied.*

4.5 Simulation

In this section, numerical simulations are performed to show the effectiveness of some theoretical results obtained in the previous sections. Let's consider a group of six followers and one virtual leader. From the communication graph among mobile robots shown in Fig. 3.2, it can be note that the undirected graph \mathcal{G} for all followers F_1 to F_6 is connected, and the follower F_1 can receive information from the virtual leader L . Let $a_{ij} = 1$ if robot i can receive information from robot j , $a_{ij} = 0$ otherwise; also $b_j = 1$ if the virtual leader's information is available to the follower j , and $b_j = 0$ otherwise, where $i \in \{1, \dots, 6\}$ and $j \in \{1, \dots, 6\}$.

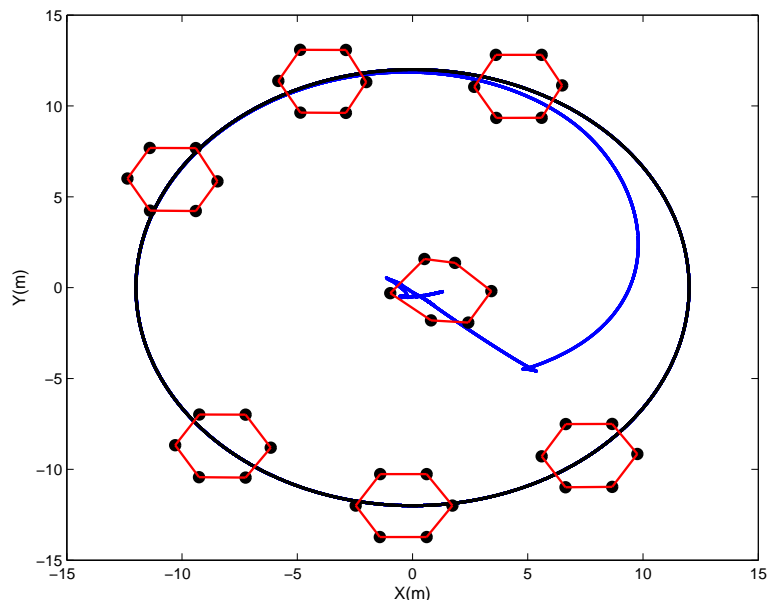


Figure 4.1: The trajectory of virtual leader (black line), the trajectory of centroid of the six followers (blue line), and the formation positions and pattern of the six followers at some moments.

4. DISTRIBUTED ADAPTIVE FORMATION CONTROL FOR MULTIPLE NONHOLONOMIC WHEELED MOBILE ROBOTS

In this simulation, we assume that the desired formation pattern \mathcal{F} is defined by orthogonal coordinates as $(p_{1x}, p_{1y}) = (2, 0)$, $(p_{2x}, p_{2y}) = (1, \sqrt{3})$, $(p_{3x}, p_{3y}) = (-1, \sqrt{3})$, $(p_{4x}, p_{4y}) = (-2, 0)$, $(p_{5x}, p_{5y}) = (-1, -\sqrt{3})$, and $(p_{6x}, p_{6y}) = (1, -\sqrt{3})$. Also assume the parameters $\hat{m} = 5$ kg and $I = 3$ kg $\cdot m^2$. The trajectory of the virtual leader is chosen as $(x_0(t), y_0(t), \theta_0(t)) = (12 \sin(t/3), -12 \cos(t/3), t/3)$. According to the coordinate transformation (4.13), $z_{20} = 12k_0$. Thus, $\dot{z}_{20} = 0 \leq \kappa$. The control gain parameters are chosen as $\alpha = 3$, $\beta = 0.64$ and $k_0 = 2$, $K_j = \text{diag}\{130, 130\}$. Obviously, these parameters satisfy the constraints in Theorem 4.12 and Theorem 4.14.

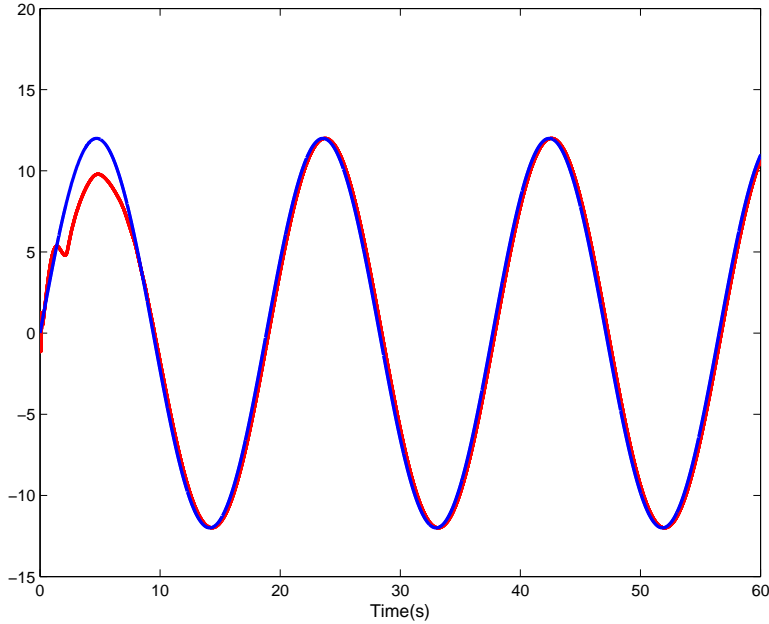


Figure 4.2: The trajectories of x_0 (blue line) and the centroid of x_i ($1 \leq i \leq 6$)(red line).

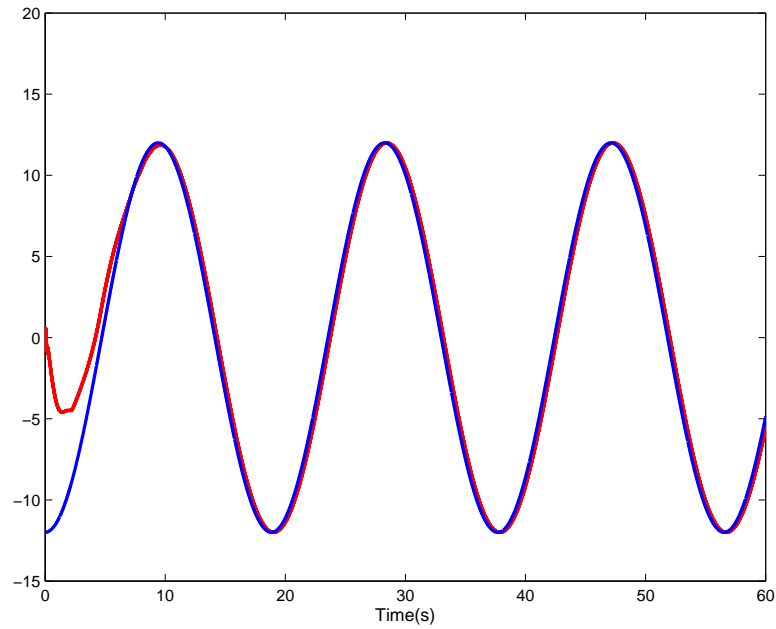


Figure 4.3: The trajectories of y_0 (blue line) and the centroid of y_i ($1 \leq i \leq 6$) (red line).

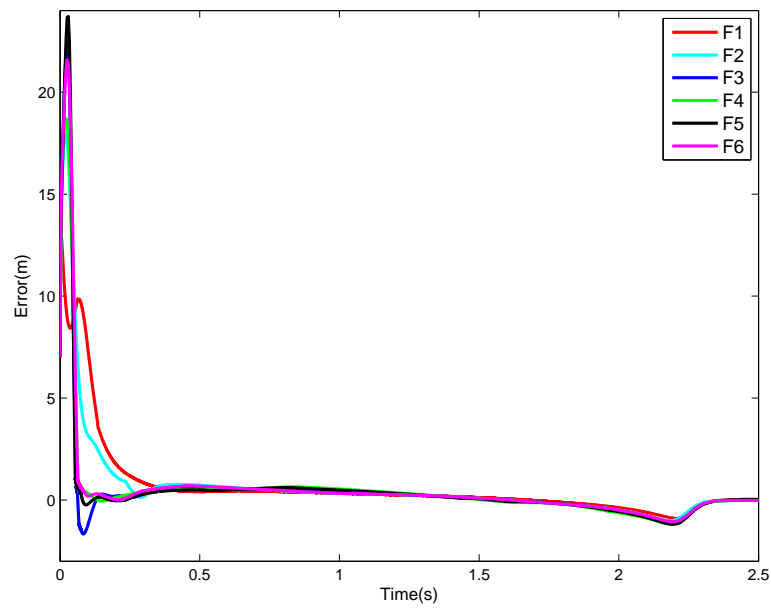


Figure 4.4: The tracking error \tilde{u}_{wi} for ($1 \leq i \leq 6$).

4. DISTRIBUTED ADAPTIVE FORMATION CONTROL FOR MULTIPLE NONHOLONOMIC WHEELED MOBILE ROBOTS

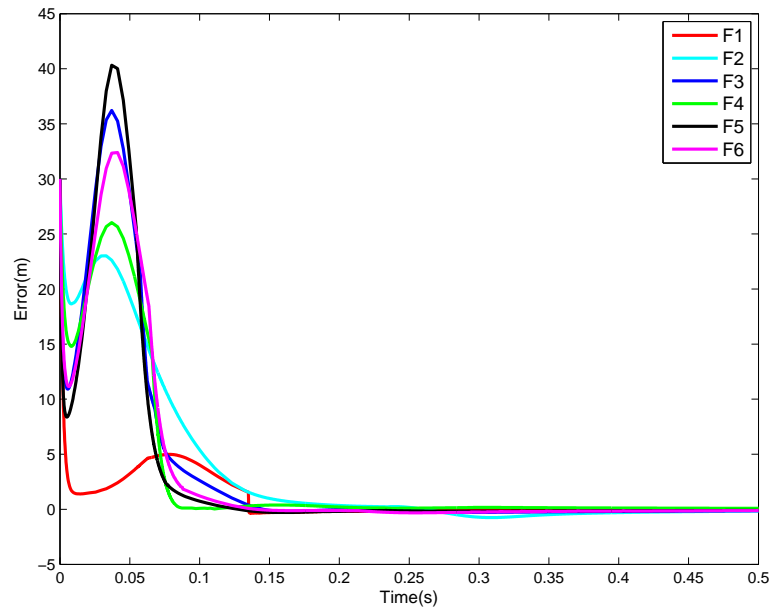


Figure 4.5: The tracking error \tilde{u}_{vi} for $(1 \leq i \leq 6)$.

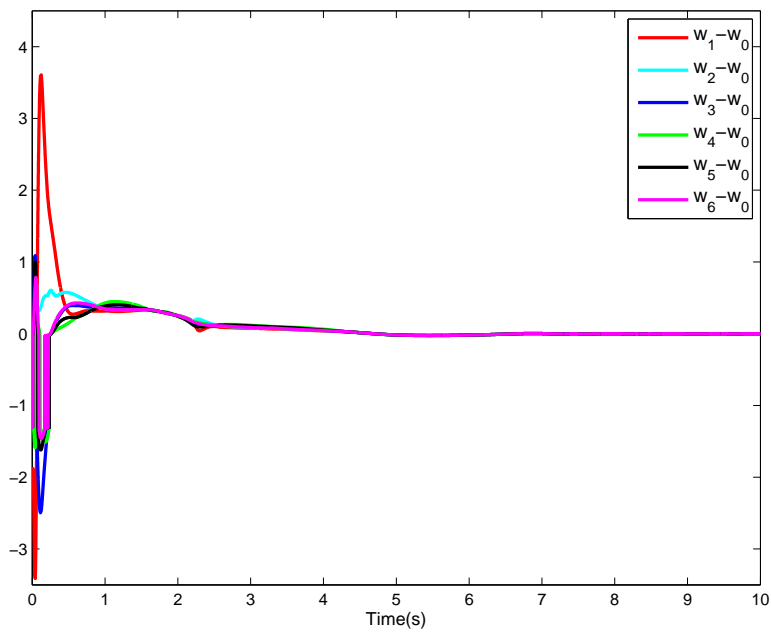


Figure 4.6: The tracking errors $w_i - w_0$ ($1 \leq i \leq 6$).

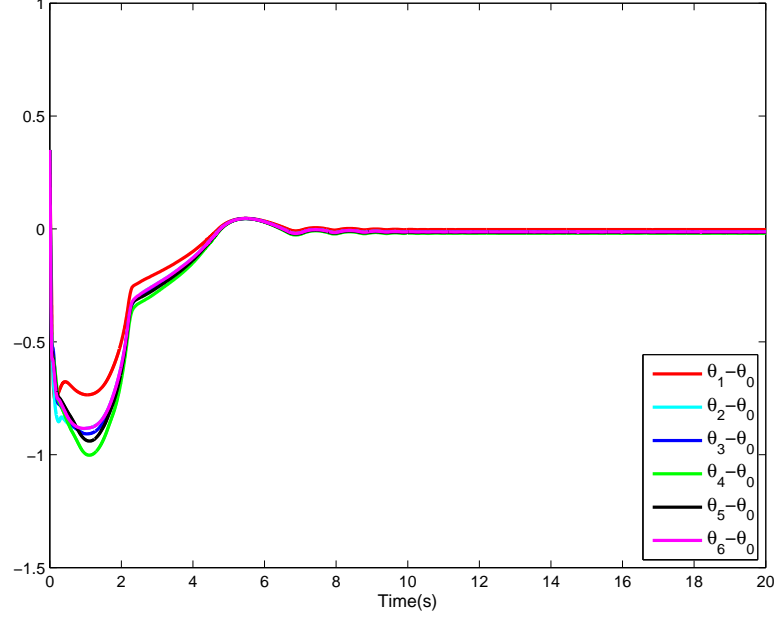


Figure 4.7: The tracking errors $\theta_i - \theta_0$ ($1 \leq i \leq 6$).

Fig. 4.1 shows the trajectory of virtual leader (black line), the trajectory of centroid of the six followers (blue line), and the formation positions and pattern of the six followers at some moments. It can be seen from Fig. 4.1 that the six robots converge to a desired geometry pattern under the proposed distributed controllers (4.22) and (4.21), i.e., the equation (4.9) is verified. Fig. 4.2 shows the trajectories of x_0 (blue line) and the centroid of x_i ($1 \leq i \leq 6$) (red line). Fig. 4.3 shows the trajectories of y_0 (blue line) and the centroid of y_i ($1 \leq i \leq 6$) (red line). From Fig. 4.2 and Fig. 4.3, the trajectory of the formation geometric centroid converges to the trajectory of virtual leader, that is to say, the equation (4.11) is verified. Fig. 4.4 and Fig. 4.5 show the tracking error \tilde{u}_{wi} for ($1 \leq i \leq 6$) and \tilde{u}_{vi} for ($1 \leq i \leq 6$) under the torque controller (4.43). From Fig. 4.4 and Fig. 4.5, \tilde{u}_{wi} and \tilde{u}_{vi} respectively converge to zero. The perfect tracking of velocity and angular velocity has been guaranteed. Fig. 4.6 and Fig. 4.7 respectively show the angular velocity tracking errors $w_i - w_0$ and the orientation tracking errors $\theta_i - \theta_0$ between follower Fi ($1 \leq i \leq 6$) and virtual leader. It can be seen from Fig. 4.6 and Fig. 4.7 that $w_i - w_0$ and $\theta_i - \theta_0$ converge to zero over time, i.e., the equation (4.10) and (4.20) are verified.

4. DISTRIBUTED ADAPTIVE FORMATION CONTROL FOR MULTIPLE NONHOLONOMIC WHEELED MOBILE ROBOTS

4.6 Conclusion

In this chapter, the distributed adaptive formation control of multiple nonholonomic wheeled robots has been discussed. The distributed control laws and adaptive dynamics controllers for mobile robots have been developed with the aid of algebraic graph theory, matrix theory, and Lyapunov control approach. In this chapter, the desired trajectory has been considered as the trajectory of a virtual leader, whose information is not required to be available to each robot. Simulation results have verified the effectiveness of theoretical results obtained in previous sections.

Chapter 5

Distributed Consensus-Based Formation Control for Nonholonomic Wheeled Mobile Robots Using Adaptive Neural Network

Contents

5.1	Introduction	108
5.2	Preliminary	108
5.2.1	Dynamics of Nonholonomic Wheeled Mobile robot	110
5.2.2	Neural Network	111
5.2.3	Problem Description	113
5.3	Distributed Control Algorithm	114
5.4	Adaptive Dynamic Controller Design	116
5.4.1	Robot Model and its Properties	116
5.4.2	Controller Design	117
5.5	Neural Network Control Design	122
5.6	Simulation	129
5.6.1	Verification of Formation Control Based on Robust Adaptive Techniques	130

5. DISTRIBUTED CONSENSUS-BASED FORMATION CONTROL FOR NONHOLONOMIC WHEELED MOBILE ROBOTS USING ADAPTIVE NEURAL NETWORK

5.6.2	Verification of Formation Control Based on Neural Network Techniques	134
5.7	Conclusion	140

5.1 Introduction

In this chapter, we will consider the formation control problem for the wheeled mobile robots, in which the dynamic model of the wheeled mobile robot has the friction term and bounded disturbance term. In the previous chapter, we considered the dynamics model of the wheeled mobile robot ignoring the friction term and bounded disturbance term. In some practical applications, the friction term and bounded disturbance term should not be ignored and practical control strategies accounting for the friction term and bounded disturbance term should be implemented. Firstly, we consider that the partial knowledge of the mobile robot dynamics is available. An asymptotically stable torque controller is proposed by using robust adaptive control techniques to account for unmodeled dynamics and bounded disturbances. Next, we consider that the dynamics of the mobile robot are unknown. Note that from the previous literatures (Fierro & Lewis (1998)) the neural network controller can relax the knowledge of the dynamics. Therefore the universal approximation property of neural network is used to relax the knowledge of the dynamics system, and an asymptotically robust adaptive controller augmented with the neural network is derived to achieve asymptotic tracking.

5.2 Preliminary

Let \mathbb{R} denote the real numbers, \mathbb{R}^p denote the real p vectors, $\mathbb{R}^{p \times q}$ denote the real $p \times q$ matrices, and the $\|\cdot\|_m$ denote the m -norm.

Definition 5.1 (Meyer 2000) *Let $x = (x_1, x_2, \dots, x_p) \in \mathbb{R}^p$, the \mathbb{R}^p is Euclidean Space, if $1 \leq m < +\infty$,*

$$\|x\|_m = \left(\sum_{j=1}^p (x_j)^m \right)^{1/m}$$

if $m = \infty$,

$$\|x\|_\infty = \max_{1 \leq j \leq p} |x_j|$$

Especially, if $m = 1$, $\|x\|_1 = \sum_{j=1}^p |x_j|$, and if $m = 2$, named the Euclid norm, denote $\|\cdot\|_2$, $\|x\|_2 = \sqrt{\sum_{j=1}^p (x_j)^2}$.

Definition 5.2 (*Meyer 2000*) *The Cauchy-Bunyakovskii-Schwarz (CBS) Inequality:*

$$\|x^T y\|_2 \leq \|x\|_2 \cdot \|y\|_2, \quad \text{for all } x, y \in \mathbb{R}^{p \times 1} \quad (5.1)$$

Equality holds if and only if $y = \alpha x$ for $\alpha = \frac{x^T y}{x^T x}$.

Definition 5.3 (*Meyer 2000*) *Given $A = [a_{ij}]$, $B \in \mathbb{R}^{p \times q}$, the Frobenius norm is defined by*

$$\|A\|_F^2 = \text{tr}(A^T A) = \sum_{i,j} a_{ij}^2,$$

and the associated inner product is defined by

$$\langle A, B \rangle_F = \text{tr}(A^T B),$$

where $\text{tr}(\cdot)$ is the trace, and $\text{tr}(A) = \sum_{i=1}^p a_{ii}$.

Matrix multiplication distinguishes matrix spaces from more general vector spaces, but the three vector-norm properties say nothing about products. The CBS inequality insures that

$$\|Ax\|_2^2 \leq \left(\sum_{i,j} a_{ij}^2 \right) \cdot \|x\|_2^2 = \|A\|_F^2 \|x\|_2^2, \quad (5.2)$$

where $A \in \mathbb{R}^{q \times p}$ and $x \in \mathbb{R}^p$ and we express this by saying that the Frobenius matrix norm $\|\cdot\|_F$ and the Euclidean vector norm $\|\cdot\|_2$ are compatible.

From the compatible condition (5.2), it can be obtained that

$$\langle A, B \rangle_F = \text{tr}(A^T B) = \|AB\|_F \leq \|A\|_F \|B\|_F, \quad (5.3)$$

Definition 5.4 (*Petersen & Pedersen 2012*) *Assume $F(x)$ to be a differentiable function of each of the elements of x . It then holds that*

$$\frac{d \text{tr}(F(x))}{dx} = f(x)^T,$$

5. DISTRIBUTED CONSENSUS-BASED FORMATION CONTROL FOR NONHOLONOMIC WHEELED MOBILE ROBOTS USING ADAPTIVE NEURAL NETWORK

where $f(\cdot)$ is the scalar derivative of $F(\cdot)$.

The derivatives of traces have the following properties (Petersen & Pedersen 2012):

$$\frac{dtr(x)}{dx} = I, \quad (5.4)$$

$$\frac{dtr(x^T A)}{dx} = \frac{dtr(A^T x)}{dx} = A, \quad (5.5)$$

$$\frac{dtr(xA)}{dx} = \frac{dtr(Ax^T)}{dx} = A^T, \quad (5.6)$$

$$\frac{dtr(x^T Ax)}{dx} = (A + A^T)x \quad (5.7)$$

5.2.1 Dynamics of Nonholonomic Wheeled Mobile robot

Consider a multi-robot system consisting of m nonholonomic wheeled mobile robots indexed by $1, 2, \dots, m$. The nonholonomic dynamics model of the mobile robot j can be described by the Euler-Lagrange equation as follows

$$M_j(q_j)\ddot{q}_j + C_j(q_j, \dot{q}_j)\dot{q}_j + F_j(\dot{q}_j) + G_j(q_j) + \tau_{dj} = B(q_j)\tau_j - A^T(q_j)\lambda, \quad j = 1, \dots, m, \quad (5.8)$$

where q_j is the generalized coordinates, $M_j(q_j) \in \mathbb{R}^{3 \times 3}$ is a symmetric positive definite inertia matrix, $C_j(q_j, \dot{q}_j) \in \mathbb{R}^{3 \times 3}$ is the bounded centripetal and coriolis matrix, $F_j(\dot{q}_j) \in \mathbb{R}^{3 \times 1}$ denotes surface friction. $G_j(q_j) \in \mathbb{R}^{3 \times 1}$ is the gravitations vector, τ_{dj} denotes bounded unknown disturbances including unstructured unmodeled dynamics. $B_j(q_j) \in \mathbb{R}^{3 \times 2}$ is the input transformation matrix, $\tau_j \in \mathbb{R}^{2 \times 1}$ is the control torque vector, $A_j(q) \in \mathbb{R}^{1 \times 3}$ is the matrix associated with the constraints, and $\lambda_j \in \mathbb{R}^{1 \times 1}$ is the vector of constraint forces.

Similar to the discussions in Section 4.2.1, all the kinematic equality constraints are independent of time, and can be expressed as follows:

$$A(q_j)\dot{q}_j = 0, \quad (5.9)$$

the wheeled mobile robot satisfies the following nonholonomic constraint:

$$\dot{y}_j \cos \theta_j - \dot{x}_j \sin \theta_j = 0. \quad (5.10)$$

and the kinematics model of the mobile robot $j \in \{1, \dots, m\}$ can be written as

$$\dot{q}_j = \begin{bmatrix} \dot{x}_j \\ \dot{y}_j \\ \dot{\theta}_j \end{bmatrix} = \begin{bmatrix} \cos \theta_j & 0 \\ \sin \theta_j & 0 \\ 0 & 1 \end{bmatrix} \begin{bmatrix} v_j \\ w_j \end{bmatrix} = S(q_j) \bar{v}_j. \quad (5.11)$$

From (5.9) and (5.11), it is easily obtained that

$$S^T(q_j) A^T(q_j) = 0. \quad (5.12)$$

We consider the wheeled mobile robot with two driving wheels, which is shown in Fig. 3.1. The geometrical center of robot is C , which is the center of mass of the robot. The trajectory of the mobile robot is constrained to the horizontal plane, i.e. $G_j(q_j) = 0$.

The equation (5.8) has the following properties (Lewis *et al.* (1993)).

Property 5.5 *The inertia matrix $M_j(q_j)$ is symmetric positive definite, and satisfies the following inequality*

$$m_1 \|q_j\|^2 \leq q_j^T M_j(q_j) q_j \leq m_2 \|q_j\|^2, q_j \in \mathbb{R}^3, \quad (5.13)$$

where m_1, m_2 are positive constants, and $\|\cdot\|$ is the standard Euclidean norm.

Property 5.6 *$\dot{M}_j(q_j) - 2C_j(q_j, \dot{q}_j)$ is skew symmetric, that is to say,*

$$\xi^T \left[\frac{1}{2} \dot{M}_j(q_j) - C_j(q_j, \dot{q}_j) \right] \xi = 0. \quad \forall \xi \in \mathbb{R}^3. \quad (5.14)$$

Property 5.7 *The unknown disturbance satisfies $\|\tau_{dj}\| < d_M$ with d_M a known positive constant.*

5.2.2 Neural Network

The Fig. 5.1 shows a two-layer feedforward Neural Network. The Neural Network output y is a vector with m components determined in terms of the n components of the input vector x by the following formula Fierro & Lewis (1998)

$$y_i = \sum_{j=1}^{N_b} [w_{ij} \sigma(\sum_{k=1}^p v_{jk} x_k + \theta_{vj}) + \theta_{wi}], \quad i = 1, \dots, m, \quad (5.15)$$

5. DISTRIBUTED CONSENSUS-BASED FORMATION CONTROL FOR NONHOLONOMIC WHEELED MOBILE ROBOTS USING ADAPTIVE NEURAL NETWORK

where $\sigma(\cdot)$ are the activation functions N_h is the number of hidden-layer neurons. The inputs-to-hidden-layer interconnection weights are denoted by v_{jk} and the hidden-layer-to-outputs interconnection weights by w_{ij} . The threshold offset are denoted by θ_{vj} , θ_{wi} . The sigmoid activation function is given by

$$\sigma(x) = \frac{1}{1 + e^{-x}}. \quad (5.16)$$

Let $f(x)$ be a smooth function from \mathcal{R}^p to \mathcal{R}^q . According to the function approximations property, it can be shown that as long as x is restricted to a compact set U_x of \mathcal{R}^p , for some number of hidden layer neurons N_h , there exist weights and thresholds such that

$$f(x) = W^T \sigma(V^T x) + \epsilon. \quad (5.17)$$

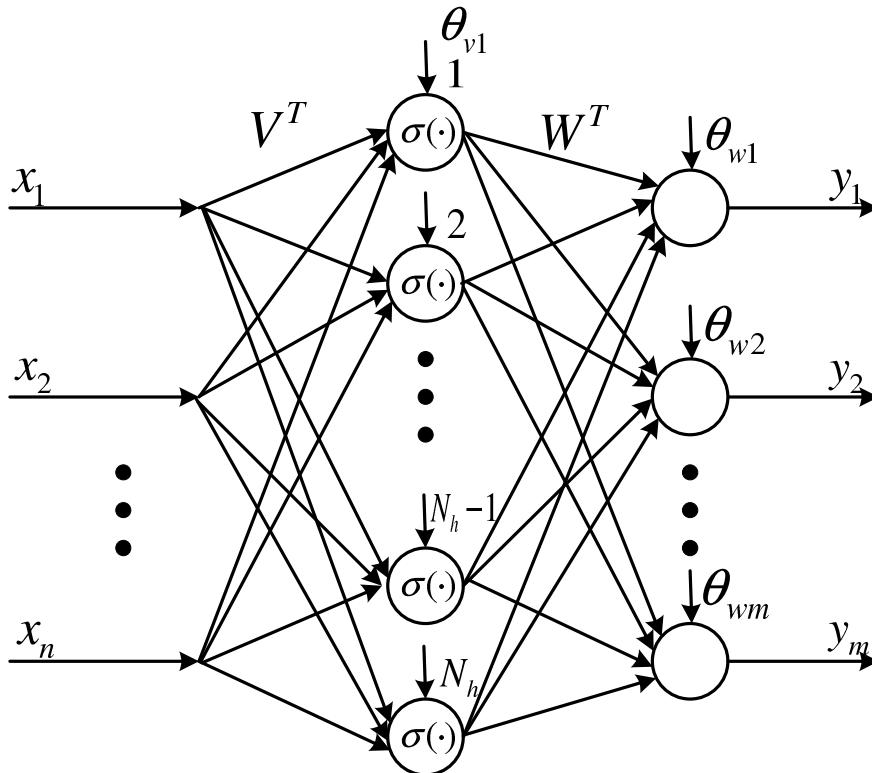


Figure 5.1: Two-layer feedforward Neural Network structure

5.2.3 Problem Description

Similar to Chapter 3 and 4, in this chapter the desired geometric pattern \mathcal{F} of m mobile robots is still defined by using orthogonal coordinates (p_{jx}, p_{jy}) , which satisfies

$$\sum_{j=1}^m p_{jx} = p_{0x}, \quad \sum_{j=1}^m p_{jy} = p_{0y}. \quad (5.18)$$

where (p_{0x}, p_{0y}) is the center of the geometric pattern \mathcal{F} . Without loss of generality, we also assume that $p_{0x} = 0, p_{0y} = 0$.

In this chapter, we will still design the control inputs v_j and w_j for the wheeled nonholonomic mobile robot j using its states (q_j, \dot{q}_j) , (p_{jx}, p_{jy}) , and its neighbors's states (q_i, \dot{q}_i) and (p_{ix}, p_{iy}) for $i \in \mathcal{N}_j$, to achieve our control objective (1): a group of such robots converge to the desired formation pattern \mathcal{F} , (2): the orientation of each robot converges to a desired value θ_0 , and (3): the geometric centroid of the formation converges to the desired reference trajectory (x_0, y_0) , that is to say,

$$\lim_{t \rightarrow \infty} \begin{bmatrix} x_j - x_i \\ y_j - y_i \end{bmatrix} = \begin{bmatrix} p_{jx} - p_{ix} \\ p_{jy} - p_{iy} \end{bmatrix}, \quad (5.19)$$

$$\lim_{t \rightarrow \infty} (\theta_j - \theta_0) = 0, \quad (5.20)$$

$$\lim_{t \rightarrow \infty} \left(\sum_{j=1}^m \frac{x_j}{m} - x_0 \right) = 0, \quad \lim_{t \rightarrow \infty} \left(\sum_{j=1}^m \frac{y_j}{m} - y_0 \right) = 0. \quad (5.21)$$

Similarly, the geometric centroid (x_0, y_0) and the desired value θ_0 are considered as the posture of a virtual leader 0,

$$\dot{x}_0 = v_0 \cos \theta_0, \quad \dot{y}_0 = v_0 \sin \theta_0, \quad \dot{\theta}_0 = w_0. \quad (5.22)$$

To achieve our control objective, the same assumptions Assumption 3.1 and Assumption 3.3 in Section 3.3 are needed.

5. DISTRIBUTED CONSENSUS-BASED FORMATION CONTROL FOR NONHOLONOMIC WHEELED MOBILE ROBOTS USING ADAPTIVE NEURAL NETWORK

5.3 Distributed Control Algorithm

In this chapter, we consider the same transformation used in Chapter 4:

$$\begin{aligned}
 z_{1j} &= \theta_j, \\
 z_{2j} &= (x_j - p_{jx}) \cos \theta_j + (y_j - p_{jy}) \sin \theta_j + k_0 \text{sign}(u_{1j}) z_{3j}, \\
 z_{3j} &= (x_j - p_{jx}) \sin \theta_j - (y_j - p_{jy}) \cos \theta_j, \\
 u_{1j} &= w_j, \\
 u_{2j} &= v_j - (1 + k_0^2) u_{1j} z_{3j} + k_0 |u_{1j}| z_{2j},
 \end{aligned} \tag{5.23}$$

where $0 \leq j \leq m$, $k_0 > 0$, and $\text{sign}(\cdot)$ is the signum function. The dynamic system of (5.23) is given as follows

$$\dot{z}_{1j} = u_{1j}, \tag{5.24}$$

$$\dot{z}_{2j} = u_{2j}, \tag{5.25}$$

$$\dot{z}_{3j} = u_{1j} z_{2j} - k_0 |u_{1j}| z_{3j}. \tag{5.26}$$

Then according to (5.23)-(5.26), we obtain the same control objective in Chapter 4 as

$$\lim_{t \rightarrow \infty} (z_{1j} - z_{10}) = 0, \tag{5.27}$$

$$\lim_{t \rightarrow \infty} (z_{2j} - z_{20}) = 0, \tag{5.28}$$

$$\lim_{t \rightarrow \infty} (z_{3j} - z_{30}) = 0, \tag{5.29}$$

$$\lim_{t \rightarrow \infty} (u_{1j} - u_{10}) = 0. \tag{5.30}$$

Lemma 5.8 *If the equations (5.27)-(5.30) hold for $0 \leq j \leq m$, then the m mobile robots can converge to the formation pattern \mathcal{F} , i.e., the equations (5.19)-(5.21) can be satisfied.*

Proof: The proof is similar to that of Lemma 3.5 and is therefore omitted here.

5.3 Distributed Control Algorithm

Let's consider the same desired control inputs used in Chapter 4 for the mobile robot j as

$$\begin{aligned} u_{1jr} = & u_{10} - \alpha \sum_{i \in \mathcal{N}_j} a_{ji}(z_{1j} - z_{1i}) - \alpha b_j(z_{1j} - z_{10}) \\ & - \beta \text{sign}\left(\sum_{i \in \mathcal{N}_j} a_{ji}(z_{1j} - z_{1i}) + b_j(z_{1j} - z_{10})\right), \end{aligned} \quad (5.31)$$

$$\begin{aligned} u_{2jr} = & -\alpha \sum_{i \in \mathcal{N}_j} a_{ji}(z_{2j} - z_{2i}) - \alpha b_j(z_{2j} - z_{20}) \\ & - \beta \text{sign}\left(\sum_{i \in \mathcal{N}_j} a_{ji}(z_{2j} - z_{2i}) + b_j(z_{2j} - z_{20})\right), \end{aligned} \quad (5.32)$$

where $j = 1, \dots, m$, b_j is a positive constant if the virtual leader's position is available to the follower j , and $b_j = 0$ otherwise, $|\dot{z}_{20}| \leq \kappa$, κ is a positive constant, α is a nonnegative constant, β is a positive constant and satisfies $\beta > \kappa$.

Using the same operation in Section 4.3, define the auxiliary velocity tracking error as

$$\tilde{u}_j = \begin{bmatrix} \tilde{u}_{wj} \\ \tilde{u}_{vj} \end{bmatrix} = \begin{bmatrix} u_{1jr} \\ u_{2jr} \end{bmatrix} - \begin{bmatrix} u_{1j} \\ u_{2j} \end{bmatrix}. \quad (5.33)$$

Then the dynamic system (5.24)-(5.26) become

$$\dot{z}_{1j} = u_{1jr} - \tilde{u}_{wj}, \quad (5.34)$$

$$\dot{z}_{2j} = u_{2jr} - \tilde{u}_{vj}, \quad (5.35)$$

$$\dot{z}_{3j} = (u_{1jr} - \tilde{u}_{wj})z_{2j} - k_0|(u_{1jr} - \tilde{u}_{wj})|z_{3j}. \quad (5.36)$$

The error dynamic system can be rewritten in a vector form as

$$\dot{\tilde{Z}} = -\alpha \mathcal{M} \tilde{Z} - \beta \text{sign}(\mathcal{M} \tilde{Z}) - \dot{f}_0 - \hat{u}, \quad (5.37)$$

where $\hat{u} = [\hat{u}_w, \hat{u}_v]^T = [\tilde{u}_{w1}, \dots, \tilde{u}_{wm}, \tilde{u}_{v1}, \dots, \tilde{u}_{vm}]^T$.

Remark 5.9 Note that the stability of the kinematic error system (5.37) is now dependent on the error \tilde{Z} and the velocity tracking error \hat{u} . The following Theorem 5.10 is given to prove that when $\hat{u} = 0$ (i.e., perfect velocity tracking) the state \tilde{Z} of system (5.37) can converge to zero in finite time.

5. DISTRIBUTED CONSENSUS-BASED FORMATION CONTROL FOR NONHOLONOMIC WHEELED MOBILE ROBOTS USING ADAPTIVE NEURAL NETWORK

Theorem 5.10 *Suppose that the communication graph \mathcal{G} is connected, Assumption 3.3 is satisfied, and the controller for the system (5.37) is chosen by (5.31) and (5.32), if the auxiliary velocity tracking error $\hat{u} = 0$, then the state \tilde{Z} of system (5.37) can converge to zero in finite time, that is to say, $z_{1j} - z_{10}$, $u_{1j} - u_{10}$ and $z_{2j} - z_{20}$ converge to zero in finite time.*

Proof: The proof is same to that of Theorem 4.7 and is therefore omitted here.

Remark 5.11 *From Theorem 5.10, when $\hat{u} = 0$ (i.e., perfect velocity tracking), the state \tilde{Z} of system (5.37) can converge to zero in finite time. As our previous discussion, the “perfect velocity tracking” for mobile robot may not hold in practice, due to the fact that the dynamic model of the wheeled mobile robot has unmodeled dynamics and unknown dynamical disturbances, which will affect the robust tracking of the system. In the next section, we will consider that “perfect velocity tracking” assumption doesn’t hold in practice. Hence, it is necessary to design a suitable torque controller τ_j based on the controller (5.31) and (5.32), guaranteeing the stability of the kinematic error system (30).*

5.4 Adaptive Dynamic Controller Design

5.4.1 Robot Model and its Properties

From the (5.23), it can be easily obtained that

$$\bar{v}_j = \begin{bmatrix} 1 & 0 \\ A & 1 \end{bmatrix} u_j,$$

where $A = (1 + k_0^2) - k_0 \text{sign}(u_{1j})z_{2j}$. According to the (5.11), it follows that

$$\dot{q}_j = s(q)_j \bar{v}_j = S(q_j) \begin{bmatrix} 1 & 0 \\ A & 1 \end{bmatrix} u_j = \hat{S}(q_j) u_j \quad (5.38)$$

where

$$\hat{S} = \begin{bmatrix} (1 + k_0^2)z_{3j} \cos \theta_j + k_0 \text{sign}(u_{1j})z_{2j} & \cos \theta_j \\ (1 + k_0^2)z_{3j} \cos \theta_j + k_0 \text{sign}(u_{1j})z_{2j} & \cos \theta_j \\ 1 & 0 \end{bmatrix}.$$

5.4 Adaptive Dynamic Controller Design

The dynamics (5.8) of the mobile robot can be rewritten as follows

$$\hat{S}^T M_j \hat{S} \dot{u}_j + \hat{S}^T (M_j \dot{\hat{S}} + C_j \hat{S}) u_j + \hat{S}^T F_j + \hat{S}^T G_j = \hat{S}^T B \tau_j - \hat{S}^T \tau_{dj}, \quad j = 1, \dots, m, \quad (5.39)$$

i.e.

$$\bar{M}_j \dot{u}_j + \bar{C}_j u_j + \bar{F}_j + \bar{G}_j = \bar{\tau}_j - \bar{\tau}_{dj}, \quad j = 1, \dots, m, \quad (5.40)$$

where $\bar{M}_j = \hat{S}^T M_j \hat{S}$ is a symmetric positive definite inertia matrix. $\bar{C}_j = \hat{S}^T (M_j \dot{\hat{S}} + C_j \hat{S})$ is the centripetal and coriolis matrix, $\bar{G}_j = \hat{S}^T G_j$ is the gravitation vector, and $\bar{G}_j = 0$. $\bar{F}_j = \hat{S}^T F_j$ is the surface friction, $\bar{\tau}_{dj} = \hat{S}^T \tau_{dj}$ denotes the bounded unknown disturbances including unstructured unmodeled dynamics, and $\bar{\tau}_j = \hat{S}^T B \tau_j$ is the input vector.

Similar to the properties 5.5-5.7, the equation (5.40) has the following properties.

Property 5.12 *The inertia matrix $\bar{M}_j(q_j)$ is symmetric positive definite.*

Property 5.13 *The matrix $\dot{\bar{M}}_j - 2\bar{C}_j$ is skew symmetric.*

Property 5.14 *The unknown disturbance satisfies $\|\bar{\tau}_{dj}\| < \bar{d}_M$ with \bar{d}_M a known positive constant.*

5.4.2 Controller Design

Taking the derivative of (5.33) and multiplying by the inertia matrix \bar{M}_j both sides gives

$$\begin{aligned} \bar{M}_j \dot{\tilde{u}}_j &= \bar{M}_j \dot{u}_{jr} - \bar{M}_j \dot{u}_j \\ &= -\bar{C}_j \tilde{u}_j - \bar{\tau}_j + f_j(u_{jr}, \dot{u}_{jr}) + w_j(t), \quad j = 1, \dots, m, \end{aligned} \quad (5.41)$$

where $f_j(u_{jr}, \dot{u}_{jr}) = \bar{M}_j \dot{u}_{jr} + \bar{C}_j u_{jr}$ is composed of known quantities, and the disturbance term is

$$w_j(t) = \Delta_j + \bar{\tau}_{dj}, \quad j = 1, \dots, m, \quad (5.42)$$

where Δ_j represents any model uncertainties and unmodeled dynamics, and $\bar{\tau}_{dj}$ is the unknown bounded disturbance which could represent any inaccurately modeled dynamics.

5. DISTRIBUTED CONSENSUS-BASED FORMATION CONTROL FOR NONHOLONOMIC WHEELED MOBILE ROBOTS USING ADAPTIVE NEURAL NETWORK

Lemma 5.15 (*Bounds on the Disturbance Term*) (*Fierro & Lewis 1998*) *The disturbance term $w_j(t)$ is bounded according to*

$$\|w_j(t)\| \leq C_0 + C_1\|\tilde{u}_j\| + C_2\|\tilde{u}_j\|^2 = Y_j\Theta_j, \quad (5.43)$$

with C_0, C_1, C_2 depending on the terms like the disturbance bound, the changes in the mass of the robot due to payload, and friction coefficients with Y_j being a known regression vector.

When the robot dynamics are partially known, the torque control algorithm for the dynamics system (5.41) is designed to be

$$\bar{\tau}_j = K_j\tilde{u}_j + f_j(u_{jr}, \dot{u}_{jr}) + \mu_{jr}, \quad (5.44)$$

where K_j is a symmetric positive-definite matrix defined by $K_j = k_j I_2$ with k_j being a positive gain constant and $I_2 \in \mathbb{R}^{2 \times 2}$ being the identity matrix. The nonlinear term μ_{jr} is an adaptive robustifying term and defined as (*Kwan et al. 1995*)

$$\begin{aligned} \mu_{jr} &= \frac{\tilde{u}_j(Y_j\hat{\Theta}_j)^2}{(Y_j\hat{\Theta}_j)\|\tilde{u}_j\| + \delta_j} \\ \dot{\delta}_j &= -\gamma_j\delta_j, \quad \delta_j(0) = C_\delta > 0 \end{aligned} \quad (5.45)$$

where γ_j and C_δ are positive design constants and $Y_j\hat{\Theta}_j$ is the adaptive estimate of the known function $Y_j\Theta_j$. $\hat{\Theta}_j$ is the estimate of Θ_j , and the parameter turning law for the estimate $\hat{\Theta}_j$ is defined as

$$\dot{\hat{\Theta}}_j = \Gamma_j Y_j \|\tilde{u}_j\|, \quad (5.46)$$

where Γ_j is a symmetric and positive definite matrix. Let $\tilde{\Theta}_j$ be the estimation error of the parameter turning law, and $\tilde{\Theta}_j = \Theta_j - \hat{\Theta}_j$. It then follows that $\dot{\hat{\Theta}}_j = -\dot{\tilde{\Theta}}_j$.

Substituting (5.44) into (5.41) and writing in a vector form gives

$$\bar{M}(q)\dot{\tilde{u}} + \bar{C}(q, \dot{q})\tilde{u} = -K\tilde{u} - \mu_r + w(t), \quad (5.47)$$

5.4 Adaptive Dynamic Controller Design

where $\bar{M}(q)$, $\bar{C}(q, \dot{q})$ and K are respectively the block diagonal matrices of $\bar{M}_j(q_j)$, $\bar{C}_j(q_j, \dot{q}_j)$ and K_j , $\mu_r = [\mu_{1r}, \dots, \mu_{mr}]^T$, $w(t) = [w_1, \dots, w_m]^T$, $\bar{\tau}_d = [\bar{\tau}_{d1}, \dots, \bar{\tau}_{dm}]^T$, and $\Delta = [\Delta_1, \dots, \Delta_m]^T$.

Theorem 5.16 *Suppose that the communication graph \mathcal{G} is connected, Assumption 3.3 is satisfied, the velocity controllers for (5.34) and (5.35) are respectively designed by (5.31) and (5.32), and the torque control input for the dynamics system (5.41) is designed by (5.44), if the control gains is chosen as $\alpha \geq \frac{1}{2\lambda_{\max}(\mathcal{M})}$, $\beta \geq \kappa$ and $k_{\max} \geq \frac{\lambda_{\max}(\mathcal{M})}{2}$, where $k_{\max} = \max\{k_1, k_2, \dots, k_m\}$, then, for $1 \leq j \leq m$, the errors $\tilde{z}_{1j} = 0$, $\tilde{z}_{2j} = 0$, $\tilde{u}_{wj} = 0$ and $\tilde{u}_{vj} = 0$ are globally asymptotically stable.*

Proof: Choose the Lyapunov candidate as

$$V = V_1 + V_2, \quad (5.48)$$

where V_1 and V_2 are chosen as

$$V_1 = \frac{1}{2} \tilde{Z}^T \mathcal{M} \tilde{Z}, \quad (5.49)$$

$$V_2 = \frac{1}{2} \tilde{u}^T \bar{M} \tilde{u} + \frac{1}{2} \tilde{\Theta}^T \Gamma^{-1} \tilde{\Theta} + \delta_1 / \gamma_1, \quad (5.50)$$

with $\tilde{\Theta} = [\tilde{\Theta}_1, \dots, \tilde{\Theta}_m]^T$, Γ is the block diagonal matrices of Γ_j . Using the properties of $\mathcal{K}[\cdot]$, the set-valued Lie derivative of V can be obtained as follows

$$\begin{aligned} \dot{V} &= \mathcal{K}[V_1 + V_2] \subseteq \mathcal{K}[V_1] + \mathcal{K}[V_2] \\ &= \dot{V}_1 + \dot{V}_2. \end{aligned} \quad (5.51)$$

Since V_2 is continuous, according to Lemma 1.7, the equality (5.69) holds.

Using the Properties of $\mathcal{K}[\cdot]$, the set-valued Lie derivative of V_1 can be obtained as follows

$$\dot{V}_1 \triangleq \bigcap_{\xi \in \partial V(\tilde{Z})} \xi^T \mathcal{K}[-\alpha \mathcal{M} \tilde{Z} - \beta \text{sign}(\mathcal{M} \tilde{Z}) - \dot{\mathbf{f}}_0 - \hat{u}].$$

where $\partial V_1(\tilde{Z})$ is the generalized gradient of V at \tilde{Z} . Because V_1 is continuously differentiable with respect to \tilde{Z} , $\partial V_1(\tilde{Z}) = \{\mathcal{M} \tilde{Z}\}$, which is a singleton. Therefore, it follows that

5. DISTRIBUTED CONSENSUS-BASED FORMATION CONTROL FOR NONHOLONOMIC WHEELED MOBILE ROBOTS USING ADAPTIVE NEURAL NETWORK

$$\begin{aligned}\dot{\tilde{V}}_1(\tilde{Z}) &= \mathcal{K}[-\alpha \tilde{Z}^T \mathcal{M}^2 \tilde{Z} - \beta \tilde{Z}^T \mathcal{M} \text{sgn}(\mathcal{M} \tilde{Z}) - \tilde{Z}^T \mathcal{M} \dot{\mathbf{f}}_0 - \tilde{Z}^T \mathcal{M} \hat{u}] \\ &= \{-\alpha \tilde{Z}^T \mathcal{M}^2 \tilde{Z} - \beta \tilde{Z}^T \mathcal{M} \text{sgn}(\mathcal{M} \tilde{Z}) - \tilde{Z}^T \mathcal{M} \dot{\mathbf{f}}_0 - \tilde{Z}^T \mathcal{M} \hat{u}\},\end{aligned}\quad (5.52)$$

where the fact that $x^T \text{sign}(x) = \|x\|_1$ has been used. By Lemma 1.7 and Paden & Sastry (1987), if f is continuous, then $\mathcal{K}[f] = \{f\}$. Note that the set-valued Lie derivative $\dot{\tilde{V}}_1$ is a singleton, whose only element is actually \dot{V}_1 . Therefore, it follows that

$$\begin{aligned}\max \dot{\tilde{V}}_1 = \dot{V} &\leq -\alpha \tilde{Z}^T \mathcal{M}^2 \tilde{Z} - (\beta - \kappa) \|\tilde{Z}^T \mathcal{M}\|_1 - \tilde{Z}^T \mathcal{M} \hat{u} \\ &\leq -\alpha \tilde{Z}^T \mathcal{M}^2 \tilde{Z} - (\beta - \kappa) \|\tilde{Z}^T \mathcal{M}\|_1 + \frac{\lambda_{\max}(\mathcal{M})}{2} (\|\tilde{Z}\|_2^2 + \|\hat{u}\|_2^2),\end{aligned}\quad (5.53)$$

where $\beta > \kappa$ and α is positive. Note that \mathcal{M}^2 is symmetric positive definite.

Since V_2 is continuous, it follows that the set-valued Lie derivative of V_2 satisfies $\max \dot{\tilde{V}}_2 = \dot{V}_2$. Hence, we have

$$\begin{aligned}\dot{V}_2 &= \tilde{u}^T \bar{M} \dot{\tilde{u}} + \frac{1}{2} \tilde{u}^T \dot{\bar{M}} \tilde{u} + \tilde{\Theta}^T \Gamma^{-1} \dot{\tilde{\Theta}} + \dot{\delta}_1 / \gamma_1 \\ &= \tilde{u}^T \{-\bar{C} \tilde{u} - K \tilde{u} - \mu_r + w(t)\} + \frac{1}{2} \tilde{u}^T \dot{\bar{M}} \tilde{u} + \tilde{\Theta}^T \Gamma^{-1} \dot{\tilde{\Theta}} - \delta_1 \\ &= -\tilde{u}^T K \tilde{u} + \tilde{u}^T \left(\frac{1}{2} \dot{\bar{M}} - \bar{C}\right) \tilde{u} - \tilde{u}^T \mu_r + \tilde{u}^T w(t) + \tilde{\Theta}^T \Gamma^{-1} \dot{\tilde{\Theta}} - \delta_1.\end{aligned}\quad (5.54)$$

Since the matrix $(\dot{\bar{M}}_j - 2\bar{C}_j)$ is skew symmetric, we have $\tilde{u}_j^T \left[\frac{1}{2} \dot{\bar{M}}_j(q) - \bar{C}_j(q, \dot{q})\right] \tilde{u}_j = 0$. Let $g_j = -\delta_j - \tilde{u}_j^T \mu_{rj} + \tilde{\Theta}^T \Gamma^{-1} \dot{\tilde{\Theta}} + \tilde{u}_j^T w_j(t)$, ($1 \leq j \leq m$). Substituting the robustifying term (5.45) and the disturbance (5.42) into g_j gives

$$\begin{aligned}g_j &\leq -\delta_j - \frac{\|\tilde{u}_j\|^2 (Y_j \hat{\Theta}_j)^2}{(Y_j \hat{\Theta}_j) \|\tilde{u}_j\| + \delta_j} + \|\tilde{u}_j\| Y_j \hat{\Theta}_j \\ &\leq -\delta_j + \frac{\delta_j \|\tilde{u}_j\| (Y_j \hat{\Theta}_j)}{(Y_j \hat{\Theta}_j) \|\tilde{u}_j\| + \delta_j} \\ &\leq -\delta_j \left(1 - \frac{\|\tilde{u}_j\| (Y_j \hat{\Theta}_j)}{(Y_j \hat{\Theta}_j) \|\tilde{u}_j\| + \delta_j}\right) \leq 0.\end{aligned}$$

5.4 Adaptive Dynamic Controller Design

Hence, it can be obtained that

$$\tilde{u}^T \mu_r + \tilde{u}^T (\epsilon + \tau_d) + \dot{\tilde{\Theta}}^T \Gamma \tilde{\Theta} + \dot{\delta}_1 / \gamma_1 \leq 0. \quad (5.55)$$

Substituting (5.55) into (5.54) gives the following inequality

$$\begin{aligned} \dot{V}_2 &\leq -\tilde{u}^T K \tilde{u} + \tilde{u}^T w(t) - \tilde{u}^T \mu_r - \|\tilde{u}\| Y \tilde{\Theta} - \delta_1 \\ &\leq -\tilde{u}^T K \tilde{u}. \end{aligned} \quad (5.56)$$

Now, Substituting (5.53) and (5.56) into the set-valued Lie derivative \dot{V} reveals

$$\begin{aligned} \max \dot{V} = \dot{V} &\leq -\alpha \tilde{Z}^T \mathcal{M}^2 \tilde{Z} - (\beta - \kappa) \|\tilde{Z}^T \mathcal{M}\|_1 + \frac{\lambda_{\max}(\mathcal{M})}{2} (\|\tilde{Z}\|_2^2 + \|\hat{u}\|_2^2) - \tilde{u}^T K \tilde{u} \\ &= -\alpha \tilde{Z}^T \mathcal{M}^2 \tilde{Z} - (\beta - \kappa) \|\tilde{Z}^T \mathcal{M}\|_1 + \frac{\lambda_{\max}(\mathcal{M})}{2} (\|\tilde{Z}\|_2^2 + \|\tilde{u}\|_2^2) - \tilde{u}^T K \tilde{u} \\ &\leq -\alpha \lambda_{\max}^2(\mathcal{M}) \|\tilde{Z}\|_2^2 - (\beta - \kappa) \|\tilde{Z}^T \mathcal{M}\|_1 \\ &\quad + \frac{\lambda_{\max}(\mathcal{M})}{2} (\|\tilde{Z}\|_2^2 + \|\tilde{u}\|_2^2) - k_{\max} \|\tilde{u}\|_2^2 \\ &\leq -\left(\alpha \lambda_{\max}^2(\mathcal{M}) - \frac{\lambda_{\max}(\mathcal{M})}{2}\right) \|\tilde{Z}\|_2^2 - (\beta - \kappa) \|\tilde{Z}^T \mathcal{M}\|_1 \\ &\quad - \left(k_{\max} - \frac{\lambda_{\max}(\mathcal{M})}{2}\right) \|\tilde{u}\|_2^2, \end{aligned}$$

and it is clear that $\max \dot{V} \leq 0$ provided by $\dot{z}_{20} \leq \kappa$, $\alpha > \frac{1}{2\lambda_{\max}(\mathcal{M})}$, $\beta > \kappa$ and $k_{\max} > \frac{\lambda_{\max}(\mathcal{M})}{2}$. It then from Lemma 1.10 that $\tilde{u} \rightarrow 0$ and $\tilde{Z} \rightarrow 0$ as $t \rightarrow \infty$, i.e., $\tilde{z}_{1j} \rightarrow 0$, $\tilde{z}_{2j} \rightarrow 0$, $\tilde{u}_{wj} \rightarrow 0$ and $\tilde{u}_{vj} \rightarrow 0$ as $t \rightarrow \infty$. Therefore, the errors $\tilde{z}_{1j} = 0$, $\tilde{z}_{2j} = 0$, $\tilde{u}_{wj} = 0$ and $\tilde{u}_{vj} = 0$ are globally asymptotically stable. This proof is completed.

Remark 5.17 *From the Theorem 5.16, we have proved that the variables z_{1j} ($1 \leq j \leq m$) and z_{2j} ($1 \leq j \leq m$) respectively converge to z_{10} and z_{20} globally asymptotically under the proposed control laws (5.31), (5.32) and (5.44). In the following Theorem 5.18, we will prove that z_{3j} asymptotically converges to z_{30} under the control laws (5.31), (5.32) and (5.44).*

Theorem 5.18 *Suppose that the communication graph \mathcal{G} is connected, Assumption 3.3 is satisfied, the velocity controllers for (5.34) and (5.35) are respectively designed by (5.31) and (5.32), and the torque control input for the dynamics sys-*

5. DISTRIBUTED CONSENSUS-BASED FORMATION CONTROL FOR NONHOLONOMIC WHEELED MOBILE ROBOTS USING ADAPTIVE NEURAL NETWORK

tem (5.41) is designed by (5.44), If z_{1j} and z_{2j} asymptotically converge to z_{10} and z_{20} , then z_{3j} also asymptotically converges to z_{30} .

Proof: The proof is similar to that of Theorem 4.14 and is therefore omitted here.

Remark 5.19 From the Theorems 5.16 and 5.18, our control objectives (5.27)-(5.30) is held under the distributed kinematic controller (5.31),(5.32) and the torque controller (5.44). Therefore from the Lemma 5.8, the m mobile robots converge to the formation pattern \mathcal{F} , i.e., the equations (5.19)-(5.21) are satisfied.

5.5 Neural Network Control Design

In the previous sections, the distributed control laws have been proposed under the assumption that the dynamics are partially known. In this section, we assume that the dynamics are not known.

When the robot dynamics are known, the torque controller for the (5.41) is (5.44), where $f_j(u_{jr}, \dot{u}_{jr})$ is known. However since the knowledge of the robot dynamics is no longer available, $f_j(u_{jr}, \dot{u}_{jr})$ can no longer be computed. Therefore, according to the function approximation property, there exists an ideal Neural Network weights W_j and V_j , such that the nonlinear function $H_j(\chi_j) = f_j(u_{jr}, \dot{u}_{jr}) + \Delta_j$ can be given as

$$H_j(\chi_j) = W_j^T \sigma(V_j^T \chi_j) + \epsilon_j. \quad (5.57)$$

where ϵ_j is the Neural Network approximation error, and ϵ_j is bounded by a known constant ϵ_N .

Assumption 5.20 The ideal weights are bounded by known positive values so that

$$\|V_j\|_F \leq V_M, \quad \|W_j\|_F \leq W_M. \quad (5.58)$$

Define the Neural Network function estimate by

$$\hat{H}_j(\chi_j) = \hat{W}_j^T \sigma_j(\hat{V}_j^T \chi_j), \quad (5.59)$$

5.5 Neural Network Control Design

where \hat{W}_j is the estimate of the ideal Neural Network weight. Design the torque inputs for the robot j as

$$\bar{\tau}_j = K_j \tilde{u}_j + \hat{W}_j^T \sigma_j(V_j^T \chi_j) + \mu_{jr}, \quad (5.60)$$

where K_j is a symmetric positive-definite matrix defined by $K_j = k_j I$ with k_j being a positive gain constant and I being the identity matrix. \hat{W}_j is the estimate of the ideal Neural Network weight that is provided by on-line weight turning algorithm. The weight turning algorithm is defined as

$$\dot{\hat{W}}_j = \Xi_j \sigma_j(V_j^T x) \tilde{u}_j - \phi_j \|\tilde{u}_j\| \Xi_j \hat{W}_j, \quad (5.61)$$

where Ξ_j is a symmetric and positive definite matrix governing the speed of convergence of the algorithm, and $\phi_j > 0$ is a small design parameter. The weight estimation error for robot j can be defined as $\tilde{W}_j = W_j - \hat{W}_j$. The nonlinear term μ_j to be defined later is used to compensate for error function robustness in the face of functional reconstruction error and the bounded disturbance $\bar{\tau}_{dj}$.

Substituting (5.44) into (5.41), the error dynamic of robot j produces the closed-loop error dynamics shown below

$$\begin{aligned} \bar{M}_j \dot{\tilde{u}}_j &= -(K_j + \bar{C}_j) \tilde{u}_j + H_j(\chi_j) - \hat{W}_j^T \sigma_j(V_j^T \chi_j) - \mu_{jr} + \bar{\tau}_{dj} + \epsilon_j, \\ &= -(K_j + \bar{C}_j) \tilde{u}_j + \tilde{W}_j^T \sigma_j(V_j^T \chi_j) - \mu_{jr} + \bar{\tau}_{dj} + \epsilon_j, \quad j = 1, \dots, m, \end{aligned} \quad (5.62)$$

where $\tilde{W}_j^T \sigma_j(V_j^T \chi_j) = W_j \sigma_j(V_j^T \chi_j) - \hat{W}_j \sigma_j(V_j^T \chi_j)$ is the Neural Network error estimation function. Let the disturbance terms $w_j(t) = \bar{\tau}_{dj} + \epsilon_j$. Hence, the closed-loop system (5.62) can be written in a vector form as

$$\bar{M}(q) \dot{\tilde{u}} + \bar{C}(q, \dot{q}) \tilde{u} = -K \tilde{u} + \tilde{W}^T \sigma(V^T \chi) - \mu_r + \epsilon + \bar{\tau}_d, \quad (5.63)$$

where \bar{M} , \bar{C} and K are respectively the block diagonal matrices of $\bar{M}_j(q_j)$, $\bar{C}_j(q_j, \dot{q}_j)$ and K_j , ($1 \leq j \leq m$), $\mu_r = [\mu_{1r}, \dots, \mu_{mr}]^T$, $\bar{\tau}_d = [\bar{\tau}_{d1}, \dots, \bar{\tau}_{dm}]^T$, $\epsilon = [\epsilon_1, \dots, \epsilon_m]^T$, and $\tilde{W} = [\tilde{W}_1, \dots, \tilde{W}_m]^T$.

Define the function $\varphi_j(t)$ as

$$\begin{aligned} \varphi_j(t) &= \epsilon_N + \bar{d}_M + \phi_j W_M \|\hat{W}\|_F + \nu_{j1} \|\tilde{z}_{1j}\| + \nu_{j2} \|\tilde{z}_{2j}\| + \nu_{j3} \|\tilde{u}_j\| \\ &\quad + \nu_{j4} \|\tilde{z}_{1j}\|^2 + \nu_{j5} \|\tilde{z}_{2j}\|^2 + \nu_{j6} \|\tilde{u}_j\|^2, \end{aligned} \quad (5.64)$$

5. DISTRIBUTED CONSENSUS-BASED FORMATION CONTROL FOR NONHOLONOMIC WHEELED MOBILE ROBOTS USING ADAPTIVE NEURAL NETWORK

which can be linearly parameterized as $\varphi_j(t) = Y_j\Theta_j$, where the vectors Y_j and Θ_j are respectively defined as follows

$$\begin{aligned} Y_j &= [1 \quad \phi_j \|\hat{W}\|_F \quad \|\tilde{z}_{1j}\| \quad \|\tilde{z}_{2j}\| \quad \|\tilde{u}_j\| \quad \|\tilde{z}_{1j}\|^2 \quad \|\tilde{z}_{2j}\|^2 \quad \|\tilde{u}_j\|^2]^T, \\ \Theta_j &= [\lambda_{j1} \quad \lambda_{j2} \quad \lambda_{j3} \quad \lambda_{j4} \quad \lambda_{j5} \quad \lambda_{j6} \quad \lambda_{j7} \quad \lambda_{j8}]^T, \end{aligned}$$

with Y_j being a known regression vector, λ_{j*} being a positive bounding constant which depends on the disturbance bound, friction coefficients, Neural Network approximation error bound, and the ideal Neural Network weights.

The nonlinear term μ_{jr} in (5.62) is an adaptive robustifying term and is defined as [Kwan *et al.* \(1995\)](#)

$$\mu_{jr} = \frac{\tilde{u}_j(Y_j\hat{\Theta}_j)^2}{(Y_j\hat{\Theta}_j)\|\tilde{u}_j\| + \delta_j}, \quad (5.65)$$

where δ_j satisfies $\dot{\delta}_j = -\gamma_j\delta_j$, $\delta_j(0) = C_\delta > 0$ with γ_j and C_δ being positive design constants, $Y_j\hat{\Theta}_j$ is the adaptive estimate of the known function $Y_j\Theta_j$, $\hat{\Theta}_j$ is the estimate of Θ_j , and the parameter turning law for the estimate $\hat{\Theta}_j$ is defined as

$$\dot{\hat{\Theta}}_j = \Gamma_j Y_j \|\tilde{u}_j\|, \quad (5.66)$$

with Γ_j being a symmetric and positive definite matrix. Let $\tilde{\Theta}_j$ be the estimation error of the parameter turning law, and $\tilde{\Theta}_j = \Theta_j - \hat{\Theta}_j$. It then follows that $\dot{\tilde{\Theta}}_j = -\dot{\hat{\Theta}}_j$.

Theorem 5.21 *Suppose that the communication graph \mathcal{G} is connected, Assumption 3.3 is satisfied, the velocity controllers for (5.34) and (5.35) are respectively designed by (5.31) and (5.32), and the torque control input for the dynamics system (5.62) is designed by (5.60), if the control gains are chosen as $\alpha > \frac{1}{2\lambda_{max}(\mathcal{M})}$, $\beta > \kappa$ and $k_{max} > \frac{\lambda_{max}(\mathcal{M})}{2}$, where $k_{max} = \max\{k_1, k_2, \dots, k_m\}$, then, for $1 \leq j \leq m$, the errors $\tilde{z}_{1j} = 0$, $\tilde{z}_{2j} = 0$, $\tilde{u}_{wj} = 0$ and $\tilde{u}_{vj} = 0$ are globally asymptotically stable.*

Proof: Consider the Lyapunov function candidate as follows

$$V = V_1 + V_2, \quad (5.67)$$

where V_1 is defined in (5.49),

$$V_2 = \frac{1}{2}\tilde{u}^T \bar{M} \tilde{u} + \frac{1}{2}tr\{\tilde{W}^T \Xi^{-1} \tilde{W}\} + \frac{1}{2}\tilde{\Theta}^T \Gamma \tilde{\Theta} + \delta_1/\gamma_1, \quad (5.68)$$

with $\tilde{\Theta} = [\tilde{\Theta}_1, \dots, \tilde{\Theta}_m]^T$, and Γ is the block diagonal matrices of Γ_j . Using the properties of $\mathcal{K}[\cdot]$, the set-valued Lie derivative of V can be obtained as follows

$$\begin{aligned} \dot{V} &= \mathcal{K}[V_1 + V_2] \subseteq \mathcal{K}[V_1] + \mathcal{K}[V_2] \\ &= \dot{V}_1 + \dot{V}_2. \end{aligned} \quad (5.69)$$

Since V_2 is continuous, according to Lemma 1.7, the equality (5.69) holds.

The set-valued Lie derivative of V_1 satisfies the inequality (5.53). Since V_2 is continuous, it follows that the set-valued Lie derivative of V_2 satisfies $\max \dot{V}_2 = \dot{V}_2$. Hence, we have

$$\begin{aligned} \dot{V}_2 &= \tilde{u}^T \bar{M} \dot{\tilde{u}} + \frac{1}{2}\tilde{u}^T \dot{\bar{M}} \tilde{u} + tr\{\tilde{W}^T \Gamma^{-1} \dot{\tilde{W}}\} + \dot{\tilde{\Theta}}^T \Gamma \tilde{\Theta} + \dot{\delta}_1/\gamma_1 \\ &= \tilde{u}^T \{-\bar{C} \tilde{u} - K \tilde{u} + \tilde{W}^T \sigma(V^T x) - \mu_r + \epsilon + \bar{\tau}_d\} + \frac{1}{2}\tilde{u}^T \dot{\bar{M}} \tilde{u} \\ &\quad + tr\{\tilde{W}^T \Xi^{-1} \dot{\tilde{W}}\} + \dot{\tilde{\Theta}}^T \Gamma \tilde{\Theta} + \dot{\delta}_1/\gamma_1. \end{aligned} \quad (5.70)$$

Note that if $x \in \mathcal{R}$ and a is a constant value, the following properties are satisfied,

$$\begin{aligned} tr\{x\} &= x, \\ tr\{a \cdot x\} &= a \cdot tr\{x\}. \end{aligned}$$

Then, it follows that $tr\{-\tilde{W}^T \sigma(V^T \chi) \tilde{u}\} = -\tilde{W}^T \sigma(V^T \chi) \tilde{u}$. Since $\dot{M}_j(q) - 2\bar{C}_j$ is skew symmetry, it follows that

$$\tilde{u}_j^T \left[\frac{1}{2} \dot{M}_j(q) - \bar{C}_j(q, \dot{q}) \right] \tilde{u}_j = 0.$$

5. DISTRIBUTED CONSENSUS-BASED FORMATION CONTROL FOR NONHOLONOMIC WHEELED MOBILE ROBOTS USING ADAPTIVE NEURAL NETWORK

Then substituting the Neural Network weight (5.61) into (5.70), we get

$$\begin{aligned}
\dot{V}_2 &= \tilde{u}^T \{-\bar{C}\tilde{u} - K\tilde{u} + \tilde{W}^T \sigma(V^T x) - \mu_r + \epsilon + \bar{\tau}_d\} + \frac{1}{2} \tilde{u}^T \dot{M} \tilde{u} \\
&\quad + \text{tr}\{\tilde{W}^T \Xi^{-1} \{\Xi_j \sigma(V^T \chi) \tilde{u} - \phi \|\tilde{u}\| \Xi \hat{W}\} + \dot{\Theta}^T \Gamma \tilde{\Theta} + \delta_1 / \gamma_1 \\
&= -\tilde{u}^T K \tilde{u} + \tilde{u}^T \left\{ \frac{1}{2} \dot{M} - \bar{C} \right\} \tilde{u} - \tilde{u}^T \mu_r + \tilde{u}^T (\epsilon + \bar{\tau}_d) + \tilde{\Theta}^T \Gamma \dot{\Theta} \\
&\quad + \tilde{u}^T \tilde{W}^T \sigma(V^T \chi) + \text{tr}\{\tilde{W}^T \Xi^{-1} \{-\Xi \sigma(V^T \chi) \tilde{u} + \phi \|\tilde{u}\| \Xi \hat{W}\}\} + \delta_1 / \gamma_1 \\
&= -\tilde{u}^T K \tilde{u} - \tilde{u}^T \mu_r + \tilde{u}^T (\epsilon + \bar{\tau}_d) + \dot{\Theta}^T \Gamma \tilde{\Theta} \tag{5.71} \\
&\quad + \tilde{u}^T \tilde{W}^T \sigma(V^T \chi) + \text{tr}\{-\tilde{W}^T \sigma(V^T \chi) \tilde{u} + \phi \|\tilde{u}\| \tilde{W}^T \hat{W}\} + \delta_1 / \gamma_1 \\
&= -\tilde{u}^T K \tilde{u} - \tilde{u}^T \mu_r + \tilde{u}^T (\epsilon + \bar{\tau}_d) + \dot{\Theta}^T \Gamma \tilde{\Theta} \\
&\quad + \tilde{u}^T \tilde{W}^T \sigma(V^T \chi) + \text{tr}\{-\tilde{W}^T \sigma(V^T \chi) \tilde{u}\} + \text{tr}\{\phi \|\tilde{u}\| \tilde{W}^T \hat{W}\} + \delta_1 / \gamma_1 \\
&= -\tilde{u}^T K \tilde{u} - \tilde{u}^T \mu_r + \tilde{u}^T (\epsilon + \bar{\tau}_d) + \dot{\Theta}^T \Gamma \tilde{\Theta} + \phi \|\tilde{u}\| \text{tr}\{\tilde{W}^T \hat{W}\} + \delta_1 / \gamma_1,
\end{aligned}$$

where the fact $\dot{\Theta}_j = -\dot{\Theta}_j$ has been used. Since

$$\begin{aligned}
\text{tr}\{\tilde{W}^T \hat{W}\} &= \langle \tilde{W}, W \rangle - \|\tilde{W}\|_F^2 \\
&\leq \|\tilde{W}\|_F \|W\|_F - \|\tilde{W}\|_F^2, \tag{5.72}
\end{aligned}$$

Hence, the (5.71) can obtain the following inequality,

$$\begin{aligned}
\dot{V}_2 &= -\tilde{u}^T K \tilde{u} - \tilde{u}^T \mu_r + \tilde{u}^T (\epsilon + \bar{\tau}_d) + \dot{\Theta}^T \Gamma \tilde{\Theta} + \phi \|\tilde{u}\| \text{tr}\{\tilde{W}^T \hat{W}\} + \delta_1 / \gamma_1 \\
&\leq -\tilde{u}^T K \tilde{u} - \tilde{u}^T \mu_r + \tilde{u}^T (\epsilon + \bar{\tau}_d) + \dot{\Theta}^T \Gamma \tilde{\Theta} \\
&\quad + \phi \|\tilde{u}\| \{ \|\tilde{W}\|_F \|W\|_F - \|\tilde{W}\|_F^2 \} + \delta_1 / \gamma_1 \tag{5.73} \\
&= -\tilde{u}^T K \tilde{u} - \phi \|\tilde{u}\| \|\tilde{W}\|_F^2 - \tilde{u}^T \mu_r + \tilde{u}^T (\epsilon + \bar{\tau}_d) + \dot{\Theta}^T \Gamma \tilde{\Theta} \\
&\quad + \phi W_M \|\tilde{u}\| \|\tilde{W}\|_F + \delta_1 / \gamma_1.
\end{aligned}$$

Define the function Ω_j , ($1 \leq j \leq m$) as follows

$$\Omega_j = -\delta_j - \tilde{u}_j^T \mu_{rj} + \dot{\Theta}_j^T \Gamma^{-1} \tilde{\Theta}_j + \tilde{u}_j^T (\epsilon_j + \bar{\tau}_{dj}) + \phi_j W_M \|\tilde{u}_j\| \|\tilde{W}_j\|_F.$$

Substituting the robustifying term (5.65) into Ω_j gives

$$\begin{aligned}
 \Omega_j &= -\delta_j - \tilde{u}_j^T \mu_{rj} + \dot{\tilde{\Theta}}_j^T \Gamma^{-1} \tilde{\Theta}_j + \tilde{u}_j^T (\epsilon_j + \bar{\tau}_{dj}) + \phi_j W_M \|\tilde{u}_j\| \|\tilde{W}_j\|_F \\
 &\leq -\delta_j - \frac{\|\tilde{u}_j\|^2 (Y_j \hat{\Theta}_j)^2}{(Y_j \hat{\Theta}_j) \|\tilde{u}_j\| + \delta_j} - \|\tilde{u}_j\| Y_j \tilde{\Theta}_j \\
 &\quad + \|\tilde{u}_j\| \{ \epsilon_N + \bar{d}_M + \phi_j W_M \|\hat{W}\|_F + \nu_{j1} \|\tilde{z}_{1j}\| + \nu_{j2} \|\tilde{z}_{2j}\| + \nu_{j3} \|\tilde{u}_j\| \\
 &\quad + \nu_{j4} \|\tilde{z}_{1j}\|^2 + \nu_{j5} \|\tilde{z}_{2j}\|^2 + \nu_{j6} \|\tilde{u}_j\|^2 \} \\
 &= -\delta_j - \frac{\|\tilde{u}_j\|^2 (Y_j \hat{\Theta}_j)^2}{(Y_j \hat{\Theta}_j) \|\tilde{u}_j\| + \delta_j} - \|\tilde{u}_j\| Y_j \tilde{\Theta}_j + \|\tilde{u}_j\| Y_j \Theta_j \\
 &= -\delta_j - \frac{\|\tilde{u}_j\|^2 (Y_j \hat{\Theta}_j)^2}{(Y_j \hat{\Theta}_j) \|\tilde{u}_j\| + \delta_j} + \|\tilde{u}_j\| Y_j \hat{\Theta}_j \\
 &\leq -\delta_j + \frac{\delta_j \|\tilde{u}_j\| (Y_j \hat{\Theta}_j)}{(Y_j \hat{\Theta}_j) \|\tilde{u}_j\| + \delta_j} \\
 &\leq -\delta_j \left(1 - \frac{\|\tilde{u}_j\| (Y_j \hat{\Theta}_j)}{(Y_j \hat{\Theta}_j) \|\tilde{u}_j\| + \delta_j} \right) \leq 0.
 \end{aligned}$$

Hence, it can be obtained that

$$\tilde{u}^T \mu_r + \tilde{u}^T (\epsilon + \bar{\tau}_d) + \dot{\tilde{\Theta}}^T \Gamma \tilde{\Theta} + \dot{\delta}_1 / \gamma_1 + \phi W_M \|\tilde{u}\| \|\tilde{W}\|_F \leq 0. \quad (5.74)$$

Then, substituting (5.74) and (5.72) into (5.73), the following inequality is obtained

$$\begin{aligned}
 \dot{V}_2 &\leq -\tilde{u}^T K \tilde{u} - \tilde{u}^T \mu_r + \tilde{u}^T (\epsilon + \bar{\tau}_d) + \tilde{\Theta}^T \Gamma \dot{\tilde{\Theta}} + \phi \|\tilde{u}\| \text{tr}\{\tilde{W}^T \hat{W}\} + \dot{\delta}_1 / \gamma_1 \\
 &\leq -\tilde{u}^T K \tilde{u} - \phi \|\tilde{u}\| \|\tilde{W}\|_F^2. \quad (5.75)
 \end{aligned}$$

Thus, from (5.53) and (5.75), the set-valued Lie derivative \dot{V} satisfies the following

5. DISTRIBUTED CONSENSUS-BASED FORMATION CONTROL FOR NONHOLONOMIC WHEELED MOBILE ROBOTS USING ADAPTIVE NEURAL NETWORK

inequality

$$\begin{aligned}
\max \tilde{V} = \dot{V} &\leq -\alpha \tilde{Z}^T \mathcal{M}^2 \tilde{Z} - (\beta - \kappa) \|\tilde{Z}^T \mathcal{M}\|_1 + \frac{\lambda_{max}(\mathcal{M})}{2} (\|\tilde{Z}\|_2^2 \\
&\quad + \|\tilde{u}\|_2^2) - \tilde{u}^T K \tilde{u} - \phi \|\tilde{u}\| \|\tilde{W}\|_F^2 \\
&= -\alpha \tilde{Z}^T \mathcal{M}^2 \tilde{Z} - (\beta - \kappa) \|\tilde{Z}^T \mathcal{M}\|_1 + \frac{\lambda_{max}(\mathcal{M})}{2} (\|\tilde{Z}\|_2^2 \\
&\quad + \|\tilde{u}\|_2^2) - \tilde{u}^T K \tilde{u} - \phi \|\tilde{u}\| \|\tilde{W}\|_F^2 \\
&\leq -\alpha \lambda_{max}^2(\mathcal{M}) \|\tilde{Z}\|_2^2 - (\beta - \kappa) \|\tilde{Z}^T \mathcal{M}\|_1 + \frac{\lambda_{max}(\mathcal{M})}{2} (\|\tilde{Z}\|_2^2 + \|\tilde{u}\|_2^2) \\
&\quad - k_{max} \|\tilde{u}\|_2^2 - \phi \|\tilde{u}\| \|\tilde{W}\|_F^2 \\
&\leq -\left(\alpha \lambda_{max}^2(\mathcal{M}) - \frac{\lambda_{max}(\mathcal{M})}{2}\right) \|\tilde{Z}\|_2^2 - (\beta - \kappa) \|\tilde{Z}^T \mathcal{M}\|_1 \\
&\quad - \left(k_{max} - \frac{\lambda_{max}(\mathcal{M})}{2}\right) \|\tilde{u}\|_2^2 - \phi \|\tilde{u}\| \|\tilde{W}\|_F^2,
\end{aligned}$$

and it is clear that $\max \dot{V} \leq 0$ provided by $\dot{z}_{20} \leq \kappa$, $\alpha \geq \frac{1}{2\lambda_{max}(\mathcal{M})}$, $\beta \geq \kappa$ and $k_{max} \geq \frac{\lambda_{max}(\mathcal{M})}{2}$. and it is clear that $\max \dot{V} < 0$ provided by $\dot{z}_{20} \leq \kappa$, $\alpha > \frac{1}{2\lambda_{max}(\mathcal{M})}$, $\beta > \kappa$ and $k_{max} > \frac{\lambda_{max}(\mathcal{M})}{2}$. It then from Lemma 1.10 that, $\tilde{u} \rightarrow 0$ and $\tilde{Z} \rightarrow 0$ as $t \rightarrow \infty$, i.e., $\tilde{z}_{1j} \rightarrow 0$, $\tilde{z}_{2j} \rightarrow 0$, $\tilde{u}_{wj} \rightarrow 0$ and $\tilde{u}_{vj} \rightarrow 0$ as $t \rightarrow \infty$. Therefore, the errors $\tilde{z}_{1j} = 0$, $\tilde{z}_{2j} = 0$, $\tilde{u}_{wj} = 0$ and $\tilde{u}_{vj} = 0$ are globally asymptotically stable. This proof is completed.

Theorem 5.22 *Suppose that the communication graph \mathcal{G} is connected, Assumption 3.3 is satisfied, the velocity controllers for (5.34) and (5.35) are respectively designed by (5.31) and (5.32), and the torque control input for the dynamics system (5.62) is designed by (5.60), If z_{1j} and z_{2j} asymptotically converge to z_{10} and z_{20} , then z_{3j} also asymptotically converges to z_{30} .*

Proof: The proof is similar to that of Theorem 4.14 and is therefore omitted here.

Remark 5.23 *From the Theorems 5.21 and 5.22, our control objectives (5.27)-(5.30) hold under the distributed kinematic controller (5.31), (5.32) and the torque controller (5.60). Therefore from the Lemma 5.8, the m mobile robots converge to the formation pattern \mathcal{F} , i.e., the equations (5.19)-(5.21) are satisfied.*

5.6 Simulation

In this section, some simulations results have been provided to demonstrate the effectiveness of some theoretical results of the previous sections. Consider a multiple mobile robot system with six followers denoted by F_1 - F_6 and one virtual leader denoted by L , respectively. The communication graph of the multiple mobile robot system is shown in Fig. 3.2.

For simplicity, suppose that $a_{ij} = 1$ if robot i can receive information from robot j , $a_{ij} = 0$ otherwise; $b_j = 1$ if the virtual leader's information is available to the follower j , and $b_j = 0$ otherwise, where $i \in \{1, \dots, m\}$ and $j \in \{1, \dots, m\}$.

The desired formation geometric pattern \mathcal{F} is defined by orthogonal coordinates as $(p_{1x}, p_{1y}) = (2, 0)$, $(p_{2x}, p_{2y}) = (1, \sqrt{3})$, $(p_{3x}, p_{3y}) = (-1, \sqrt{3})$, $(p_{4x}, p_{4y}) = (-2, 0)$, $(p_{5x}, p_{5y}) = (-1, -\sqrt{3})$, and $(p_{6x}, p_{6y}) = (1, -\sqrt{3})$ in Fig. 3.3. The reference trajectory of the virtual leader is chosen as

$$\begin{aligned} x_0 &= 10 \sin(t/2) \\ y_0 &= -10 \cos(t/2). \end{aligned}$$

The control gain parameters are chosen as $\alpha = 10$, $\beta = 0.99$, $k_0 = 2$. For $1 \leq j \leq 6$, the design parameters for the robust adaptive terms are selected as $\delta_j(0) = 30$, $\gamma_j = 0.5$, and

$$\Gamma_j = \begin{bmatrix} 0.001 & 0 \\ 0 & 0.001 \end{bmatrix}, \quad K_j = \begin{bmatrix} 1 & 0 \\ 0 & 1 \end{bmatrix}.$$

Assume the parameters for each robot are given as follows the mass $\hat{m} = 5$ kg and the moment of inertia $I = 3$ kg $\cdot m^2$. In both cases, unmodeled dynamics are introduced in the form of friction as

$$\bar{F}_j = \begin{bmatrix} a_{j1} \text{sign}(u_{2j}) + a_{j2} u_{2j} \\ a_{j3} \text{sign}(u_{1j}) + a_{j4} u_{1j} \end{bmatrix},$$

where a_{ji} are the coefficients of friction, and $a_{j1} = 0.75, a_{j2} = 0.05, a_{j3} = 0.025$ and $a_{j4} = 0.3$. The disturbance is introduced as $\bar{\tau}_{dj} = 2 \sin(2t) \cos(5t)$,

5. DISTRIBUTED CONSENSUS-BASED FORMATION CONTROL FOR NONHOLONOMIC WHEELED MOBILE ROBOTS USING ADAPTIVE NEURAL NETWORK

5.6.1 Verification of Formation Control Based on Robust Adaptive Techniques

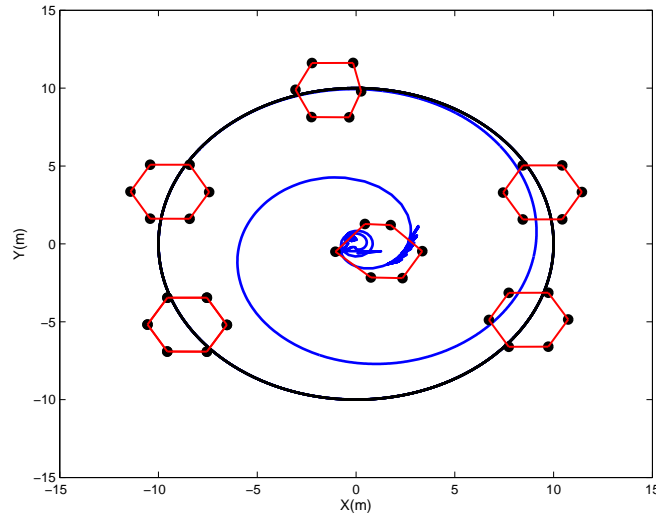
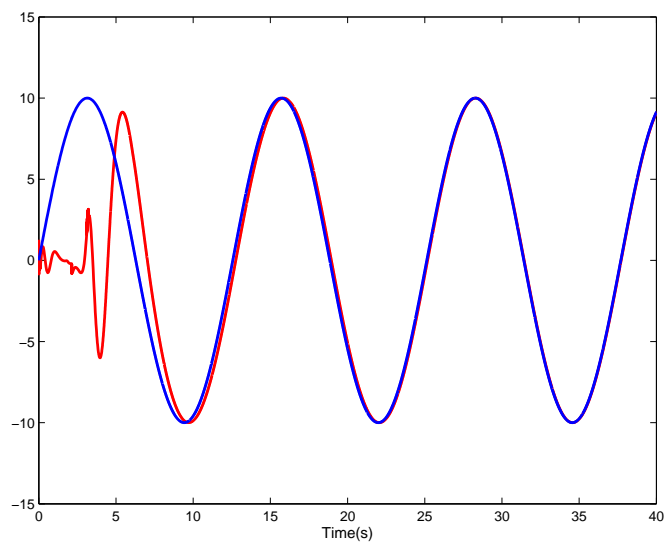


Figure 5.2: Path of the six robots' centroid (blue line), the desired trajectory of the centroid of the robots (black line), and the formation of the six robots at several moments under the distributed kinematic controller (5.31), (5.32) and the torque controller (5.44).

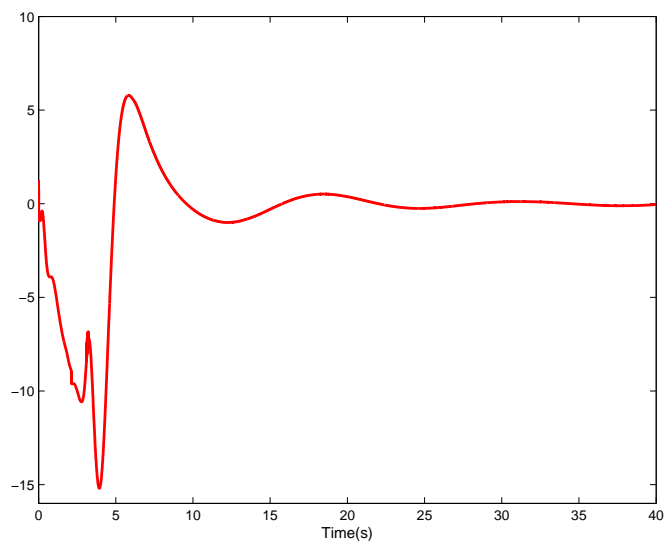
In this simulation, Fig. 5.2 shows the trajectory of virtual leader (black line), the trajectory of the six followers' centroid (blue line), and the formation positions and pattern of the six followers at some moments. It can be seen from Fig. 5.2 that the six robots converge to a desired geometry pattern under the proposed distributed controllers (5.32), (5.31) and the robust adaptive torque controller (5.44), i.e., the equation (5.19) is verified.

Fig. 5.3 shows the trajectories of x_0 (blue line) and the centroid of x_i ($1 \leq i \leq 6$); and the position error between x_0 and the centroid of x_i . Fig. 5.4 shows the trajectories of y_0 and the centroid of y_i ($1 \leq i \leq 6$); and the position error between y_0 and the centroid of y_i . From Fig. 5.3 and Fig. 5.4, the trajectory of the formation geometric centroid converges to the trajectory of virtual leader, that is to say, the equation (5.21) is verified. Fig. 5.5 and Fig. 5.6 show the tracking error \tilde{u}_{wi} for ($1 \leq i \leq 6$) and \tilde{u}_{vi} for ($1 \leq i \leq 6$) under the torque controller (5.44). From Fig. 5.5 and Fig. 5.6, \tilde{u}_{wi} and \tilde{u}_{vi} respectively converge

to zeros. The perfect tracking of velocity and angular velocity has been guaranteed. Fig. 5.7 and 5.8 respectively show the angular velocity tracking errors $w_i - w_0$ and the orientation tracking errors $\theta_i - \theta_0$ between follower F_i ($1 \leq i \leq 6$) and virtual leader. It can be seen from Fig. 5.7 and 5.8 that $w_i - w_0$ and $\theta_i - \theta_0$ converge to zero over time, i.e., the equation (5.20) and (5.30) are verified.



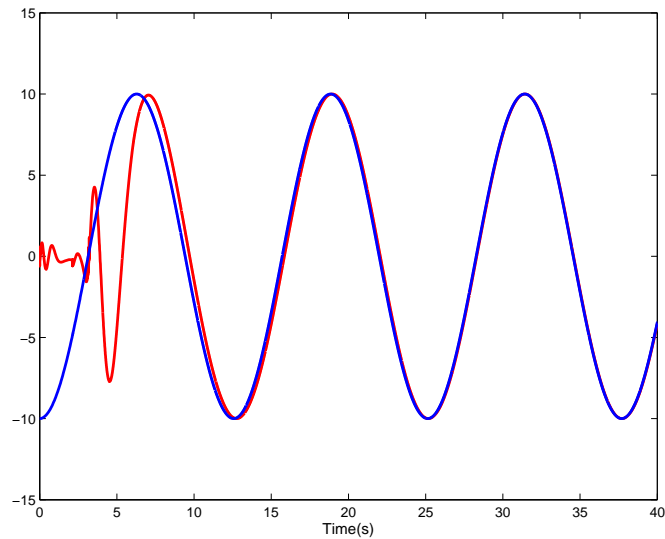
(a)



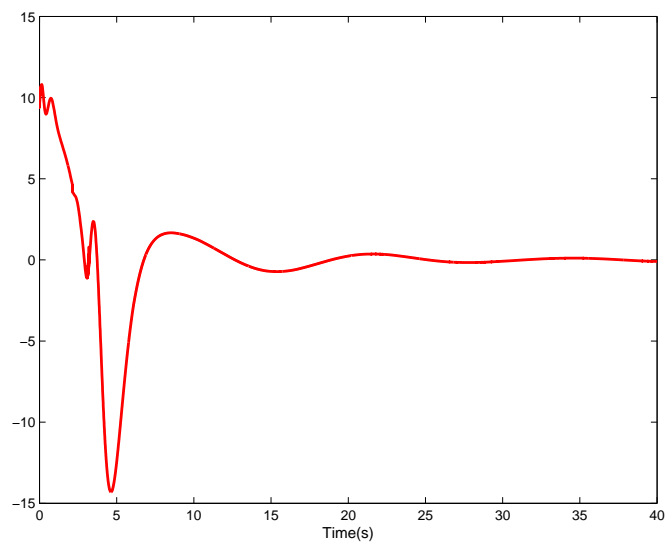
(b)

Figure 5.3: (a)The trajectories of x_0 (blue line) and the centroid of x_i ($1 \leq i \leq 6$)(red line); (b)The position error between x_0 and the centroid of x_i .

5. DISTRIBUTED CONSENSUS-BASED FORMATION CONTROL FOR NONHOLONOMIC WHEELED MOBILE ROBOTS USING ADAPTIVE NEURAL NETWORK



(a)



(b)

Figure 5.4: (a) The trajectories of y_0 (blue line) and the centroid of y_i ($1 \leq i \leq 6$) (red line); (b) The position error between y_0 and the centroid of y_i .

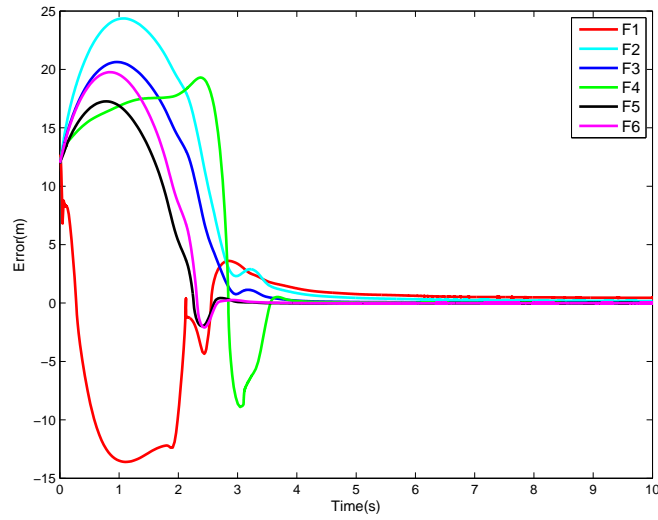


Figure 5.5: The tracking error \tilde{u}_{wi} for $(1 \leq i \leq 6)$ using the torque controller (5.44).

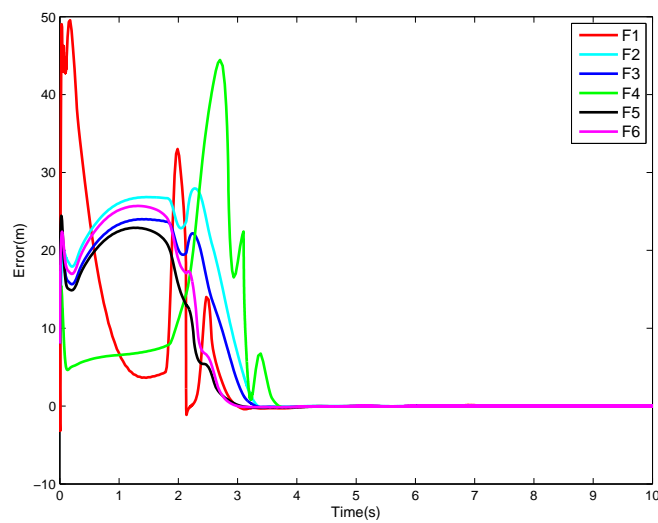


Figure 5.6: The tracking error \tilde{u}_{vi} for $(1 \leq i \leq 6)$ using the torque controller (5.44).

5. DISTRIBUTED CONSENSUS-BASED FORMATION CONTROL FOR NONHOLONOMIC WHEELED MOBILE ROBOTS USING ADAPTIVE NEURAL NETWORK

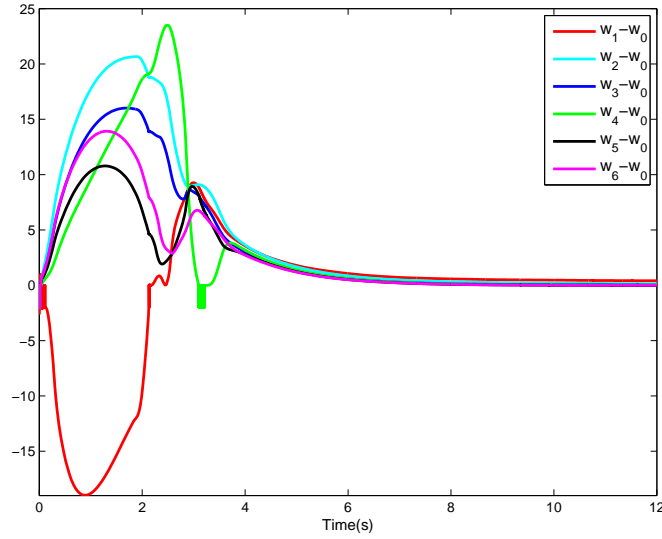


Figure 5.7: Response of the centroid of $w_i - w_0$ for $1 \leq i \leq 6$.

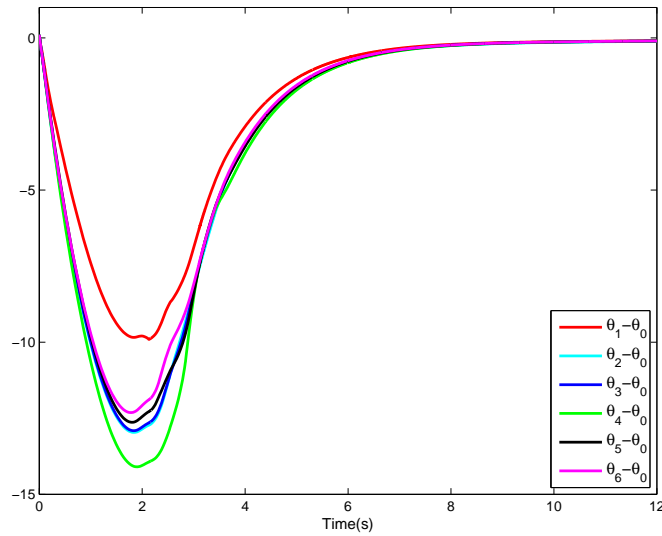


Figure 5.8: Response of the centroid of $\theta_i - \theta_0$ for $1 \leq i \leq 6$.

5.6.2 Verification of Formation Control Based on Neural Network Techniques

In this simulation, the number of hidden neuron is chosen by 5 for the mobile robot, and the Neural Network parameters for each robot are selected as $F_j =$

$\begin{bmatrix} 10 & 0 \\ 0 & 10 \end{bmatrix}$, and $\phi_j = 0.5$. The control gain Γ_j is chosen by $\Gamma_j = \begin{bmatrix} 0.001 & 0 \\ 0 & 0.008 \end{bmatrix}$.

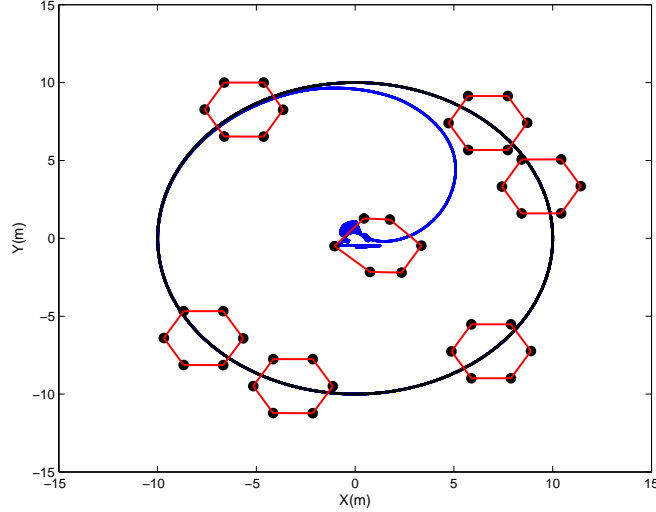
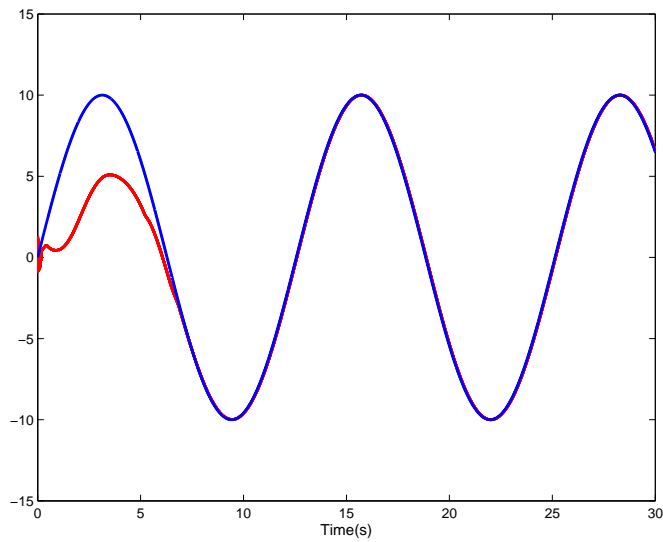


Figure 5.9: Path of the six robots' centroid(blue line), the desired trajectory of the centroid of the robots(black line), and the formation of the six robots at several moments

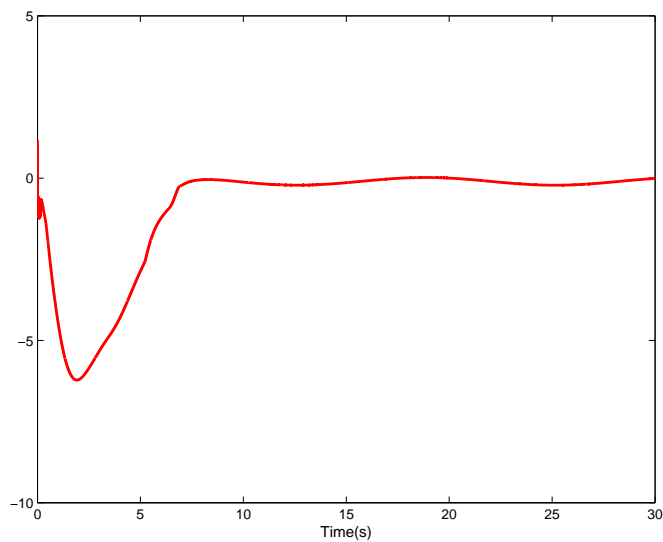
In this simulation, Fig. 5.9 shows the trajectory of virtual leader (black line), the trajectory the six followers' centroid (blue line), and the formation positions and pattern of the six followers at some moments. It can be seen from Fig. 5.9 that the six robots converge to a desired geometry pattern under the proposed distributed controllers (5.32), (5.31) and the adaptive Neural Network controller (5.60), i.e., the equation (5.19) is verified.

Fig. 5.10 shows the trajectories of x_0 (blue line) and the centroid of x_i ($1 \leq i \leq 6$)(red line); and the position error between x_0 and the centroid of x_i . Fig. 5.11 shows the trajectories of y_0 (blue line) and the centroid of y_i ($1 \leq i \leq 6$)(red line); and the position error between y_0 and the centroid of y_i . From Fig. 5.10 and Fig. 5.11, the trajectory of the formation geometric centroid converges to the trajectory of virtual leader, that is to say, the equation (5.21) is verified. Fig. 5.12 and Fig. 5.13 show the tracking error \tilde{u}_{wi} for ($1 \leq i \leq 6$) and \tilde{u}_{vi} for ($1 \leq i \leq 6$) under the torque controller (5.60). From Fig. 5.12 and Fig. 5.13, \tilde{u}_{wi} and \tilde{u}_{vi} respectively converge to zero. The perfect tracking of velocity and angular velocity has been guaranteed. Fig. 5.14 and 5.15 respectively show the

5. DISTRIBUTED CONSENSUS-BASED FORMATION CONTROL FOR NONHOLONOMIC WHEELED MOBILE ROBOTS USING ADAPTIVE NEURAL NETWORK

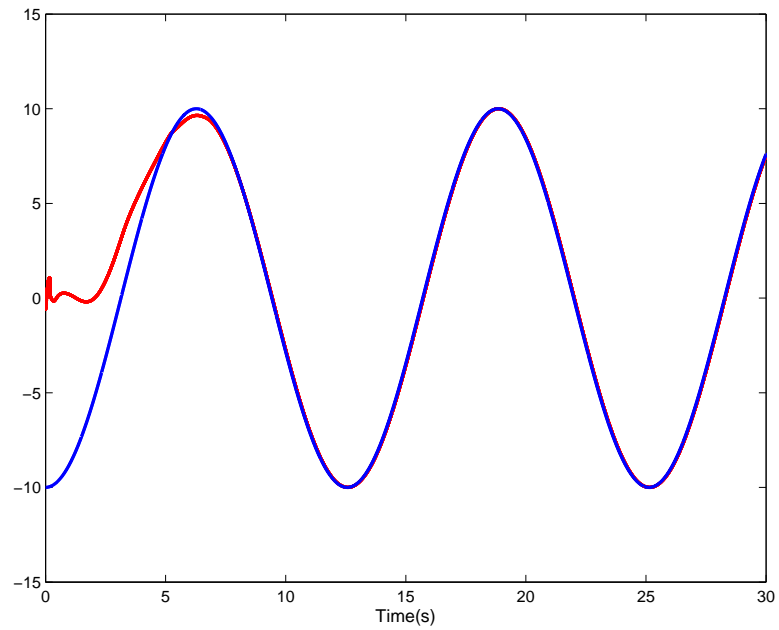


(a)

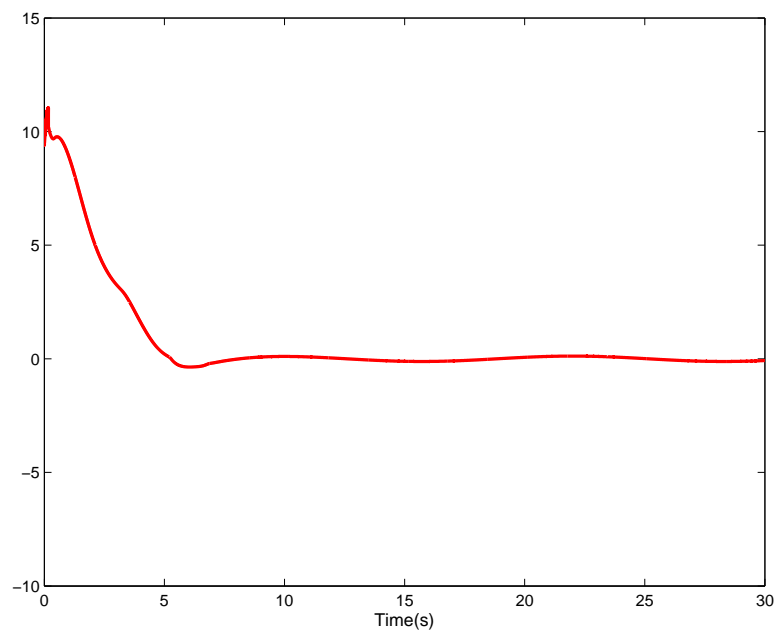


(b)

Figure 5.10: (a) The trajectories of x_0 (blue line) and the centroid of x_i ($1 \leq i \leq 6$) (red line); (b) The position error between x_0 and the centroid of x_i .



(a)



(b)

Figure 5.11: (a) The trajectories of y_0 (blue line) and the centroid of y_i ($1 \leq i \leq 6$) (red line); (b) The position error between y_0 and the centroid of y_i .

5. DISTRIBUTED CONSENSUS-BASED FORMATION CONTROL FOR NONHOLONOMIC WHEELED MOBILE ROBOTS USING ADAPTIVE NEURAL NETWORK

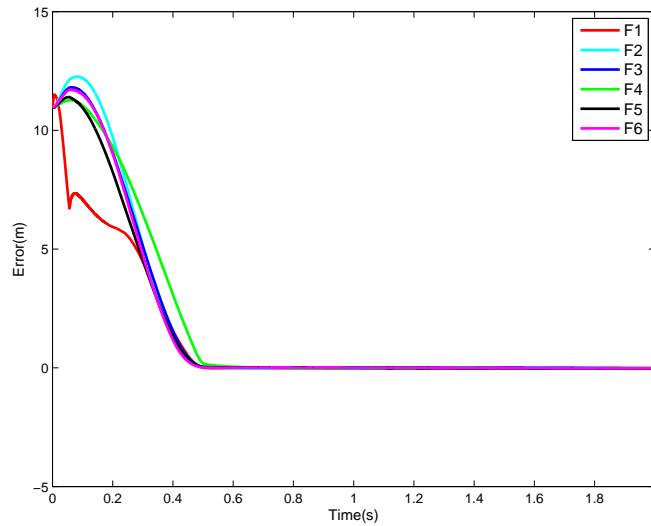


Figure 5.12: The tracking error \tilde{u}_{wi} for $(1 \leq i \leq 6)$ under the Neural Network controller (5.60).

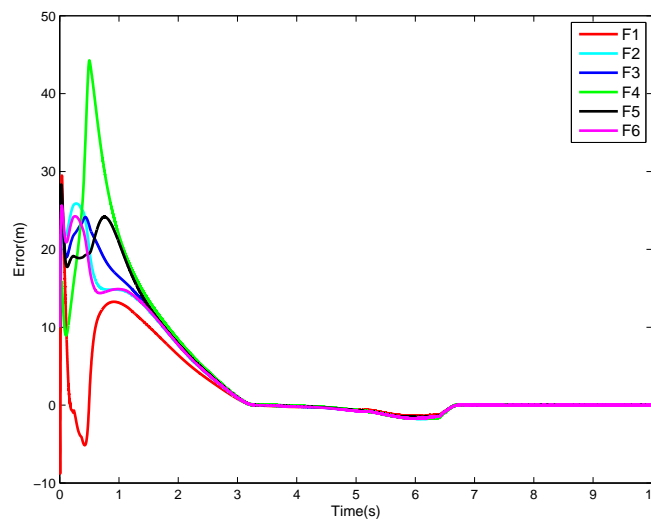


Figure 5.13: The tracking error \tilde{u}_{vi} for $(1 \leq i \leq 6)$ under the Neural Network controller (5.60).

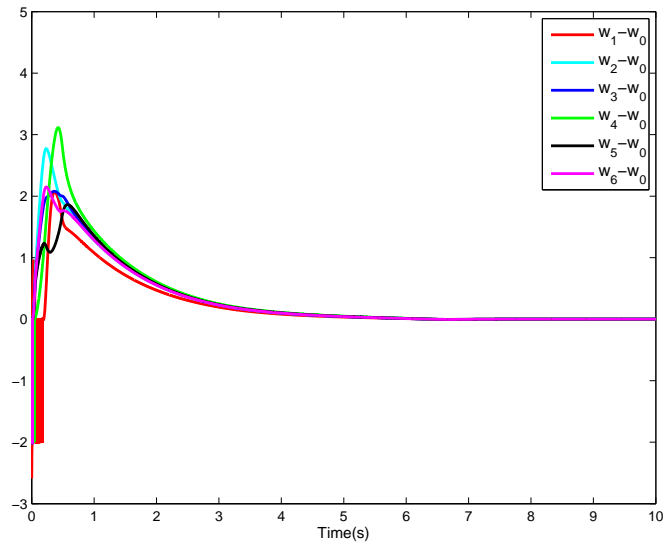


Figure 5.14: Response of the centroid of $w_i - w_0$ for $1 \leq i \leq 6$.

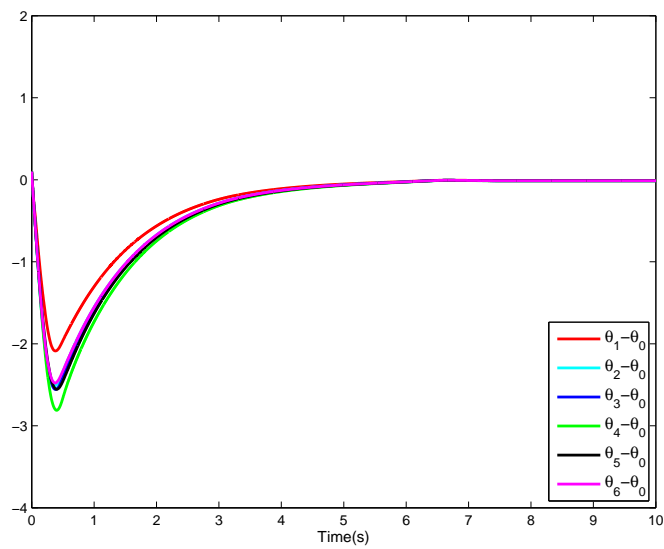


Figure 5.15: Response of the centroid of $\theta_i - \theta_0$ for $1 \leq i \leq 6$.

5. DISTRIBUTED CONSENSUS-BASED FORMATION CONTROL FOR NONHOLONOMIC WHEELED MOBILE ROBOTS USING ADAPTIVE NEURAL NETWORK

angular velocity tracking errors $w_i - w_0$ and the orientation tracking errors $\theta_i - \theta_0$ between follower F_i ($1 \leq i \leq 6$) and virtual leader. It can be seen from Fig. 5.14 and 5.15 that $w_i - w_0$ and $\theta_i - \theta_0$ converge to zero over time, i.e., the equation (5.20) and (5.30) are verified.

5.7 Conclusion

In this chapter, the formation control problem for the wheeled mobile robots has been considered, in which the dynamics model of the wheeled mobile robot has the friction term and bounded disturbance term in the dynamic model. First the partial knowledge of the mobile robot dynamics has been assumed to be available. Then an asymptotically stable torque controller has been proposed by using robust adaptive control techniques to account for unmolded dynamics and bounded disturbances. Next, with the dynamics of the mobile robot has been assumed to be unknown. Then the universal approximation property of neural network has been used to relax the knowledge of the system dynamics, and an asymptotically robust adaptive controller augmented with the neural network has been derived to achieve asymptotic tracking.

Conclusions and Future Work

The purpose of this chapter is to summarize the contributions presented in the dissertation and introduce some perspectives for future research to complete and improve this work.

Conclusions

In this thesis, we focus on the formation control of multiple nonholonomic mobile robots. The objective is to design some new control laws for each robot according to different control tasks and different constraint conditions, such that a group of mobile robots can form and maintain a desired geometric pattern and follow a desired trajectory.

In Chapter 2, the leader-follower formation control problem for nonholonomic mobile robots based on the backstepping approach has been investigated. The trajectory tracking control for a single nonholonomic mobile robot has been extended to the formation control for multiple nonholonomic mobile robots based on backstepping technique, in which follower can track its real-time leader by the proposed kinematic controller. Due to the nonholonomic constraint of each robot and the leader-follower formation control objective, an auxiliary angular velocity control law has been developed to guarantee the global asymptotic stability of the followers and to further guarantee the local asymptotic stability of the entire formation. Then an asymptotically stable control law for the formation control of multiple mobile robots has been developed by using backstepping technology, which not only guarantee all mobile robots achieve and maintain the desired formation, but also guarantee all follower robots track the time-varying trajectory of the leader robot. Since using the backstepping technology may lead to the impractical velocity jump when tracking errors suddenly occur, a bioinspired neu-

CONCLUSIONS AND PERSPECTIVES

rodynamics based approach has been developed to solve the impractical velocity jumps problem. It is shown that each robot has smooth and continuous velocities with zero initial value by using the bioinspired neurodynamics based approach. Stability analysis has been provided by using Lyapunov theory. The effectiveness of the proposed control scheme has been demonstrated by simulation results.

In Chapter 3 the distributed formation control problem for multiple nonholonomic mobile robots using consensus-based approach has been investigated. First, a variable transformation has been given to convert the formation control problem for multiple nonholonomic mobile robots into a state consensus problem. Then a set of control laws have been established using the result from graph theory and Lyapunov techniques for accomplishing our formation control objectives: a group of nonholonomic mobile robots converge to a desired geometric pattern with its centroid moving along the specified reference trajectory. In this chapter, the specified reference trajectory has been represented by the state of a virtual leader whose outputs is only its position information that is available to only a subset of a group of followers. As the control laws proposed in this chapter are distributed, it is not necessary to provide the global information for each robot. In fact, each robot can obtain information only from its neighbors. It is shown that the communication topology required in this chapter does not necessary need to be tree information sensing structures, and our proposed control laws guaranty that the nonholonomic mobile robots can at least exponentially converge to the desired geometric pattern, as well as the geometric centroid of the formation at least exponentially converges to the trajectory of the virtual leader.

In the previous Chapter 3, the formation control of nonholonomic wheeled mobile robots is based on kinematic models, which requires "perfect velocity tracking". However, in many practical situations, the dynamics of robot should not be ignored and practical control strategies accounting for both the kinematic and dynamic effect should be implemented. Hence, Chapter 4 investigates the distributed adaptive formation control problem for multiple nonholonomic wheeled mobile robots with consideration of both kinematic model and dynamics systems with unknown parameters. The objective is to develop the corresponding distributed controllers, such that a group of nonholonomic wheeled mobile robots asymptotically converges to a desired geometric pattern with its centroid moving along the specified reference trajectory. To achieve this goal, a variable trans-

formation is first given to convert the formation control problem into a state consensus problem. Then, some distributed kinematic controllers are developed. We assume that the specified reference trajectory can be considered as the trajectory of a virtual leader whose information is available to only a subset of the followers. Also the followers are assumed to have only local interaction. Next, it is well known in practice that the dynamics model of the wheel mobile robot has unknown dynamical parameters, which will affect the robust trajectory tracking of the system. Therefore, adaptive computed-torque controllers for mobile robots are developed. Sufficient conditions are derived for accomplishing the asymptotical stability of the systems based on algebraic graph theory, matrix theory, and Lyapunov control approach. Finally, simulation examples illustrate the effectiveness of the proposed controllers.

It is well known that, in some practical applications, the friction term and bounded disturbance term should not be ignored and practical control strategies accounting for the friction term and bounded disturbance term should be implemented. In Chapter 5, the formation control problem for the wheeled mobile robots has been investigated, in which the dynamics model of the wheeled mobile robot has the friction term and bounded disturbance term. First, the partial knowledge of the mobile robot dynamics has been assumed to be available. Then an asymptotically stable torque controller is proposed by using robust adaptive control techniques to account for unmolded dynamics and bounded disturbances. Second, the dynamics of the mobile robot has been assumed to be unknown. Then the universal approximation property of neural network has been used to relax the knowledge of the dynamics system, and an asymptotically robust adaptive controller augmented with the neural network has been derived to achieve asymptotic tracking.

Ongoing and Future Works

There are some challenging open topics to the problems studied in this thesis.

The proposed control laws were corroborated based on simulation results on examples in our current works. The numerical examples presented in this thesis verified the theoretical results. So in the future works we will develop a platform of robot group formation using real nonholonomic mobile robots to validate our

CONCLUSIONS AND PERSPECTIVES

theory results experimentally.

In practical applications, formation control algorithm for nonholonomic robots ensuring collision avoidance of robots in the formation is possibly the most striking issue. In the future, we will consider the formation control problem with obstacle avoidance.

In addition, it is well known that time delay is ubiquitous in many systems, and most multiple robots systems operations are naturally delayed. Moreover, it has been observed from numerical experiments in this thesis that formation control algorithms without considering time delays may lead to unexpected instability. Hence, in the future, we will also consider the formation control problem for multiple nonholonomic robots with time-varying delays.

Bibliography

- ABEL, R.O. (2010). *The Coordinated Control of Autonomous Agents*. Thesis, University of Iowa. [21](#)
- ANDERSON, B., YU, C., FIDAN, B. & HENDRICKX, J. (2008). Rigid graph control architectures for autonomous formations. *Control Systems Magazine, IEEE*, **28**, 48–63. [26](#)
- ANTONELLI, G., ARRICHIELLO, F. & CHIAVERINI, S. (2008). The null-space-based behavioral control for autonomous robotic systems. *Intelligent Service Robotics*, **1**, 27–39. [22](#)
- BALCH, T. & ARKIN, R. (1998). Behavior-based formation control for multirobot teams. *Robotics and Automation, IEEE Transactions on*, **14**, 926–939. [22](#)
- BELTA, C. & KUMAR, V. (2002). Trajectory design for formations of robots by kinetic energy shaping. In *Robotics and Automation, 2002. Proceedings. ICRA '02. IEEE International Conference on*, vol. 3, 2593–2598. [21](#)
- BENNET, D. & MCINNES, C. (2010). Distributed control of multi-robot systems using bifurcating potential fields. *Robotics and Autonomous Systems*, **58**, 256–264. [25](#)
- BLAŽIČ, S. (2011). A novel trajectory-tracking control law for wheeled mobile robots. *Robotics and Autonomous Systems*, **59**, 1001–1007. [40](#), [41](#)
- BOUKATTAYA, M., JALLOULI, M. & DAMAK, T. (2012). On trajectory tracking control for nonholonomic mobile manipulators with dynamic uncertainties and external torque disturbances. *Robotics and Autonomous Systems*, **60**, 1640–1647. [40](#), [41](#)

BIBLIOGRAPHY

- BROOKS, R.A. (1985). A robust layered control system for a mobile robot. Tech. rep., Cambridge, MA, USA. [22](#)
- BRUNETE, A., HERNANDO, M., GAMBAO, E. & TORRES, J.E. (2012). A behaviour-based control architecture for heterogeneous modular, multi-configurable, chained micro-robots. *Robotics and Autonomous Systems*, **60**, 1607–1624. [22](#)
- CHEN, H. (2009). *Towards Multi-robots Formation: Study on Vision-based Localization System*. Thesis, City University of Hong Kong. [19](#)
- CHEN, J., SUN, D., YANG, J. & CHEN, H. (2010). Leader-follower formation control of multiple non-holonomic mobile robots incorporating a receding-horizon scheme. *The International Journal of Robotics Research*, **29**, 727–747. [21](#), [86](#)
- CHEN, Y. & WANG, Z. (2005). Formation control: a review and a new consideration. In *Intelligent Robots and Systems, 2005. (IROS 2005). 2005 IEEE/RSJ International Conference on*, 3181–3186. [21](#), [22](#), [23](#)
- CHUNG, F.R.K. (1997). *Spectral Graph Theory*, vol. 92. American Mathematical Society. [29](#)
- CONSOLINI, L., MORBIDI, F., PRATTICIZZO, D. & TOSQUES, M. (2008). Leader follower formation control of nonholonomic mobile robots with input constraints. *Automatica*, **44**, 1343 – 1349. [66](#), [86](#)
- CORTES, J. (2008). Discontinuous dynamical systems. *IEEE Control Systems*, **28**, 36–73. [30](#), [31](#)
- DAS, A.K., FIERRO, R., KUMAR, V., OSTROWSKI, J.P., SPLETZER, J. & TAYLOR, C.J. (2002). A vision-based formation control framework. *IEEE Transactions on Robotics and Automation*, **18**, 813–825. [21](#), [23](#), [66](#), [86](#)
- DESAI, J., OSTROWSKI, J. & KUMAR, V. (1998). Controlling formations of multiple mobile robots. In *Robotics and Automation, 1998. Proceedings. 1998 IEEE International Conference on*, vol. 4, 2864 –2869 vol.4. [13](#), [21](#), [23](#), [24](#), [25](#), [65](#), [66](#), [86](#)

- DESAI, J.P., OSTROWSKI, J.P. & KUMAR, V. (2001). Modeling and control of formations of nonholonomic mobile robots. *IEEE Transactions on Robotics and Automation*, **17**, 905–908. [21](#), [24](#), [66](#)
- DIERKS, T. & JAGANNATHAN, S. (2007). Control of nonholonomic mobile robot formations: Backstepping kinematics into dynamics. In *IEEE International Conference on Control Applications*, 94–99. [50](#)
- DIERKS, T. & JAGANNATHAN, S. (2009a). Asymptotic adaptive neural network tracking control of nonholonomic mobile robot formations. *J. Intell. Robotics Syst.*, **56**, 153–176. [21](#), [86](#)
- DIERKS, T. & JAGANNATHAN, S. (2009b). Neural network control of mobile robot formations using rise feedback. *IEEE Transactions on Systems, Man, and Cybernetics, Part B: Cybernetics*, **39**, 332–347. [21](#), [86](#)
- DIESTEL, R., ed. (1997). *Graph Theory*. Springer-Verlag, Heidelberg. [26](#)
- DONG, W. (2012). Tracking control of multiple-wheeled mobile robots with limited information of a desired trajectory. *Robotics, IEEE Transactions on*, **28**, 262–268. [21](#), [66](#), [67](#), [86](#)
- DONG, W. & FARRELL, J. (2008). Cooperative control of multiple nonholonomic mobile agents. *Automatic Control, IEEE Transactions on*, **53**, 1434–1448. [21](#), [23](#), [66](#), [67](#), [69](#), [86](#)
- DONG, W. & FARRELL, J.A. (2009). Decentralized cooperative control of multiple nonholonomic dynamic systems with uncertainty. *Automatica*, **45**, 706–710. [21](#), [66](#), [67](#), [69](#), [86](#)
- DOUGHERTY, R., OCHOA, V., RANGLES, Z. & KITTS, C. (2004). A behavioral control approach to formation-keeping through an obstacle field. In *Aerospace Conference, 2004. Proceedings. 2004 IEEE*, vol. 1, –175 Vol.1. [22](#)
- DUDEK, G., JENKIN, M., MILIOS, E. & WILKES, D. (1996). A taxonomy for multi-agent robotics. *AUTONOMOUS ROBOTS*, **3**, 375–397. [20](#)
- EGERSTEDT, M. & HU, X. (2001). Formation constrained multi-agent control. *IEEE Transactions on Robotics and Automation*, **17**, 947–951. [21](#), [22](#)

BIBLIOGRAPHY

- EREN, T., ANDERSON, B.D.O., MORESE, A.S., WHITELEY, W. & BELHUMEUR, P.N. (2004). operations on rigid formation of autonomous agents. *Communications in Formation and Systems*, 223–258. [26](#)
- FAX, J. & MURRAY, R. (2004). Information flow and cooperative control of vehicle formations. *Automatic Control, IEEE Transactions on*, **49**, 1465 – 1476. [22](#)
- FAX, J.A. & MURRAY, R.M. (2002). Graph laplacians and stabilization of vehicle formations. In *in Proc. 15th IFAC world congress*, 238–288. [22](#)
- FIERRO, R. & LEWIS, F. (1998). Control of a nonholonomic mobile robot using neural networks. *IEEE Transactions on Neural Networks*, **9**, 589–600. [40](#), [41](#), [42](#), [49](#), [50](#), [86](#), [108](#), [111](#), [118](#)
- FUKAO, T., NAKAGAWA, H. & ADACHI, N. (2000). Adaptive tracking control of a nonholonomic mobile robot. *Robotics and Automation, IEEE Transactions on*, **16**, 609 –615. [86](#)
- GAZI, V. & PASSINO, K. (2003). Stability analysis of swarms. *IEEE Transactions on Automatic Control*, **48**, 692–697. [25](#)
- GHOMMAM, J., MEHRJERDI, H., SAAD, M. & MNIF, F. (2010). Formation path following control of unicycle-type mobile robots. *Robotics and Autonomous Systems*, **58**, 727 – 736. [23](#)
- GODSIL, C. & ROYLE, G., eds. (2001). *Algebraic Graph Theory*. Springer-Verlag, Heidelberg. [25](#), [26](#)
- GOLDSTEIN, H. (1980). Addison-Wesley series in physics, Addison-Wesley Pub. Co. [32](#)
- GU, D. & HU, H. (2006). Receding horizon tracking control of wheeled mobile robots. *IEEE Transactions on Control Systems Technology*, **14**, 743–749. [40](#), [41](#)
- GUSTAVI, T. & HU, X. (2008). Observer-based leader-following formation control using onboard sensor information. *IEEE Transactions on Robotics*, **24**, 1457–1462. [18](#)

BIBLIOGRAPHY

- HENDRICKX, J., FIDAN, B., YU, C., ANDERSON, B. & BLONDEL, V. (2008). Formation reorganization by primitive operations on directed graphs. *IEEE Transactions on Automatic Control*, **53**, 968–979. [26](#)
- HODGKIN, A.L. & HUXLEY, A.F. (1952). A quantitative description of membrane current and its application to conduction and excitation in nerve. *Journal of Physiology*, **117**, 500–554. [50](#)
- HSIEH, M. & KUMAR, V. (2006). Pattern generation with multiple robots. In *Robotics and Automation, 2006. ICRA 2006. Proceedings 2006 IEEE International Conference on*, 2442–2447. [24](#)
- JADBABAIE, A., LIN, J. & MORSE, A. (2003). Coordination of groups of mobile autonomous agents using nearest neighbor rules. *Automatic Control, IEEE Transactions on*, **48**, 988–1001. [66](#)
- JIANG, Z. & NIJMEIJER, H. (1997). Tracking control of mobile robots: A case study in backstepping. *Automatica*, **33**, 1393–1399. [40](#), [41](#)
- KANAYAMA, Y., KIMURA, Y., MIYAZAKI, F. & NOGUCHI, T. (1990). A stable tracking control method for an autonomous mobile robot. *Robotics and Automation*, **1**, 384–389. [40](#), [41](#)
- KANJANAWANISHKUL, K. (2005). Formation control of mobile robots: Survey. *eng.ubu.ac.th*, 50–64. [20](#)
- KANJANAWANISHKUL, K. (2009). Formation control of omnidirectional mobile robots using distributed model predictive control. In *Robot Communication and Coordination, 2009. ROBOCOMM '09. Second International Conference on*, 1–7. [26](#)
- KHATIB, O. (1986). Real-time obstacle avoidance for manipulators and mobile robots. *The International Journal of Robotics Research*, **5**, 90–98. [24](#)
- KOO, T. & SHAHRUZ, S. (2001). Formation of a group of unmanned aerial vehicles (uavs). In *American Control Conference, 2001. Proceedings of the 2001*, vol. 1, 69–74. [21](#)

BIBLIOGRAPHY

- KOSTIC, D., ADINANDRA, S., CAARLS, J., VAN DE WOUW, N. & NIJMEIJER, H. (2010). Saturated control of time-varying formations and trajectory tracking for unicycle multi-agent systems. In *Decision and Control (CDC), 2010 49th IEEE Conference on*, 4054–4059. [23](#)
- KUMAR, M., GARG, D. & KUMAR, V. (2008). Self-sorting in a swarm of heterogeneous agents. In *American Control Conference, 2008*, 117–122. [24](#)
- KWAN, C., DAWSON, D. & LEWIS, F. (1995). Robust adaptive control of robots using neural network: global tracking stability. In *Decision and Control, 1995., Proceedings of the 34th IEEE Conference on*, vol. 2, 1846–1851 vol.2. [118](#), [124](#)
- LALISH, E., MORGANSEN, K. & TSUKAMAKI, T. (2006). Formation tracking control using virtual structures and deconfliction. In *Decision and Control, 2006 45th IEEE Conference on*, 5699–5705. [23](#)
- LAWTON, J., BEARD, R. & YOUNG, B. (2003). A decentralized approach to formation maneuvers. *Robotics and Automation, IEEE Transactions on*, **19**, 933–941. [22](#)
- LEWIS, F.L., ABDALLAH, C.T. & DAWSON, D.M. (1993). *Control of Robot Manipulators*, vol. 92. New York: MacMillan. [88](#), [111](#)
- LEWIS, M.A. & TAN, K. (1997). High precision formation control of mobile robots using virtual structures. *Autonomous Robots*, **4**, 387–403. [22](#)
- LI, X., XIAO, J. & CAI, Z. (2005). Backstepping based multiple mobile robots formation control. In *Intelligent Robots and Systems, 2005. (IROS 2005). 2005 IEEE/RSJ International Conference on*, 887–892. [46](#)
- LIU, C. & TIAN, Y. (2009). Formation control of multi-agent systems with heterogeneous communication delays. *International Journal of Systems Science*, **40**, 627–636. [86](#)
- LONG, M., GAGE, A., MURPHY, R. & VALAVANIS, K. (2005). Application of the distributed field robot architecture to a simulated demining task. In *Robotics and Automation, 2005. ICRA 2005. Proceedings of the 2005 IEEE International Conference on*, 3193–3200. [22](#)

- LU, W. & CHEN, T. (2009). Synchronisation in complex networks of coupled systems with directed topologies. *International Journal of Systems Science*, **40**, 909–921. [66](#)
- MARIOTTINI, G.L., MORBIDI, F., PRATTICIZZO, D., PAPPAS, G.J. & DANILIDIS, K. (2007). Leader-follower formations: Uncalibrated vision-based localization and control. In *2007 IEEE International Conference on Robotics and Automation*, 2403–2408. [21](#), [24](#), [66](#), [86](#)
- MCCLINTOCK, J. & FIERRO, R. (2008). A hybrid system approach to formation reconfiguration in cluttered environments. In *2008 16th Mediterranean Conference on Control and Automation*, 83 –88. [26](#)
- MEYER, C.D., ed. (2000). *Matrix analysis and applied linear algebra*. Society for Industrial and Applied Mathematics, Philadelphia, PA, USA. [108](#), [109](#)
- MONTEIRO, S. & BICHO, E. (2010). Attractor dynamics approach to formation control: theory and application. *Autonomous Robots*, **29**, 331–355. [22](#)
- OGMEN, H. & GAGNÉ, S. (1990). Neural network architectures for motion perception and elementary motion detection in the fly visual system. *Neural Networks*, **3**, 487–505. [50](#)
- OLFATI-SABER, R. (2006). Flocking for multi-agent dynamic systems: algorithms and theory. *Automatic Control, IEEE Transactions on*, **51**, 401 – 420. [22](#), [24](#)
- OLFATI-SABER, R. & MURRAY, R. (2003). Agreement problems in networks with directed graphs and switching topology. In *Proceedings. 42nd IEEE Conference on Decision and Control*, vol. 4, 4126–4132. [25](#)
- PADEN, B.E. & SASTRY, S.S. (1987). A calculus for computing filippov’s differential inclusion with application to the variable structure control of robot manipulators. *IEEE Transactions on Circuits and Systems*, **34**, 73–82. [31](#), [72](#), [73](#), [92](#), [93](#), [120](#)
- PARK, B., PARK, J. & CHOI, Y. (2011). Robust adaptive formation control and collision avoidance for electrically driven non-holonomic mobile robots. *Control Theory Applications, IET*, **5**, 514 –522. [21](#), [86](#)

BIBLIOGRAPHY

- PENG, Z., WEN, G. & RAHMANI, A. (2013). Leader-follower formation control of multiple nonholonomic robots based on backstepping. In *Proceedings of the 28th Annual ACM Symposium on Applied Computing, SAC '13*, 211–216, ACM, New York, NY, USA. [18](#)
- PETERSEN, K.B. & PEDERSEN, M.S. (2012). The matrix cookbook. Version 20121115. [109](#), [110](#)
- PHAN, M. & BARLOW, J. (2008). Optimal model predictive control formations. In *Control and Decision Conference, 2008. CCDC 2008. Chinese*, 55–64. [26](#)
- REN, W. & BEARD, R. (2004). Formation feedback control for multiple spacecraft via virtual structures. *Control Theory and Applications, IEE Proceedings* -, **151**, 357–368. [23](#)
- REN, W. & BEARD, R.W. (2005). Consensus seeking in multiagent systems under dynamically changing interaction topologies. *Automatic Control, IEEE Transactions on*, **50**, 655–661. [66](#)
- SABATTINI, L., SECCHI, C. & FANTUZZI, C. (2009). Potential based control strategy for arbitrary shape formations of mobile robots. In *Intelligent Robots and Systems, 2009. IROS 2009. IEEE/RSJ International Conference on*, 3762–3767. [25](#)
- SHEVITZ, D. & PADEN, B. (1994). Lyapunov stability theory of nonsmooth systems. *IEEE Transactions on Automatic Control*, **39**, 1910–1914. [31](#)
- SHI, H., WANG, L. & CHU, T. (2009). Flocking of multi-agent systems with a dynamic virtual leader. *International Journal of Control*, **82**, 43–58. [22](#)
- SLOTINE, J. & LI, W. (1991). *Applied nonlinear control*. Prentice Hall. [34](#)
- SUMMERS, T., YU, C., DASGUPTA, S. & ANDERSON, B. (2011). Control of minimally persistent leader-remote-follower and coleader formations in the plane. *Automatic Control, IEEE Transactions on*, 1–1. [26](#)
- TAN, K. & LEWIS, M. (1996). Virtual structures for high-precision cooperative mobile robotic control. In *Intelligent Robots and Systems '96, IROS 96, Proceedings of the 1996 IEEE/RSJ International Conference on*, vol. 1, 132–139. [22](#), [23](#)

- TANNER, H. & PIOVESAN, J. (2010). Randomized receding horizon navigation. *IEEE Transactions on Automatic Control*, **55**, 2640–2644. [18](#)
- TANNER, H., JADBABAIE, A. & PAPPAS, G. (2003a). Stable flocking of mobile agents part i: dynamic topology. In *In proceedings of the 42th IEEE Conference on Decision and Control*, 2010–2015. [22](#)
- TANNER, H.G., JADBABAIE, A. & PAPPAS, G.J. (2003b). Stable flocking of mobile agents, part ii: Dynamic topology. In *In proceedings of the 42th IEEE Conference on Decision and Control*, 2016–2021. [22](#)
- TSAI, P.S., WANG, L.S., CHANG, F.R. & WU, T.F. (2004). Systematic backstepping design for b-spline trajectory tracking control of the mobile robot in hierarchical model. In *2004 IEEE International Conference on Networking, Sensing and Control*, vol. 2, 713–718. [50](#)
- WANG, G., LI, D., GAN, W. & JIA, P. (2013). Study on formation control of multi-robot systems. In *Intelligent System Design and Engineering Applications (ISDEA), 2013 Third International Conference on*, 1335–1339. [22](#)
- WEN, G., PENG, Z., YU, Y. & RAHMANI, A. (2012). Planning and control of three-dimensional multi-agent formations. *IMA Journal of Mathematical Control and Information*. [18](#)
- WEN, G., PENG, Z., RAHMANI, A. & YU, Y. (2013). Distributed leader-following consensus for second-order multi-agent systems with nonlinear inherent dynamics. *International Journal of Systems Science*. [66](#)
- WU, Q., ZHOU, J. & XIANG, L. (2012). Impulsive consensus seeking in directed networks of multi-agent systems with communication time delays. *International Journal of Systems Science*, **43**, 1479–1491. [66](#)
- XIANG, X., LAPIERRE, L., JOUVENCEL, B. & PARODI, O. (2009). Coordinated path following control of multiple nonholonomic vehicles. In *OCEANS 2009 - EUROPE*, 1–7. [32](#)
- YANG, S., ZHU, A., YUAN, G. & MENG, M. (2012). A bioinspired neurodynamics-based approach to tracking control of mobile robots. *IEEE Transactions on Industrial Electronics*, **59**, 3211–3220. [40](#), [41](#), [49](#)

BIBLIOGRAPHY

- YU, C., HENDRICKX, J.M., FIDAN, B., ANDERSON, B.D. & BLONDEL, V.D. (2007). Three and higher dimensional autonomous formations: Rigidity, persistence and structural persistence. *Automatica*, **43**, 387 – 402. [26](#)
- YU, J. & WANG, L. (2012). Group consensus of multi-agent systems with directed information exchange. *International Journal of Systems Science*, **43**, 334–348. [66](#)
- ZHANG, Q., SHIPPEN, J. & JONES, B. (1999). Robust backstepping and neural network control of a low-quality nonholonomic mobile robot. *International Journal of Machine Tools and Manufacture*, **39**, 1117–1134. [50](#)
- ZHAO, S. (2010). Multi-robot cooperative control:from theory to practice. Tech. rep., University of Cincinnati. [22](#)
- ZOHAR, I., AILON, A. & RABINOVICI, R. (2011). Mobile robot characterized by dynamic and kinematic equations and actuator dynamics: Trajectory tracking and related application. *Robotics and Autonomous Systems*, **59**, 343 – 353. [86](#)
- ZUO, G., HAN, J. & HAN, G. (2010). Multi-robot formation control using reinforcement learning method. In Y. Tan, Y. Shi & K. Tan, eds., *Advances in Swarm Intelligence*, vol. 6145 of *Lecture Notes in Computer Science*, 667–674, Springer Berlin Heidelberg. [26](#)

Contribution à la Commande d'un Groupe de Robots Mobiles Non-holonomes à Roues

Résumé: Ce travail s'inscrit dans le cadre de la commande d'un système multi agents / multi véhicules. Cette thèse traite en particulier le cas de la commande d'un système multi-robots mobiles non-holonomes. L'objectif est de concevoir des lois de commandes appropriées pour chaque robot de sorte que l'ensemble des robots puisse exécuter des tâches spécifiques, de suivre des trajectoires désirées tout en maintenant des configurations géométriques souhaitées. L'approche leader-suiveur pour la commande d'un groupe de robots mobiles non-holonomes est étudiée en intégrant la technologie backstepping, avec une approche basée sur les neurodynamiques bioinspirées. Le problème de commande distribuée d'un système multi robots sur le consensus est également étudié. Des lois de commandes cinématiques distribuées sont développés afin de garantir au système multi-robots la convergence exponentielle vers une configuration géométrique souhaitée. Afin de tenir compte de la dynamique des paramètres inconnus, des commandes adaptatives de couple sont développés pour que le système multi-robots puisse converger asymptotiquement vers le modèle géométrique souhaité. Lorsque la dynamique est inconnue, des commandes à base de réseaux de neurones sont proposées.

Mots-clefs: Leader-suiveur, Robots mobiles non-holonomes, Contrôle de la formation, Algorithmes de consensus, Contrôleur adaptatif distribué, Réseau de neurones, Technologie backstepping.

Formation Control of Multiple Nonholonomic Wheeled Mobile Robots

Abstract: This work is based on the multi-agent system / multi-vehicles. This thesis especially focuses on formation control of multiple nonholonomic mobile robots. The objective is to design suitable controllers for each robot according to different control tasks and different constraint conditions, such that a group of mobile robots can form and maintain a desired geometric pattern and follow a desired trajectory. The leader-follower formation control for multiple nonholonomic mobile robots is investigated under the backstepping technology, and we incorporate a bioinspired neurodynamics scheme in the robot controllers, which can solve the impractical velocity jumps problem. The distributed formation control problem using consensus-based approach is also investigated. Distributed kinematic controllers are developed, which guarantee that the multi-robots can at least exponentially converge to the desired geometric pattern under the assumption of "perfect velocity tracking". However, in practice, "perfect velocity tracking" doesn't hold and the dynamics of robots should not be ignored. Next, in consideration of the dynamics of robot with unknown parameters, adaptive torque controllers are developed such that the multi-robots can asymptotically converge to the desired geometric pattern under the proposed distributed kinematic controllers. Furthermore, When the partial knowledge of dynamics is available, an asymptotically stable torque controller has been proposed by using robust adaptive control techniques. When the dynamics of robot is unknown, the neural network controllers with the robust adaptive term are proposed to guarantee robust velocity tracking.

Keywords: Leader-follower, Nonholonomic mobile robots, Formation control, Consensus algorithms, Distributed adaptive controller, Neural Network, Backstepping technology.

BIBLIOGRAPHY
